University of Calgary

PRISM Repository **https://prism.ucalgary.ca**

The Vault Open Theses and Dissertations

2014-07-28

Measurement of the Physical Properties of MacKay River Bitumen and Solvent Mixtures

Khan, Adeem

Khan, A. (2014). Measurement of the Physical Properties of MacKay River Bitumen and Solvent Mixtures (Master's thesis, University of Calgary, Calgary, Canada). Retrieved from https://prism.ucalgary.ca. doi:10.11575/PRISM/26851

http://hdl.handle.net/11023/1657

Downloaded from PRISM Repository, University of Calgary

UNIVERSITY OF CALGARY

Measurement of the Physical Properties of MacKay River Bitumen and Solvent Mixtures

by

Adeem Hassan Khan

A THESIS

SUBMITTED TO THE FACULTY OF GRADUATE STUDIES

IN PARTIAL FULFILMENT OF THE REQUIREMENTS FOR THE

DEGREE OF MASTER OF SCIENCE

GRADUATE PROGRAM IN CHEMICAL AND PETROLEUM ENGINEERING

CALGARY, ALBERTA

JULY, 2014

© Adeem Hassan Khan 2014

ABSTRACT

Bitumen, with its high asphaltene content, has a much higher viscosity than conventional crude oils. The high viscosity of bitumen represents the greatest obstacle to both efficient recoveries by conventional processes and transportation to the refinery for upgrading. To produce bitumen, its viscosity must be reduced using techniques such as solvent aided processes (SAP).

Solvent aided processes, such as LASER (Liquid addition to steam to enhance recovery), significantly reduce the viscosity of bitumen by adding a liquid solvent to the injected steam. This process increases the production rate and reduces the ratio of required steam to oil. To improve oil recovery prediction, it is essential to have accurate measurements the physical properties of the bitumen-solvent system at conditions similar to those encountered in situ and in transport. Measurements of the viscosity of complex bitumen-solvent systems can be used to develop an appropriate model for predicting the viscosity of diluted bitumen/solvent mixtures.

This study aimed to accurately measure the physical properties (viscosity and density) of bitumen diluted with liquid solvents (hexane and toluene) over a wide range of pressures (up to 10 MPa), temperatures (ambient to 345 K), and solvent mass compositions (0.05, 0.1, 0.2, 0.35, 0.5, 0.70, and 0.80) for several bitumen-solvent systems. In addition to density and viscosity measurements, the possibility of asphaltene formation at high solvent concentration was visually investigated. The viscosity and density of the raw bitumen, pure solvents (toluene and hexane), and toluene and hexane diluted bitumen were also measured. Additional solvent mixtures were prepared by mixing hexane with toluene in different mass fractions (0.25, 0.5, and 0.75). The physical properties of bitumen diluted with these mixtures were recorded. The experimental results for all bitumen/solvents mixtures were evaluated using prediction schemes and correlation models from the literature.

The experimental results showed that the viscosity and density of the solvent diluted bitumen decreased as the temperature and mass fraction of solvents was increased, and increased as the pressure was increased. Asphaltene precipitation was detected in hexane-diluted bitumen at 0.5 mass fraction of hexane and increased significantly when the mass fraction of hexane was increased to 0.7. The addition of aromatic solvent i.e. toluene to hexane delayed the critical concentration in case of bitumen/mixture (hexane 75 mass % + toluene 25 mass %) resulting in asphaltene precipitation at only w_s= 0.80.

ACKNOWLEDGEMENTS

I am extremely grateful to everyone who has helped me on this journey. I would also like to express my profound gratitude to my honorable supervisor, Dr. Jalal Abedi, for his support, encouragement, and invaluable guidance. He has been a constant source of inspiration, and without his support, this work would not have been possible. Additionally, I would like to thank all of the members of the supervisory and examination committees of the MSc. Program.

I whole-heartedly appreciate my mentors, Hossein Nourozieh and Mohammad Kariznovi who helped and guided me to overcome any obstacle. I wish to express my appreciation for the financial support from all of the companies in the SHARP Research Consortium: Alberta Innovates Energy and Environment Solutions, Athabasca Oil Sands, BP Canada Energy Group ULC, Brion Energy, Chevron Energy Technology Co., Computer Modeling Group Ltd., ConocoPhillips Canada, Devon Canada Co., Foundation CMG, Husky Energy, Japan Canada Oil Sands Limited, Nexen Energy ULC, Laricina Energy Ltd., Natural Sciences and Engineering Research Council of Canada (NSERC), OSUM Oil Sands Co., PennWest Energy, Statoil Canada Ltd., Suncor Energy, and Total E&P Canada. The support of the Department of Chemical and Petroleum Engineering and the Schulich School of Engineering at the University of Calgary is also acknowledged.

Finally, I would like to thank all of my family members including my mom, wife, sister in law, niece, and brothers for their support, love, and care.

I wish to dedicate this thesis to:

My mother, who never asked for anything in return,

My father, for believing in me

My wife, for encouraging me

My niece and sister in law, for their prayers

My brothers, for standing right beside me in my whole life

TABLE OF CONTENTS

ABSTRACT ii
ACKNOWLEDGEMENTS iv
DEDICATION v
TABLE OF CONTENTS vi
LIST OF TABLES ix
LIST OF FIGURES xix
NOMENCLATURE xxv
Chapter 1 Introduction 1
1.1 Oil Sands Reserves 1
1.2 Oil Sands Microscopic Structure 1
1.3 Recovery of Oil Sands 2
1.3.1 Cyclic Steam Simulation 2
1.3.2 Steam Assisted Gravity Drainage 2
1.3.3 Vapor Extraction Method 3
1.3.4 Toe to Heel Air Injection (THAI) 3
1.3.5 Solvent Aided Process 3
1.4 Research Objectives 3
Chapter 2 Literature Review 5
2.1 Experimental Findings and Modelling on Rheological Properties of Raw Bitumen 5
2.2 Experimental Findings and Modelling on Pure Solvents 14
2.3 Studies on Bitumen-Solvent Systems 15
2.3.1 Experimental Findings for Gas Diluted Bitumen 16
2.3.2 Correlations Developed for Bitumen Solvent Systems 20
2.3.3 Experimental Findings for Solvent Diluted Bitumen 22
Chapter 3 Experimental Procedure and Apparatus 25
3.1 Experimental Apparatus 25
3.1.1 Density Measuring Cell 26
3.1.2 Cambridge Viscometer 27
3.2 Experimental Procedure 28
3.3 Evaluation of Calibration 28
3.3.1 Densitometer Calibration Evaluation 28

3.3.2 Viscometer Calibration Evaluation 37
Chapter 4 Experimental Results 43
4.1 Measured Density and Viscosity Data of Pure Solvents 43
4.2 Measured Density and Viscosity Data of Raw MacKay River Bitumen 46
4.3 Physical Properties of Toluene Diluted Bitumen Systems 48
4.3.1 Measured Viscosity Data of Toluene Diluted Bitumen Mixtures 48
4.3.2 Measured Density Data of Toluene Diluted Bitumen Mixtures 56
4.4 Physical Properties of Hexane Diluted Bitumen Systems 64
4.4.1 Measured Viscosity Data of Hexane Diluted Bitumen Mixtures 64
4.4.2 Measured Density Data of Hexane Diluted Bitumen Mixtures 72
4.5 Physical Properties of Pure Mixtures of Toluene and Hexane 80
4.6 Physical Properties of Bitumen/Mixture 1 (Hexane 75%-Toluene 25%) 84
4.6.1 Measured Viscosity Data of Mixture 1 Diluted Bitumen 84
4.6.2 Measured Density Data of Mixture 1 Diluted Bitumen 93
4.7 Physical Properties of Bitumen/Mixture 2 (Hexane 50%-Toluene 50%) 102
4.7.1 Measured Viscosity Data of Mixture 2 Diluted Bitumen 102
4.7.2 Measured Density Data of Mixture 2 Diluted Bitumen 111
4.8 Physical Properties of Bitumen/Mixture 3 (Hexane 25%-Toluene 75%) 120
4.8.1 Measured Viscosity Data of Mixture 3 Diluted Bitumen 120
4.8.2 Measured Density Data of Mixture 3 Diluted Bitumen 129
Chapter 5 Modelling Investigation of Experimental Data 138
5.1 Modelling of Physical Properties of Pure Solvents 138
5.1.1 Viscosity Modelling 138
5.1.2 Density Modelling 138
5.2 Modelling of Physical Properties of Raw Bitumen 139
5.2.1 Viscosity Modelling 139
5.2.2 Density Modelling 139
5.3 Modelling of Physical Properties of Binary Mixture 139
5.3.1 Viscosity Modelling 139
5.3.2 Density Modelling 141
5.4 Results and Discussion 141
5.4.1 Physical Properties of Pure Solvents 141

5.4.2 Physical Properties of Raw Bitumen 143
5.4.3 Physical Properties of Bitumen-Toluene System 148
5.4.4 Physical Properties of Bitumen-Hexane System 154
5.4.5 Physical Properties of Pure Mixtures 1, 2, 3 159
5.4.6 Physical Properties of Bitumen/Mixture 1 System 161
5.4.7 Physical Properties of Bitumen/Mixture 2 System 166
5.4.8 Physical Properties of Bitumen/Mixture 3 System 171
Chapter 6 Conclusion 176
6.1 Asphaltene Precipitation 176
6.2 Case Study of Raw MacKay River Bitumen 177
6.3 Case Study of Pure Solvents: Toluene and Hexane 178
6.4 Case Study of Bitumen/Toluene and Bitumen/Hexane Binary Mixtures 179
6.5 Case Study of Pure Mixtures 1, 2, and 3 181
6.6 Case Study of Bitumen/Mixture 1, Bitumen/Mixture 2, and Bitumen/Mixture 3 182
6.7 Future Work 184
Bibliography 185

LIST OF TABLES

Table 3-1: Features of the density-measuring cell DMA HPM. 27

Table 3-2: VISCO Pro 2000 Specifications. 28

Table 3-3: Experimental measured and NIST density data comparison for pure toluene as a function of temperatures (T) and pressures (P)..... 29

Table 3-4: Comparison of experimental measured and NIST density data for pure hexane as a function of temperatures, (T) and pressures (P)..... 31

Table 3-5: Experimental measured density data of MacKay River bitumen/n-decane mixture as a function of temperatures (T) and pressures (P) at a constant mass fraction of n-decane (w_s = 0.35) in the binary mixture..... 32

Table 3-6: Experimental measured density data of MacKay River bitumen/n-decane mixture as a function of temperatures (T) and pressures (P) at a constant mass fraction of n-decane (w_s = 0.40) in the binary mixture..... 33

Table 3-7: Experimental measured density data of MacKay River bitumen/n-decane mixture as a function of temperatures (T) and pressures (P) at a constant mass fraction of n-decane (w_s = 0.45) in the binary mixture..... 34

Table 3-8: Experimental measured density data of MacKay River bitumen/n-decane mixture as a function of temperature (T) and pressure (P) at a constant mass fraction of n-decane (w_s = 0. 50) in the binary mixture..... 35

Table 3-9: Comparison of experimental measured and NIST viscosity data for pure hexane as a function of temperature (T) and pressure (P)..... 37

Table 3-10: Experimental viscosity data for a MacKay River bitumen/n-decane mixture as a function of temperature (T) and pressure (P) at a constant mass fraction of n-decane (w_s = 0.35) in the binary mixture..... 38

Table 3-11: Experimental measured viscosity data for a MacKay River bitumen/n-decane mixture as a function of temperature (T) and pressure (P) at a constant mass fraction of n-decane (w_s = 0.40) in the binary mixture. 39

Table 3-12: Experimental measured viscosity data for a MacKay River bitumen/n-decane mixture as a function of temperature (T) and pressure (P) at a constant mass fraction of n-decane (w_s = 0.45) in the binary mixture. 40

Table 3-13: Experimental measured viscosity data for a MacKay River bitumen/n-decane mixture as a function of temperature (T) and pressure (P) at a constant mass fraction of n-decane (w_s = 0.50) in the binary mixture. 41

Table 4-1: Experimental measured density data of pure solvents (toluene and hexane) as a function of temperature (T) and pressure (P). 44

Table 4-2: Experimental measured viscosity data of pure solvents (toluene and hexane) as a function of temperatures (T) and pressure (P). 45

Table 4-3: Experimental measured density data of raw MacKay River bitumen as a function of temperature (T) and pressure (P). 46

Table 4-4: Experimental measured viscosity data for raw MacKay River bitumen as a function of temperature (T) and pressure (P). 48

Table 4-5: Experimental measured viscosity data of MacKay River bitumen/toluene mixture as a function of temperature (T) and pressure (P) at constant mass fraction of toluene (w_s = 0.05) in the binary mixture. 49

Table 4-6: Experimental measured viscosity data of MacKay River bitumen/toluene mixture as a function of temperature (T) and pressure (P) at constant mass fraction of toluene (w_s = 0.1) in the binary mixture. 50

Table 4-7: Experimental measured viscosity data of MacKay River bitumen/toluene mixture as a function of temperature (T) and pressure (P) at a constant mass fraction of toluene (w_s = 0.2) in the binary mixture. 51

Table 4-8: Experimental measured viscosity data of MacKay River bitumen/toluene mixture as a function of temperature (T) and pressure (P) at a constant mass fraction of toluene (w_s = 0.35) in the binary mixture.. 52

Table 4-9: Experimental measured viscosity data of MacKay River bitumen/toluene mixture as a function of temperature (T) and pressure (P) at a constant mass fraction of toluene (w_s = 0.5) in the binary mixture.. 53

Table 4-10: Experimental measured viscosity data of MacKay River bitumen/toluene mixture as a function of temperature (T) and pressure (P) at a constant mass fraction of toluene (w_s = 0.7) in the binary mixture.. 54

Table 4-11: Experimental measured density data of the MacKay River bitumen/toluene mixture as a function of temperature (T) and pressure (P) at a constant mass fraction of toluene (w_s = 0.05) in the binary mixture. 57

Table 4-12: Experimental measured density data for the MacKay River bitumen/toluene mixture as a function of temperature (T) and pressure (P) at a constant mass fraction of toluene (w_s = 0.1) in the binary mixture. 58

Table 4-13: Experimental measured density data for the MacKay River bitumen/toluene mixture as a function of temperature (T) and pressure (P) at a constant mass fraction of toluene (w_s = 0.2) in the binary mixture. 59

Table 4-14: Experimental measured density data for the MacKay River bitumen/toluene mixture as a function of temperature (T) and pressure (P) at a constant mass fraction of toluene (w_s = 0.35) in the binary mixture. 60

Table 4-15: Experimental measured density data for the MacKay River bitumen/toluene mixture as a function of temperature (T) and pressure (P) at a constant mass fraction of toluene (w_s = 0.5) in the binary mixture. 61

Table 4-16: Experimental measured density data for the MacKay River bitumen/toluene mixture as a function of temperature (T) and pressure (P) at a constant mass fraction of toluene (w_s = 0.7) in the binary mixture. 62

Table 4-17: Experimental measured viscosity data of the MacKay River bitumen/hexane mixture as a function of temperature (T) and pressure (P) at constant hexane mass fraction (w_s = 0.05) in the binary mixture. 65

Table 4-18: Experimental measured viscosity data of the MacKay River bitumen/hexane mixture as a function of temperature (T) and pressure (P) at constant hexane mass fraction (w_s = 0.1) in the binary mixture. 66

Table 4-19: Experimental measured viscosity data of the MacKay River bitumen/hexane mixture as a function of temperature (T) and pressure (P) at constant hexane mass fraction (w_s = 0.2) in the binary mixture. 67

Table 4-20: Experimental measured viscosity data of the MacKay River bitumen/hexane mixture as a function of temperature (T) and pressure (P) at constant hexane mass fraction (w_s = 0.35) in the binary mixture. 68

Table 4-21: Experimental measured viscosity data of the MacKay River bitumen/hexane mixture as a function of temperature (T) and pressure (P) at constant hexane mass fraction (w_s = 0.5) in the binary mixture. 69

Table 4-22: Experimental measured viscosity data of the MacKay River bitumen/hexane mixture as a function of temperature (T) and pressure (P) at constant hexane mass fraction (w_s = 0.7) in the binary mixture. 70

Table 4-23: Experimental measured density data of the MacKay River bitumen/hexane mixture as a function of temperature (T) and pressure (P) at a constant mass fraction of hexane (w_s = 0.05) in the binary mixture. 73

Table 4-24: Experimental measured density data of the MacKay River bitumen/hexane mixture as a function of temperature (T) and pressure (P) at a constant mass fraction of hexane (w_s = 0.1) in the binary mixture. 74

Table 4-25: Experimental measured density data of the MacKay River bitumen/hexane mixture as a function of temperature (T) and pressure (P) at a constant mass fraction of hexane (w_s = 0.2) in the binary mixture. 75

Table 4-26: Experimental measured density data of the MacKay River bitumen/hexane mixture as a function of temperature (T) and pressure (P) at a constant mass fraction of hexane (w_s = 0.35) in the binary mixture. 76

Table 4-27: Experimental measured density data of the MacKay River bitumen/hexane mixture as a function of temperature (T) and pressure (P) at a constant mass fraction of hexane (w_s = 0.5) in the binary mixture. 77

Table 4-28: Experimental measured density data of the MacKay River bitumen/hexane mixture as a function of temperature (T) and pressure (P) at a constant mass fraction of hexane (w_s = 0.7) in the binary mixture. 78

Table 4-29: Experimental measured density and viscosity data for pure mixture 1 (hexane 75%-toluene 25%) as a function of temperature (T) and pressure (P). 81

Table 4-30: Experimental measured density and viscosity data of pure mixture 2 (hexane 50%-toluene 50%) as a function of temperature (T) and pressure (P). 82

Table 4-31: Experimental measured density and viscosity data of pure mixture 3 (hexane 25%-toluene 75%) as a function of temperature, (T) and pressure (P). 83

Table 4-32: Experimental measured viscosity data for bitumen diluted with mixture 1 as a function of temperature (T) and pressure (P) with a constant mass fraction of mixture 1 (w_s = 0.05) in the mixture. 85

Table 4-33: Experimental measured viscosity data for bitumen diluted with mixture 1 as a function of temperature (T) and pressure (P) with a constant mass fraction of mixture 1 (w_s = 0.1) in the mixture. 86

Table 4-34: Experimental measured viscosity data for bitumen diluted with mixture 1 as a function of temperature (T) and pressure (P) with a constant mass fraction of mixture 1 (w_s = 0.2) in the mixture. 87

Table 4-35: Experimental measured viscosity data for bitumen diluted with mixture 1 as a function of temperature (T) and pressure (P) with a constant mass fraction of mixture 1 (w_s = 0.35) in the mixture. 88

Table 4-36: Experimental measured viscosity data for bitumen diluted with mixture 1 as a function of temperature (T) and pressure (P) with a constant mass fraction of mixture 1 (w_s = 0.5) in the mixture. 89

Table 4-37: Experimental measured viscosity data for bitumen diluted with mixture 1 as a function of temperature (T) and pressure (P) with a constant mass fraction of mixture 1 (w_s = 0.7) in the mixture. 90

Table 4-38: Experimental measured viscosity data for bitumen diluted with mixture 1 as a function of temperature (T) and pressure (P) with a constant mass fraction of mixture 1 (w_s = 0.8) in the mixture. 91

Table 4-39: Experimental measured density data for bitumen diluted with mixture 1 as a function of temperature (T) and pressure (P) at a constant mass fraction of mixture 1 (w_s = 0.05) in the mixture. 94

Table 4-40: Experimental measured density data for bitumen diluted with mixture 1 as a function of temperature (T) and pressure (P) at a constant mass fraction of mixture 1 (w_s = 0.1) in the mixture. 95

Table 4-41: Experimental measured density data for bitumen diluted with mixture 1 as a function of temperature (T) and pressure (P) at a constant mass fraction of mixture 1 (w_s = 0.2) in the mixture. 96

Table 4-42: Experimental measured density data for bitumen diluted with mixture 1 as a function of temperature (T) and pressure (P) at a constant mass fraction of mixture 1 (w_s = 0.35) in the mixture. 97

Table 4-43: Experimental measured density data for bitumen diluted with mixture 1 as a function of temperature (T) and pressure (P) at a constant mass fraction of mixture 1 (w_s = 0.5) in the mixture. 98

Table 4-44: Experimental measured density data for bitumen diluted with mixture 1 as a function of temperature (T) and pressure (P) at a constant mass fraction of mixture 1 (w_s = 0.7) in the mixture. 99

Table 4-45: Experimental measured density data for bitumen diluted with mixture 1 as a function of temperature (T) and pressure (P) at a constant mass fraction of mixture 1 (w_s = 0.8) in the mixture. 100

Table 4-46: Experimental measured viscosity data for bitumen diluted with mixture 2 as a function of temperature (T) and pressure (P) at constant mass fraction of mixture 2 (w_s = 0.05) in the mixture. 103

Table 4-47: Experimental measured viscosity data for bitumen diluted with mixture 2 as a function of temperature (T) and pressure (P) at constant mass fraction of mixture 2 (w_s = 0.1) in the mixture. 104

Table 4-48: Experimental measured viscosity data for bitumen diluted with mixture 2 as a function of temperature (T) and pressure (P) at constant mass fraction of mixture 2 (w_s = 0.2) in the mixture. 105

Table 4-49: Experimental measured viscosity data for bitumen diluted with mixture 2 as a function of temperature (T) and pressure (P) at constant mass fraction of mixture 2 (w_s = 0.35) in the mixture. 106

Table 4-50: Experimental measured viscosity data for bitumen diluted with mixture 2 as a function of temperature (T) and pressure (P) at constant mass fraction of mixture 2 (w_s = 0.5) in the mixture. 107

Table 4-51: Experimental measured viscosity data for bitumen diluted with mixture 2 as a function of temperature (T) and pressure (P) at constant mass fraction of mixture 2 (w_s = 0.7) in the mixture. 108

Table 4-52: Experimental measured viscosity data for bitumen diluted with mixture 2 as a function of temperature (T) and pressure (P) at constant mass fraction of mixture 2 (w_s = 0.8) in the mixture. 109

Table 4-53: Experimental measured density data of bitumen diluted with mixture 2 as a function of temperature (T) and pressure (P) at a constant mass fraction of mixture 2 (w_s = 0.05) in the mixture. 112

Table 4-54: Experimental measured density data of bitumen diluted with mixture 2 as a function of temperature (T) and pressure (P) at a constant mass fraction of mixture 2 (w_s = 0.1) in the mixture. 113

Table 4-55: Experimental measured density data of bitumen diluted with mixture 2 as a function of temperature (T) and pressure (P) at a constant mass fraction of mixture 2 (w_s = 0.2) in the mixture. 114

Table 4-56: Experimental measured density data of bitumen diluted with mixture 2 as a function of temperature (T) and pressure (P) at a constant mass fraction of mixture 2 (w_s = 0.35) in the mixture. 115

Table 4-57: Experimental measured density data of bitumen diluted with mixture 2 as a function of temperature (T) and pressure (P) at a constant mass fraction of mixture 2 (w_s = 0.5) in the mixture. 116

Table 4-58: Experimental measured density data of bitumen diluted with mixture 2 as a function of temperature (T) and pressure (P) at a constant mass fraction of mixture 2 (w_s = 0.7) in the mixture. 117

Table 4-59: Experimental measured density data of bitumen diluted with mixture 2 as a function of temperature (T) and pressure (P) at a constant mass fraction of mixture 2 (w_s = 0.8) in the mixture. 118

Table 4-60: Experimental measured viscosity data for bitumen diluted with mixture 3 as a function of temperature (T) and pressure (P) at a constant mass fraction of mixture 3 (w_s = 0.05) in the mixture. 121

Table 4-61: Experimental measured viscosity data for bitumen diluted with mixture 3 as a function of temperature (T) and pressure (P) at a constant mass fraction of mixture 3 (w_s = 0.1) in the mixture. 122

Table 4-62: Experimental measured viscosity data for bitumen diluted with mixture 3 as a function of temperature (T) and pressure (P) at a constant mass fraction of mixture 3 (w_s = 0.2) in the mixture. 123

Table 4-63: Experimental measured viscosity data for bitumen diluted with mixture 3 as a function of temperature (T) and pressure (P) at a constant mass fraction of mixture 3 (w_s = 0.35) in the mixture. 124

Table 4-64: Experimental measured viscosity data for bitumen diluted with mixture 3 as a function of temperature (T) and pressure (P) at a constant mass fraction of mixture 3 (w_s = 0.5) in the mixture. 125

Table 4-65: Experimental measured viscosity data for bitumen diluted with mixture 3 as a function of temperature (T) and pressure (P) at a constant mass fraction of mixture 3 (w_s = 0.7) in the mixture. 126

Table 4-66: Experimental measured viscosity data for bitumen diluted with mixture 3 as a function of temperature (T) and pressure (P) at a constant mass fraction of mixture 3 (w_s = 0.8) in the mixture. 127

Table 4-67: Experimental measured density data of bitumen diluted with mixture 3 as a function of temperature (T) and pressure (P) at a constant mass fraction of mixture 3 (w_s = 0.05) in the mixture.. 130

Table 4-68: Experimental measured density data of bitumen diluted with mixture 3 as a function of temperature (T) and pressure (P) at a constant mass fraction of mixture 3 (w_s = 0.1) in the mixture. 131

Table 4-69: Experimental measured density data of bitumen diluted with mixture 3 as a function of temperature (T) and pressure (P) at a constant mass fraction of mixture 3 (w_s = 0.2) in the mixture. 132

Table 4-70: Experimental measured density data of bitumen diluted with mixture 3 as a function of temperature (T) and pressure (P) at a constant mass fraction of mixture 3 (w_s = 0.35) in the mixture. 133

Table 4-71: Experimental measured density data of bitumen diluted with mixture 3 as a function of temperature (T) and pressure (P) at a constant mass fraction of mixture 3 (w_s = 0.5) in the mixture. 134

Table 4-72: Experimental measured density data of bitumen diluted with mixture 3 as a function of temperature (T) and pressure (P) at a constant mass fraction of mixture 3 (w_s = 0.7) in the mixture. 135

Table 4-73: Experimental measured density data of bitumen diluted with mixture 3 as a function of temperature (T) and pressure (P) at a constant mass fraction of mixture 3 (w_s = 0.8) in the mixture. 136

Table 5-1: Measured and correlated viscosities of toluene at different temperatures, T at a pressure of 1 MPa. 142

Table 5-2: Calculated coefficients for density of pure toluene by using Eq. [5-2] 142

Table 5-3: Calculated coefficients for density of bitumen using correlation [5-2] 143

Table 5-4: Measured μ_{exp}, and correlated, μ_{corr}, viscosity of MacKay River bitumen at different temperatures, T, and pressures, P. 145

Table 5-5: Calculated coefficients for bitumen viscosity using correlations 2-7 and 2-8..... 146

Table 5-6: Measured and correlated viscosities of mixture 1 at different temperatures, T. 159

Table 5-7: Measured and correlated viscosities of mixture 2 at different temperatures, T. 160

Table 5-8: Measured and correlated viscosities of mixture 3 at different temperatures, T. 160

Table 5-9: Calculated coefficients for density of pure mixture 1, 2, 3 by using Eq. [5-2] 160

LIST OF FIGURES

Figure 3-1: Experimental apparatus schematic diagram: (1) water storage tank, (2) nitrogen cylinder, (3) pressure gauge, (4) vacuum pump, (5) reciprocating pump, (6) sampling cell, (7) toluene cell, (8) density measuring cell, (9) viscometer, (10) pressure transducer, (11) temperature controlled oven, (12) interface module, (13) density evaluation unit, and (14) Viscopro 2000 unit. 26

Figure 3-2: Density of pure toluene versus pressure, P, at different temperature, T; ■,●,▲,♦, measured densities; ■, T = 333.3 K; ●, T=318.5 K; ▲, T = 303.6 K, ♦, T = 297.8 K; − , NIST density data. 30

Figure 3-3: Density variation of bitumen/n-decane system with temperature, at different mass fractions of n-decane and at a constant pressure of 1 MPa. 36

Figure 3-4: Density variation of bitumen/n-decane system with temperature, at different mass fractions of n-decane and at a constant pressure of 10 MPa. 36

Figure 3-5: Viscosity variation of bitumen/n-decane systems with temperature, at different mass fractions of n-decane and a constant pressure of 1 MPa. 42

Figure 3-6: Viscosity variation of bitumen/n-decane systems with temperature, at different mass fractions of n-decane and a constant pressure of 10 MPa. 42

Figure 4-1: Raw MacKay River bitumen density dependence on pressure (P) and temperature (T). 47

Figure 4-2: Calculated viscosity of the toluene-bitumen mixture versus temperature, at different mass fractions of toluene and at a constant pressure of 1 MPa. 55

Figure 4-3: Calculated viscosity of the toluene-bitumen mixture versus temperature, at different mass fractions of toluene and at a constant pressure of 10 MPa. 55

Figure 4-4: Density variation of the toluene-bitumen mixture with temperature, at different mass fractions of toluene and a constant pressure of 1 MPa. 63

Figure 4-5: Density variation of the toluene-bitumen mixture with temperature, at different mass fractions of toluene and a constant pressure of 10 MPa. 63

Figure 4-6: Viscosity variation of hexane-bitumen mixtures with temperature, at different mass fractions of hexane and a constant pressure of 1 MPa. 71

Figure 4-7: Viscosity variation of hexane-bitumen mixtures with temperature, at different mass fractions of hexane and a constant pressure of 10 MPa. 71

Figure 4-8: Density variation of hexane-bitumen mixtures with temperature, at different mass fractions of hexane and at a constant pressure of 1 MPa. 79

Figure 4-9: Density variation of hexane-bitumen mixtures with temperature at different hexane mass fractions at a constant 10MPa of pressure. 79

Figure 4-10: Viscosity variations of mixture 1 and bitumen with temperature, at different mass fractions of mixture 1 and 1 MPa constant pressure. 92

Figure 4-11: Viscosity variations of mixture 1/ bitumen with temperature, at different mass fractions of mixture 1 at constant pressure of 10 MPa. 92

Figure 4-12: Density variations of mixture 1/ bitumen with temperature, at different mass fractions of mixture 1 at a constant pressure of 1 MPa. 101

Figure 4-13: Density variations of mixture 1/ bitumen with temperature, at different mass fractions of mixture 1 at a constant pressure of 10 MPa. 101

Figure 4-14: Viscosity variations of mixture 2/ bitumen with temperature, at different mass fractions of mixture 2 at a constant pressure of 1MPa. 110

Figure 4-15: Viscosity variations of mixture 2/ bitumen with temperature, at different mass fractions of mixture 2 at a constant pressure of 10 MPa. 110

Figure 4-16: Density variations of mixture 2/ bitumen with temperature, at different mass fractions of mixture 2 at a constant pressure of 1 MPa. 119

Figure 4-17: Density variations of mixture 2/ bitumen with temperature, at different mass fractions of mixture 2 at a constant pressure of 10 MPa.....119

Figure 4-18: Viscosity variations of mixture 3/ bitumen with temperature, at different mass fractions of mixture 3 at a constant pressure of 1 MPa..... 128

Figure 4-19: Viscosity variations of mixture 3/ bitumen with temperature, at different mass fractions of mixture 3 at a constant pressure of 10 MPa..... 128

Figure 4-20: Density variations of mixture 3/ bitumen with temperature, at different mass fractions of mixture 3 at a constant pressure of 1 MPa..... 137

Figure 4-21: Density variations of mixture 3/ bitumen with temperature, at different mass fractions of mixture 3 at a constant pressure of 10 MPa..... 137

Figure 5-1: Density of raw bitumen, ρ, versus pressure, P, at different temperatures, T; ■,●,×,▲,♦, measured densities; ■, T = 303.3 K; ●, T=313.4 K; ×, T = 318.1 K; ▲, T = 323.6 K, ♦, T = 333.3 K; -----, correlated densities using Eq. [5-2]. 144

Figure 5-2: Viscosity of bitumen, μ, versus pressure, P, at different temperatures, T; ■,●,▲,♦, measured viscosities; ■, T = 344.7 K; ●, T=333.1 K; ▲, T = 326 K, ♦, T = 321.3 K; − ,correlated viscosities using Eq. [2-7]..... 147

Figure 5-3: Viscosity of bitumen, μ, versus pressure, P, at different temperature, T; ■,●,▲,♦, measured viscosities; ■, T = 344.7 K; ●, T=333.1 K; ▲, T = 326 K, ♦, T = 321.3 K; − ,correlated viscosities using Eq. [2-8]..... 147

Figure 5-4: Density of toluene/bitumen system, ρ_m, versus toluene concentration, W_S, at different temperatures, T; and a pressure of 1 MPa; measured densities;−, correlated densities; ■, T = 333 K; ●, T=318 K; ▲, T = 303 K, ♦, T = 297.6 K..... 149

Figure 5-5: Density of toluene/bitumen system, ρ_m, versus toluene concentration, W_S, at different temperatures, T; and a pressure of 10 MPa; measured densities;−, correlated densities; ■, T = 333 K; ●, T=318 K; ▲, T = 303 K, ♦, T = 297.6 K..... 149

Figure 5-6: Density of toluene/bitumen system, ρ_m, versus pressure, P, at different temperatures, T; and a toluene concentration of 0.05; measured densities;−, correlated densities; ■, T = 333 K; ●, T=318 K; ▲, T = 303 K, ♦, T = 297.6 K. 150

Figure 5-7: Density of toluene/bitumen system, ρ_m, versus pressure, P, at different temperatures, T; and a toluene concentration of 0.7; measured densities;−, correlated densities; ■, T = 333 K; ●, T=318 K; ▲, T = 303 K, ♦, T = 297.6 K. 151

Figure 5-8: Experimental bitumen/toluene mixture viscosities, μ_{exp}, versus correlated viscosities, μ_{corr}, by using several models; ▲, Arrhenius's model; ●, power law model; ■, Lederer's model; ×, Shu correlation. 152

Figure 5-9: Viscosity, μ_m, of toluene diluted bitumen mixtures versus toluene mass fraction, W_S, at different temperatures and a pressure of 1 MPa; ▲,●,■,♦, measured viscosities; −, Lederer's model; ---, power law model; ▲, 302.1 K; ●, 311.3 K; ■, 327 K; ♦, 344.6 K. 153

Figure 5-10: Viscosity, μ_m, of toluene diluted bitumen mixtures versus toluene mass fraction, W_S, at different temperatures and a pressure of 10 MPa; ▲,●,■,♦, measured viscosities; −, Lederer's model; ---, power law model; ▲, 302.1 K; ●, 311.3 K; ■, 327 K; ♦, 344.6 K. 154

Figure 5-11: Density of hexane/bitumen system, ρ_m, versus hexane concentration, W_S, at different temperatures, T; and a pressure of 1 MPa; measured densities;−, correlated densities; ■, T = 333.2 K; ●, T=318.4 K; ▲, T = 303.4 K, ♦, T = 296.4 K. 155

Figure 5-12: Density of hexane/bitumen system, ρ_m, versus hexane concentration, W_S, at different temperatures, T; and a pressure of 10 MPa; measured densities;−, correlated densities; ■, T = 333.2 K; ●, T=318.4 K; ▲, T = 303.4 K, ♦, T = 296.4 K. 156

Figure 5-13: Experimental bitumen/hexane mixture viscosities, μ_{exp}, versus correlated viscosities, μ_{corr}, by using several models; ▲, Arrhenius's model; ●, power law model; ■, Lederer's model; ×, Shu correlation. 157

Figure 5-14: Viscosity, μ_m, of hexane diluted bitumen mixtures versus pressure, P, at different temperatures and a hexane concentration of 0.05; ■,●,▲ ,♦, measured viscosities; −, Lederer's model; ---, power law model; ■, 344 K; ●, 328 K; ▲, 311.3 K; ♦, 300.9 K. 158

Figure 5-15: Viscosity, μ_m, of hexane diluted bitumen mixtures versus pressure, P, at different temperatures and a hexane concentration of 0.7; ■,●,▲ ,♦, measured viscosities; −, Lederer's model; ⋯⋯, power law model; ■, 344 K; ●, 328 K; ▲, 311.3 K; ♦, 300.9 K. 158

Figure 5-16: Density of bitumen/mixture 1 system, ρ_m, versus temperature, T, at different mixture 1 concentrations, W_S; and at a pressure of 1 MPa; measured densities;−, correlated densities; □, W_S = 0.8; ○, W_S = 0.7; ◊, W_S = 0.5; ■, W_S = 0.35; ●, W_S = 0.2; ▲, W_S = 0.1, ♦, W_S = 0.05... 162

Figure 5-17: Density of bitumen/mixture 1 system, ρ_m, versus temperature, T, at different mixture 1 concentrations, W_S; and at a pressure of 10 MPa; measured densities;−, correlated densities; □, W_S = 0.8; ○, W_S = 0.7; ◊, W_S = 0.5; ■, W_S = 0.35; ●, W_S = 0.2; ▲, W_S = 0.1, ♦, W_S = 0.05... 162

Figure 5-18: Experimental bitumen/ mixture 1 viscosities, μ_{exp}, versus correlated viscosities, μ_{corr}, by using several models; ▲, Arrhenius's model; ●, power law model; ■, Lederer's model; ×, Shu correlation. 164

Figure 5-19: Viscosity of bitumen/mixture 1 system, μ_m, versus pressure, P, at different mixture 1 concentrations, W_S; and at a Temperature of 344 K; measured viscosities;− , correlated viscosities; □, W_S = 0.8; ○, W_S = 0.7; ◊, W_S = 0.5; ■, W_S = 0.35; ●, W_S = 0.2; ▲, W_S = 0.1, ♦, W_S = 0.05. 165

Figure 5-20: Viscosity of bitumen/mixture 1 system, μ_m, versus pressure, P, at different mixture 1 concentrations, W_S; and at a Temperature of 299 K; measured viscosities;− , correlated viscosities; □, W_S = 0.8; ○, W_S = 0.7; ◊, W_S = 0.5; ■, W_S = 0.35; ●, W_S = 0.2; ▲, W_S = 0.1, ♦, W_S = 0.05 165

Figure 5-21: Density of bitumen/mixture 2 system, ρ_m, versus pressure, P, at different temperatures, T; and a mixture 2 concentration of 0.05; measured densities;− , correlated densities; ■, T = 333 K; ●, T=318 K; ▲, T = 303 K, ♦, T = 298 K..... 167

Figure 5-22: Density of bitumen/mixture 2 system, ρ_m, versus pressure, P, at different temperatures, T; and a mixture 2 concentration of 0.8; measured densities;−, correlated densities; ■, T = 333 K; ●, T=318 K; ▲, T = 303 K, ♦, T = 298 K..... 167

Figure 5-23: Experimental bitumen/ mixture 2 viscosities, μ_{exp}, versus correlated viscosities, μ_{corr}, by using several models; ▲, Arrhenius's model; ●, power law model; ■, Lederer's model; ×, Shu correlation. 169

Figure 5-24: Viscosity, μ_m, of mixture 2 diluted bitumen system versus mixture 2 mass fraction, W_S, at different temperatures and a pressure of 1 MPa; ▲,●,■,♦, measured viscosities; −, Lederer's model; ⋯⋯, power law model; ▲, 300 K; ●, 311 K; ■, 327 K; ♦, 344 K. 170

Figure 5-25: Viscosity, μ_m, of mixture 2 diluted bitumen system versus mixture 2 mass fraction, W_S, at different temperatures and a pressure of 10 MPa; ▲,●,■,♦, measured viscosities; −, Lederer's model; ⋯⋯, power law model; ▲, 300 K; ●, 311 K; ■, 327 K; ♦, 344 K. 170

Figure 5-26: Density of bitumen/mixture 3 system, ρ_m, versus mixture 3 mole fraction, X_S, at different temperatures, T; and a constant pressure of 1 MPa; measured densities;−, correlated densities; ■, T = 333 K; ●, T=318 K; ▲, T = 303 K, ♦, T = 296 K. 172

Figure 5-27: Density of bitumen/mixture 3 system, ρ_m, versus mixture 3 mole fraction, X_S, at different temperatures, T; and a constant pressure of 10 MPa; measured densities;−, correlated densities; ■, T = 333 K; ●, T=318 K; ▲, T = 303 K, ♦, T = 296 K. 172

Figure 5-28: Experimental bitumen/ mixture 3 viscosities, μ_{exp}, versus correlated viscosities, μ_{corr}, by using several models; ▲, Arrhenius's model; ●, power law model; ■, Lederer's model; ×, Shu correlation. 173

Figure 5-29: Viscosity μ_m, of bitumen/mixture 3 systems, versus mixture 3 mole fraction, X_S, at different temperatures, T; and a pressure of 1 MPa; measured data;−, correlated data; ■, T = 343 K; ●, T=326 K; ▲, T = 311.7 K, ♦, T = 301.3 K. 174

Figure 5-30: Viscosity μ_m, of bitumen/mixture 3 systems, versus mixture 3 mole fraction, X_S, at different temperatures, T; and a pressure of 10 MPa; measured data;−, correlated data; ■, T = 343 K; ●, T=326 K; ▲, T = 311.7 K, ♦, T = 301.3 K. 175

NOMENCLATURE

μ	Dynamic viscosity, mPa.s (cp)
ρ	Density, kg/m^3
Pg	Gauge pressure (MPa)
$T_{c,\,r}$	Critical, reduced temperature (K)
Θ	Energy shape factor
Φ	Size shape factor
ω	Pitzer's acentric factor
V	Molar Volume (m^3/kmol)
Ap	Multiplying factor
Z	Compressibility factor
h	Equivalent substance volume reducing ratio
Γ	Equivalent substance temperature reducing ratio
M	Molar mass (g/mol)
α, β	Components
V_{ci}	Critical volume of component i
x	Mole fraction
ψ	Binary interaction parameter

a_1, a_2, a_3	Empirical constants in Eq. [2-7, 2-8]
a, b	Adjustable parameters in Eq. [5-1]
T	Temperature, K in Eq. [5-2]
P	Pressure in kPa in Eq. [5-2]
w_s	Mass fraction of solvent
p_m, p_s	Density of mixture and solvents
v_s	Volume fraction of solvent
n	Adjustable parameter in Eq. [5-5]
α	Adjustable parameter in Eq. [5-6]

Subscripts

i, j	Components
m	Mixture
exp	Experimental
corr	Correlated

Chapter 1 Introduction

Increase in global energy demand and depletion of conventional light oil reserves has driven increasing interest in the recovery of non-conventional petroleum deposits over the last few years. Additionally, non-conventional oil represents much greater reserves at around 6 trillion barrels of oil in place, compared to conventional oil reserves of approximately 1 trillion barrels (Das and Butler, 1998).

The oil sands are a major type of non-conventional petroleum deposit composed of bitumen, clay, water, and sand particles. Bitumen is defined as an organic substance, which is solid at room temperature and contains hydrocarbons greater than pentane. Bitumen has a high viscosity which prevents it from flowing in its natural state.

1.1 Oil Sands Reserves

Oil sands are found in many countries but the majority of the deposits are in Venezuela and Canada. In Canada, these reserves are found in four different locations; Athabasca River, Cold Lake, Wabasca, and Peace River. The Athabasca reserves are the largest.

The Canadian oil sands account for 97% of Canada's total oil reserves. Approximately 80% of the oil sands reserves are recoverable using in-situ processes while 20% can be recovered by surface mining, as they are easily accessible from the surface.

1.2 Oil Sands Microscopic Structure

(Takamura, 1982) proposed a refined model for the Athabasca oil sands. He concluded that oil sand consist of sand grains, fines, water and bitumen. The porosity of sand grains was observed to be 35 %, and 10 to 15 % of the pore spaces were occupied by water. The bitumen and sand grains were separated by a thin film of water about 10 nm thick.

The viscosity and density of bitumen are the most important properties to recovering and transporting it. The viscosity of bitumen at reservoir conditions is extremely high making it difficult to recover and transport. Therefore, the following techniques should be employed to decrease its viscosity.

1.3 Recovery of Oil Sands

Recovering oil sands in an economical and environmentally friendly way is the greatest challenge faced by the oil sands industry. Two main recovery methods are employed depending on the depth of the oil sands. In surface mining, oil sands located closer to the surface are dug out of the ground and transported in large trucks to a facility where the bitumen is separated and upgraded. In situ recovery methods are the most suitable for recovering bitumen that is located at a depth of 70 meter or more. In situ recovery is further divided into the following processes.

1.3.1 Cyclic Steam Simulation

In this technique, steam is injected into the well for several weeks at such a rate that allow minimum heat loss. This step is followed by shut-in period to allow steam to condense resulting in reduction of viscosity of heavy oil bitumen. The well is placed on production after shut-in period to produce the condense water at first followed by oil production.

1.3.2 Steam Assisted Gravity Drainage

In this technique two horizontal wells are drilled into the reservoir. Steam is injected through upper horizontal pipe, which heats bitumen and it is allowed to flow to the lower horizontal pipe along with the condensed water.

1.3.3 Vapor Extraction Method

The vapour extraction method is one of the evolving methods used to recover bitumen. This method uses solvents such as propane, butane or their mixture instead of steam and has a working mechanism similar to SAGD technology, except the upper drilled well is used for injecting solvent. The solvent in the upper well reduces the viscosity of the heavy oil and bitumen which then flows to the lower drilled well and is brought to the surface.

1.3.4 Toe to Heel Air Injection (THAI)

THAI uses underground combustion to move the viscous oil in the reservoir. This process requires less water because air is injected instead.

1.3.5 Solvent Aided Process

In this process, the viscosity of the bitumen is reduced using different solvents that have a lesser viscosity and density. The process is relatively energy efficient compared to thermal processes. However, a lack of experimental data and viscosity correlations makes it difficult to fully utilize this approach. Measuring the physical properties of solvent/bitumen mixtures in different proportions and at various temperatures and pressures is of utmost importance to optimizing this process.

1.4 Research Objectives

The study aims to accurately measure the physical properties (viscosity and density) of raw MacKay River bitumen, pure solvents (hexane and toluene), bitumen diluted with toluene, bitumen/hexane, pure solvent mixtures *(hexane 75 mass % + toluene 25 mass %, hexane 50 mass % + toluene 50 mass %, and hexane 25 mass % + toluene 75 mass %)* and bitumen diluted with these mixtures at pressures and temperatures suitable to in situ recovery and transportation

of bitumen. The relationship of each property of the bitumen diluted with liquid solvents was also determined. The research was divided into two main sections.

1. Experimental Measurement

    - Viscosity and density measurement of raw MacKay River bitumen at different temperatures and pressures.
    - Measurement of the physical properties of pure hexane, toluene, and their mixtures with bitumen at similar temperatures and pressures.
    - Investigation of the dependence of viscosity and density on temperature, pressure, and mixture composition.
    - Investigation of asphaltene precipitation for bitumen/solvent systems

2. Modelling Prediction

    - Correlation of the measured data of raw MacKay River bitumen and bitumen diluted with various mixtures.
    - Several mixing rules were also investigated

Chapter 2 Literature Review

Several experimental and modelling studies measuring the rheological properties of bitumen have been completed in the last couple of years. The literature on the physical properties of bitumen has been documented in various formats and each research project has its own significance. This chapter will discuss most of the research on raw bitumen and its binary mixtures with various solvents, including both experimental studies and modelling prediction schemes.

2.1 Experimental Findings and Modelling on Rheological Properties of Raw Bitumen

(Ward and Clark, 1950) determined the viscosity and specific gravity of samples of oil from different sites of Athabasca bituminous sands. They found that the viscosity of the oil varied significantly and the specific gravity varied from 1.005 to 1.027 depending on the location where the samples were taken. They used a pressure capillary tube viscometer and observed that at 84.4°C the viscosity was proportional to the shear rate leading them to believe that the oil samples were Newtonian. The viscosity-temperature relationship was inversely proportional and the viscosity was dependent on the type of extraction process.

(Dealy, 1979) studied the rheological properties of bitumen from three different regions, Athabasca, Cold Lake, and Lloydminster using a mechanical spectrometer. He observed slight non-Newtonian behaviour for the oil samples and found that their rheological properties were affected when the sample was exposed to air or high temperatures. He measured a 10% decrease in viscosity for a small change in shear rate.

(Ukwuoma and Ademodi, 1999) measured the viscosities of Nigerian oil sand bitumen (extracted with toluene) over various temperatures and shear rate ranges. They found that at

higher temperatures the bitumen behaves as a Newtonian fluid. They measured viscosity using a rotational viscometer and found that at 50 °C, the bitumen behaves as a non-Newtonian fluid and the effect of the shear rate was not significant. A non-linear relationship between the viscosity of bitumen and shear rate was found at various temperatures.

(Moran and Yeung, 2004) measured the viscosities of oils A and B (polybutene oils) at room temperature and of Coker feed bitumen at 22.5 °C using the drop shape recovery method. Due to the limitations of this technique, the viscosity was measured at low shear rates to avoid heating the samples. This can be compared with conventional rotational viscometers, which are operated at higher shear rates. (Moran and Yeung, 2004) measured the viscosity of bitumen at 22.5 °C to be 1250 Pa.s.

(Khan et al., 1984) developed two empirical viscosity models involving minimal adjustable parameters as opposed to the modified Eyring's and Hildebrand's models, which contain more than four adjustable parameters. The modified Eyring's equation was:

$$\frac{\mu}{d} = 6.466126 * 10^{-4} exp \frac{\Delta F}{1.987T} \qquad 2\text{-}1$$

where,

$$d = 0.120(616.62 - T)^{\frac{1}{3}}, \qquad 2\text{-}2$$

$$\ln \Delta F = \frac{b_1}{T^{b_2}}, \qquad 2\text{-}3$$

where, ΔF is viscous free energy of activation and b_1 and b_2 were adjustable parameters.

The Hildebrand's equation was modified to the following equation:

$$ln\left(\frac{1}{\mu}\right) = B_o + B_1 \sinh \beta + B_2 \sinh \beta^2 + B_3 \sinh \beta^3 \qquad 2\text{-}4$$

where,

B_0 to B_3 Constants

β $(v- v_o)/ v_o$

v Molar volume (cm^3/gmol)

v_o Corresponding state fraction of critical volume (cm^3/gmol)

The following two models were developed by (Khan et al., 1984). The average deviation for these two models was ranged from 3.6 % to 10.7 % for the experimental data.

Non-linear viscosity model:

$$\ln \ln(\mu) = [1.0 + b_1 T + b_2 (b_1 T)^2] e^{b_1 T} \quad \text{2-5}$$

Linear viscosity model:

$$\ln \ln(\mu) = C_2 lnT + C_2 \quad \text{2-6}$$

(Mehrotra and Svrcek, 1986) performed experiments to measure the effects of temperature and pressure on the properties of gas free Athabasca bitumen. They observed a significant increase in viscosity compared to the increase in density when bitumen was compressed under similar conditions. They also proposed new correlations for measuring the effects of temperature and pressure on viscosity by modifying the equation presented by (Khan et al., 1984) to include the pressure. They proposed the following two models:

$$\ln \mu = \exp[a_1 + a_2 \ln T] + a_3 P_g \quad \text{(Model I)} \quad \text{2-7}$$

$$\ln \ln(\mu) = [a_1 + a_2 \ln T] + a_3 P_g \quad \text{(Model II)} \quad \text{2-8}$$

where;

μ Dynamic viscosity (mPa.s)

T Temperature (K)

P_g Gauge pressure (MPa)

a_1, a_2, a_3 Empirical constants

The authors concluded that model II showed less deviation from the experimental results than model I.

(Mehrotra and Svrcek, 1987 a) measured the viscosity of four Alberta bitumens; Athabasca, Peace River, Marguerite Lake, and Wabasca by applying the theory of corresponding states over a wide range of temperatures. In this study, bitumens from these areas were characterized into two, three, and four pseudo components and the Kessler-Lee correlations were found to best characterize the pseudo components. The calculated viscosities of all four bitumens matched the viscosity data over 0.5 Pa.s. The correlations used were as follows:

$$f_{\alpha,o} = (\frac{Tc_a}{Tc_0})\theta_{a,o} \quad \text{2-9}$$

$$h_{a,o} = (\frac{\rho c_o}{\rho c_a})\phi_{a,o} \quad \text{2-10}$$

$$\emptyset_{a,o}(Tr_a, Vr_a, \omega) = [1 + (\omega_a - \omega_o)(a_2 Ap(V_{a^+} + b_2 Ap) + c_2 Ap(V_{a^+} + d_2 Ap) lnT_{a^+}]\frac{Z_{co}}{Z_{ca}} \quad \text{2-11}$$

$$T_{a^+} = \min[2, \max\ (T_{ra}, 0.5)] \quad \text{2-12}$$

$$V_{a^+} = \min\ [2, \max\ (V_{ra}, 0.5)] \quad \text{2-13}$$

$$\eta_x(\rho, T) = \eta_0[\rho h_{x,0}, \frac{T}{f_{x,o}}](\frac{M_x}{M_0})^{\frac{1}{2}} h_{x,o}{}^{\frac{-2}{3}} f_{x,o}{}^{\frac{-1}{3}} \quad \text{2-14}$$

$$h_{x,o} = \sum_{\alpha} \sum_{\beta} X_{\alpha} X_{\beta} h_{\alpha\beta,o} \qquad 2\text{-}15$$

$$\Gamma_{x,o} h_{x,o} = \sum_{\alpha} \sum_{\beta} X_{\alpha} X_{\beta} h_{\alpha\beta,o} T_{\alpha\beta,o} \qquad 2\text{-}16$$

$$f_{\alpha\beta,o} = (1 - k_{\alpha\beta})(f_{\alpha,o} f_{\beta,o})^{\frac{1}{l}} \qquad 2\text{-}17$$

$$h_{\alpha\beta,o} = \left(1 - l_{\alpha\beta}\right)\left(\frac{1}{2} h_{\alpha,o}{}^{\frac{1}{l}} + \frac{1}{2} h_{\beta,o}{}^{\frac{1}{l}}\right)^{3} \qquad 2\text{-}18$$

$$f_{x,o}{}^{\frac{1}{2}} M_{x}{}^{\frac{1}{2}} = h_{x,o} = \sum_{\alpha} \sum_{\beta} X_{\alpha} X_{\beta}\ h_{\alpha\beta,o}{}^{\frac{3}{4}} f_{\alpha\beta,o}{}^{\frac{3}{4}} M_{\alpha\beta,o}{}^{\frac{1}{2}} \qquad 2\text{-}19$$

where,

$T_{c,\,r}$	Critical, reduced temperature (K)
Θ	Energy shape factor
Φ	Size shape factor
ω	Pitzer's acentric factor
V	Molar Volume (m^3/kmol)
Ap	Multiplying factor
Z	Compressibility factor
h	Equivalent substance volume reducing ratio
Γ	Equivalent substance temperature reducing ratio
M	Molar mass (g/mol)
α,β	Components

a,b,c,d Constants

(Mehrotra and Svrcek, 1987 b) performed experiments on Cold Lake bitumen at different temperatures ranging from 37 to 115 °C and pressures from atmospheric to 10 MPa. They observed that Cold Lake bitumen, having less molecular mass, showed less increase in viscosity with increased pressure than the Athabasca River bitumen. The experimental viscosity data was correlated using two models derived in a previous study (Mehrotra and Svrcek, 1986) , model II produced a lower average absolute deviation than model I.

(Johnson et al., 1987) predicted the viscosity of gas-free and gas diluted Athabasca bitumen with the help of an extended corresponding states principle requiring only three parameters for each pseudo component of bitumen, the critical properties, acentric factor, and mole fraction. 1,2,3,4,5,6,7,8-octahydrophenanthrene was used as a reference material instead of methane resulting in higher accuracy predictions with a deviation of less than 6%. For heavier hydrocarbons, the authors modified the shape factor to obtain more accurate density predictions. The multiplication factor Ap for this reference fluid was found to be dependent on the critical pressure instead of the acentric factor. The bitumen viscosity predictions were more accurate when the bitumen was characterized into four components. The Teja-Rice mixing rule gave the best predictions and is outlined below:

$$T_{cm}V_{cm} = \sum_i \sum_j x_i x_j T_{cij} V_{cij} \qquad 2\text{-}20$$

$$V_{cm} = \sum_i \sum_j x_i x_j V_{cj} \qquad 2\text{-}21$$

$$\omega_m = \sum_i x_i \omega_i \qquad 2\text{-}22$$

$$M_m = \sum_i x_i M_i \qquad 2\text{-}23$$

$$T_{cij}V_{cij} = \Psi_{ij}(T_{ci}V_{ci}T_{cj}V_{cj})^{\frac{1}{2}} \quad 2\text{-}24$$

$$V_{cij} = \frac{1}{8}(V_{ci}^{\frac{1}{3}} + V_{cj}^{\frac{1}{3}})^3 \quad 2\text{-}25$$

where,

T_{ci} Critical temperature (K) of component i

T_{cm} Critical temperature (K) of mixture

V_{ci} Critical volume of component i

x Mole fraction

ω Pitzer's acentric factor

M Molecular weight

ψ Binary interaction parameter

i, j Components

(Mehrotra et al., 1989) measured the viscosity of Cold Lake bitumen at its five "cuts". Various viscometers (depending on the viscosity of "cuts") were used at several temperatures and pressures. The authors also conducted an elemental analysis of each of the samples. The experimental viscosity data was determined to be more correlated with the double-log correlation as shown below.

$$\log\log(\mu + 0.7) = b_1 + b_2 \log T \quad 2\text{-}26$$

where b_1, b_2 varied with the bitumen samples over a range of values. The values of b_1 for Cold Lake bitumen and 5 "cuts" were 9.1451, 11.6244, 11.2120, 10.4535, 10.1941 and 8.9592,

respectively. The values of b_2 were -3.4281, 4.7535, -4.4068, -3.9527, -3.8016 and -3.1573, respectively. The viscosity of the whole bitumen was predicted by the following correlation.

$$log(\mu_m + 0.7) = \sum_{i=1}^{n} \left[x_i \left(\frac{M_i}{M} \right)^{0.5} \right] \log(\mu_i + 0.7) \qquad 2\text{-}27$$

where, x_i is the mole fraction of component i, M is the molar mass, and μ is the dynamic viscosity in mPa.s. The average absolute deviation determined by comparing this equation with the measured data was 38%.

(Mehrotra, 1992) presented a one-parameter correlation to predict the effect of temperature on the viscosity of several liquid hydrocarbons and their mixtures. The presented equation was validated for 360 pure liquid hydrocarbons.

$$\log(\mu + 0.8) = \Theta\ (\Phi T)^b \qquad 2\text{-}28$$

where, μ is in mPa.s, **Θ** = 100, **Φ** =0.01, T is in Kelvin for pure hydrocarbons, and **Θ** = 160, **Φ** =0.008 for Canadian oil-sands. Following two mixing rules were introduced to calculate the viscosity of CO_2 diluted or toluene-diluted bitumen. Mixing rule I fit significantly better with the experimental results compared to mixing rule II.

$$\text{Mixing Rule I: } \log(\mu + 0.8) = \sum V_i\ \Theta\ (\Phi T)^b \qquad 2\text{-}29$$

$$\text{Mixing Rule II: } \log(\mu + 0.8) = \sum V_i\ \Theta\ (\Phi T)^b + \sum_i \sum_j v_i v_j B_{ij} \qquad 2\text{-}30$$

where, T is absolute temperature (K), b is single viscosity parameter, v is geometric mean of mass and mole fraction, and B_{ij} is binary viscous interaction term.

(Puttagunata et al., 1993) presented a correlation that includes the effects of combined pressures and temperatures on Canadian bitumen and heavy oil. The correlation was developed

using data from Svrcek's group and 570 data points of Alberta heavy oil and bitumens from Cold Lake, Athabasca, Cold Bailed Cold Lake bitumen, and Lloydminster. The predicted results were close to the experimental results for these bitumens, and the correlation produced average absolute deviations of 2.32%, 4.43%, 3.85% and 10.27%, respectively. The correlation is as follows:

$$\ln \mu = 2.30259 \left[\frac{b}{1+\frac{(T-30)}{303.15}} + C \right] + B_0 P exp(dt) \qquad 2\text{-}31$$

where, b is characterization coefficient and is given by

$$b = \log_{10} \mu_{30\,C} - C \qquad 2\text{-}32$$

$$C = -3.0020 \qquad 2\text{-}33$$

$$S = 0.0066940b + 3.53641 \qquad 2\text{-}34$$

$$B_o = 0.0047424b + 0.0081709 \qquad 2\text{-}35$$

$$d = -0.0015646b + 0.0061814 \qquad 2\text{-}36$$

(Miadonye et al., 1995) developed a correlation to predict the viscosity of bitumen with certain diluents. Among the diluents, the difference between the calculated and experimental viscosities for the bitumen-GCOS (Great Canadian Oil Sands) synthetic crude mixtures was small. This behaviour is reasonable due to the similar characteristics of bitumen and GCOS synthetic crude oil. The developed correlation showed an average absolute deviation of 8.7 % for the 300 experimental data points.

(Zhang et al., 2007) presented a viscosity temperature correlation after measuring the viscosity of samples of dead oils from the Liaohe basin in northeast China at various

temperatures between 40-90 °C at 10 °C intervals. The authors observed a relationship between the viscosity of the samples at 50 °C and their viscosities at other temperatures. The relationship is defined as:

$$\mu_T = a\mu_{50}{}^b \qquad 2\text{-}37$$

where

μ_T is viscosity in mPa.s,

T is in °C,

μ_{50} is viscosity at 50 °C ,

a and b are viscosity parameters

2.2 Experimental Findings and Modelling on Pure Solvents

(Allan and Teja, 1991) presented a new method for predicting the viscosity of liquid hydrocarbons and their mixtures. This method was based on the effective carbon number concept. The Vogel equation was found to fit the viscosity data of n-alkanes in the literature with an error of less than 10%. The authors also used a mixing rule to calculate the effective carbon number of the mixtures of hydrocarbons and showed that only the effective carbon number and composition of the mixture are required to calculate the viscosity of hydrocarbon mixtures. The Vogel equation is given as:

$$\ln \mu = A \left[\frac{-1}{B} + \frac{1}{T+C}\right] \qquad 2\text{-}38$$

where,

$$A = 145.73 + 99.01n + 0.83n^2 - 0.125n^3 \qquad 2\text{-}39$$

$$B = 30.48 + 34.01n - 1.23n^2 + 0.017n^3 \quad \text{2-40}$$

$$C = -3.01 - 1.99n \quad \text{2-41}$$

n is effective number of carbon atoms

In the same year, (Mehrotra, 1991) modified the Walther correlation to calculate and predict the viscosity of pure heavy hydrocarbons. The resulting one parameter equation depicts the relationship between viscosity and temperature and is defined by:

$$\log(\mu + 0.8) = 100(0.01T)^b \quad \text{2-42}$$

where

$$b = Bt_0 + \frac{Bt_1}{{T_b}^{10}} \quad \text{2-43}$$

The authors measured an average absolute deviation of less than 10 % for most of the compounds that they considered.

2.3 Studies on Bitumen-Solvent Systems

Current bitumen recovery technologies were outlined in the last chapter, however, their economic and environmental sustainability is limited. Techniques involving the use of solvents to reduce the viscosity of bitumen have proven more efficient for producing and transporting bitumen when compared with other techniques such as SAGD. This is largely because of the additional cost incurred by the generation of steam. Various experiments and correlations have been developed to measure the effects of various solvents on the properties of bitumen.

2.3.1 Experimental Findings for Gas Diluted Bitumen

(Jacobs et al., 1980) performed experiments to measure the effect of CO_2, N_2, and methane saturation on bitumen samples. They used a Contraves model DC 44 viscometer and a Kay-Ray model 7050B gamma ray densitometer. The bitumen was extracted from oil sand samples using toluene, which was subsequently evaporated using a rotary evaporator. In the CO_2 diluted bitumen samples, increased temperature and pressure resulted in a significant viscosity reduction. However, as the temperature exceeds 100 °C, the change in pressure no longer has a significant impact on viscosity. In the methane and nitrogen diluted bitumen samples, the impact of increased temperature and pressure on the viscosities of the samples was not as significant as it was in the CO_2 diluted bitumen, although both decreased the viscosities of the samples. The study found that N_2 was the least effective of the three gases studied.

(Svrcek and Mehrotra, 1982) measured variations in density, viscosity, and solubility of different gases (CO_2, CH_4, and N_2) in Athabasca bitumen at different temperatures and pressures. The authors determined that CO_2 diluted bitumen produced greater viscosity reduction than other gases at similar pressures and temperature. Saturating N_2 in bitumen produced very small or negligible effects with temperature and pressure on bitumen viscosity. Pressure increase was found to be more significant on the reduction of methane diluted bitumen density.

(Mehrotra and Svrcek, 1984) measured the effects of temperature and pressure on CO_2 solubility, density, and viscosity for Marguerite Lake bitumen samples. They used a Contraves DC44 viscometer in their experiments and covered the bitumen sample with a N_2 cloud in order to minimize the interaction between the bitumen and atmospheric oxygen. As described earlier, N_2 has a minimal effect on viscosity reduction. The Marguerite Lake bitumen was less viscous than Athabasca bitumen and had a greater difference between the experimental and calculated

viscosities. The researchers observed a reduction in viscosity with increased pressure at all isotherms. The viscosity reduction curve was steeper in the low temperature regions than the high temperature regions. The viscosity reduction at the 12 $^{\circ}$C isotherm was significant up to 4.5 MPa and after which the viscosity reduction curve becomes flat, due to the interaction between liquid CO_2 and the bitumen. The density of bitumen sample decreased as the temperature increased at constant pressure but there was no definite trend for density with pressure at all temperatures. They measured an increase in solubility of CO_2 in bitumen with pressure at all temperatures and a decreasing solubility trend with increasing temperature.

(Mehrotra and Svrcek, 1985 a) determined the effects on the density and viscosity of Athabasca bitumen diluted with CO and ethane. The bitumen sample was extracted using toluene, which was then removed using vacuum distillation. They measured the viscosity reduction of dead bitumen with increasing temperature. The Mehrotra and Svrcek results differed from those measured by (Jacobs et al., 1980) in low temperature regions but were similar at higher temperatures. The reduction in viscosity for CO diluted bitumen when pressure was increased was greater than that of CH_4 diluted bitumen and less than that of N_2 diluted bitumen. A decreasing trend in the solubility of CO in bitumen with increased temperature was measured for all pressures. At constant temperature, increasing the pressure resulted in an increase in solubility that was double that of N_2 diluted bitumen at similar conditions.

For CO diluted bitumen, a slight increase in density was measured with increasing pressure and similar behaviour was observed for the average densities with increasing temperature as found with the CO_2, N_2, and CH_4 diluted samples (Svrcek and Mehrotra, 1982). When the pressure of C_2H_6 diluted bitumen was increased at all temperatures, the reduction in viscosity was much more significant than was seen in the CO_2 diluted samples at similar conditions. A

similar trend was found when the temperature was increased. The solubility of ethane was greater than that of CO_2 in bitumen at the same conditions and the reduction in density was quite large when pressure and temperature were increased.

(Mehrotra and Svrcek, 1985 b) measured the viscosity, density, and solubility of gases (N_2, CO, CH_4, CO_2, C_2H_6) in Peace River bitumen. The bitumen samples were extracted using a hot water process and then filtered to remove any sand particles. The study found that the viscosity of Peace River bitumen was higher than that of Athabasca bitumen. Similar viscosity reduction behaviour was seen for both N_2 diluted Peace River and Athabasca River bitumen with increasing pressure at all temperatures. At the lower isotherm, increasing pressure resulted in high solubility of N_2 in bitumen but the solubility values were closer to each other at the higher isotherms. Increasing the pressure did not greatly influence the density but did reduce the average density. For the CO diluted bitumen samples, very little reduction in viscosity was measured with increasing pressure at all temperatures. A significant increase in solubility was measured with increased pressure compared to increased temperature, which showed no effect on solubility.

The CH_4 diluted samples experienced a greater reduction in viscosity at lower isotherms when the pressure was increased. In the lower pressure regions, the methane solubility values were close to each other at different temperatures but as the pressure increased, the solubility also increased and the bitumen density decreased with increasing temperature as well as pressure. The CO_2 diluted bitumen showed a significant viscosity reduction at low temperatures with increasing pressure. The solubility of the sample increased linearly with pressure and CO_2 was more soluble than N_2, CO, and CH_4 diluted bitumen at similar conditions. The density of the sample decreased when the temperature was increased. Ethane diluted bitumen showed dramatic

viscosity reduction with increased pressure in the low temperature regions. However, as the temperature and pressure were increased, the viscosity curve became less steep. The solubility of ethane in bitumen increased significantly with increased pressure at various temperatures. The measured density values showed pressure dependence.

(Mehrotra and Svrcek, 1985 c) went on to measure the same properties from their preceding experiments (Mehrotra and Svrcek, 1985 a, 1985 b) for Wabasca bitumen. The density and viscosity of the dead bitumen was less than that of the bitumen samples from Athabasca and Peace River. Similar behaviour, for density reduction with increasing pressure and temperature was measured for both live (diluted with N_2, CO, CH_4, CO_2, C_2H_6) and dead bitumens. The viscosity reduction for the N_2 diluted sample was greater when the temperature was increased and was less dependent on increasing pressure at all temperatures. Increasing the temperature resulted in a very small decrease in solubility but the influence of increasing pressure was quite significant. The viscosity of the CO diluted samples was not significantly affected by increasing pressure but was considerably reduced when the temperature of the sample was increased. The solubility of the CO diluted sample in bitumen increased with pressure.

In the methane diluted bitumen sample, the reduction in viscosity was measured as the pressure was increased and the resulting reduction curve was steeper at lower isotherms. The solubility of Wabasca River bitumen was greater than that of Athabasca River bitumen and at low pressure the effect of increasing temperature on solubility was small compared to the increase in pressure. The viscosity reduction curve was steeper for CO_2 diluted bitumen at lower isotherms with increase in pressure. The solubility-pressure curve was linear and the CO_2 was more soluble in the Wabasca bitumen than the Athabasca and Peace River bitumen. Increasing the pressure decreased the viscosity and increased the solubility of the ethane. The key results of

the experiments (Mehrotra and Svrcek, 1985 b, 1985 c) demonstrated that the properties of bitumen are dependent on the quantities of ethane and bitumen.

(Mehrotra and Svrcek, 1988) measured the effects of temperature and pressure change on viscosity, density, and gas solubility of Cold Lake bitumen. Their focus was determining the properties of bitumen diluted with gas mixtures (methane rich and CO_2 rich). Increasing the temperature resulted in a similar reduction in viscosity for gas free Cold Lake and Marguerite Lake bitumen and their average densities were found to decrease linearly with temperature. Mehrotra and Svrcek studied the properties of Cold Lake bitumen diluted with various gases (N_2, CH_4, CO_2, and C_2H_6) and found similar behaviour to that found in previous studies. The methane rich bitumen sample exhibited viscosity behaviour with increased pressure similar to that of the CO_2 diluted bitumen due to the greater solubility of CO_2. The density-temperature relationship for the gas free and CH_4 rich samples were similar but the density values were lower for the latter cases. Increasing pressure resulted in higher viscosity reductions at the lower isotherm for the CO_2 rich diluted bitumen but the effect of increased pressure was significantly less on viscosity and gas solubility.

2.3.2 Correlations Developed for Bitumen Solvent Systems

(Shu, 1984) developed a correlation for calculating the viscosity of Cold Lake bitumen-solvent samples and showed excellent results with the experimental values. The correlation proved to be more applicable for determining the viscosity of mixtures with high viscosities. The key feature of this correlation in determining mixture viscosity is that it requires only the density and viscosities of the components forming mixtures. The applicability of this correlation is limited to systems in which blending results in asphaltene precipitation. The correlation is as follows (equation 1-4):

$$\ln \mu = x_A \ln \mu_A + x_B \ln \mu_B \quad \text{2-44}$$

$$x_A = \frac{\alpha V_A}{\alpha V_A + V_B} \quad \text{2-45}$$

$$x_B = 1 - x_A \quad \text{2-46}$$

$$\alpha = \frac{17.04 \Delta p^{0.5237} {p_A}^{3.2745} {p_B}^{1.6316}}{\ln\left(\frac{\mu_A}{\mu_B}\right)} \quad \text{2-47}$$

where, μ is the dynamic viscosity (mPa.s), v_A is the volume fraction of component A, and ρ_A is the density of component A.

(Mehrotra, 1990) also developed a model for determining the viscosity of fractions of Cold Lake bitumen and toluene. Different approaches were used to determine the viscosity of toluene-diluted bitumen based on the number of pseudo-components in the bitumen.

(Miadonye et al., 2000) developed a correlation for the viscosity of bitumen-diluents mixtures. The solvent mass fraction relationship with mixture viscosity was also considered and is described by the following equation.

$$V_m = \exp\{\exp[a(1 - {X_D}^n)] + \ln V_D - 1\} \quad \text{2-48}$$

where,

$$a = \ln(\ln v_B - ln\, v_D + 1) \quad \text{2-49}$$

$$n = \frac{V_D}{0.1351 + 0.9029 V_D} \quad \text{2-50}$$

(Wen and Kantzas, 2006) measured the experimental viscosity data for four different bitumens with six solvents in different fractions. They compared the experimental values with the predicted viscosity values using four models. The regression model was only effective for

specific heavy oil-solvent systems. The Cragoe model produced good results only when lighter oil was used. The difference between the experimental and predicted viscosities was very small with the low field nuclear magnetic resonance relaxometer (NMR) compared to the Shu and Cragoe models. However, the results of the Shu model were superior to those of the Cragoe model.

2.3.3 Experimental Findings for Solvent Diluted Bitumen

(Badamchi-zadeh et al., 2009 a) determined the density and viscosity of mixtures of propane and bitumen at various temperatures, pressures, and mass fractions of propane. A considerable reduction in the density and viscosity of bitumen was measured by adding propane but this viscosity reduction at reservoir conditions was smaller than that achieved in other thermal recovery processes. It was concluded that an additional heat source should be employed in the reservoir along with addition of propane in order to achieve a greater viscosity reduction. There was a risk of asphaltene precipitation when propane was used. However, another study (Badamchi-zadeh et al., 2009 b) by the same authors showed less asphaltene precipitation with mixtures of CO_2, propane, and bitumen.

(Kariznovi et al., 2010) performed a different test using new experimental equipment to study the phase behaviour and density of various bitumen-solvent systems. The authors compared the applicability and limitations of the new apparatus to the previous apparatus. They concluded that the capacity of the new apparatus to detect and measure the properties of different phases and phase behaviour of simple tertiary and binary fluids such as bitumen-propane validated the new equipment. It was also determined that bitumen viscosity was the key factor in determining the equilibration time; the higher the viscosity, the greater the equilibration time.

(Kariznovi et al., 2011) measured the solubility of propane in bitumen and found that the solubility of the propane increased with increasing pressure. This effect was greater at lower temperatures than at higher temperatures. The increase in propane solubility resulted in a decrease in the viscosity of the diluted bitumen. The authors compared the experimental results (which included six pseudo-components) with the calculated values for bitumen-solvent phase behaviour and concluded that due to the very small difference in values, these six pseudo-components best depict bitumen phase behaviour.

(Kariznovi et al., 2012) also measured the density and viscosity for two systems of methane diluted and ethane diluted bitumen using the same equipment used in the previous experimental study (Kariznovi et al., 2011). In the methane diluted bitumen systems, a linear relationship between viscosity and density with pressure was observed at all temperatures but for ethane diluted bitumen the linear relationship was only found at a few temperatures. They also measured a considerable reduction in the density of the ethane-diluted system at 50 °C due to the higher solubility at these conditions.

(Guan et al., 2013) measured the viscosity and density of xylene and toluene diluted Athabasca bitumen at different temperatures, pressures, and individual solvent concentrations using a new apparatus. The experimental values of the pure solvent viscosities were fitted with the correlation as follows;

$$\ln \mu = a + \frac{b}{T} \qquad \text{2-51}$$

where;

μ Viscosity (mPa.s)

a, b Correlation coefficients (different for each solvent)

T Temperature (K)

Similarly, the equations presented by Mehrotra and Svrcek were used to fit the bitumen viscosity values. The mixture densities for both solvents increased linearly with pressure at all temperatures. The following equation best represents the experimental data based on the assumption that no volume change occurs after mixing.

$$p_m = \frac{1}{\left(\frac{w_S}{p_S} + \frac{1-w_S}{p_B}\right)} \qquad 2\text{-}52$$

where;

w_s Mass fraction solvents

p_m,p_S,p_B Density of mixture, solvents and bitumen, respectively

They measured a significant impact of pressure on the viscosity of the mixture at low solvent mass fractions.

A later study by (Nourozieh et al., 2013) used the same experimental procedure as (Guan et al., 2013) to determine the density and viscosity of solvent-bitumen mixture. In this study, n-decane was used as a solvent to dilute the Athabasca bitumen. The concentration of n-decane used in the experiments was below its critical value in order to prevent the bitumen from becoming unstable and to prevent asphaltene precipitation. They measured a linear reduction in the density of n-decane diluted bitumen with mass fraction of n-decane and a non-linear density reduction with its mole fractions for all temperatures and pressures. The mixture viscosity increased linearly (especially at low concentrations) with pressure and decreased linearly with mole fraction (non-linear reduction with mass fractions) of n-decane.

Chapter 3 Experimental Procedure and Apparatus

3.1 Experimental Apparatus

The physical properties of raw bitumen and its mixtures with liquid solvents were measured using an apparatus consisting of a viscometer, density measuring cell, reciprocating pump, vacuum pump, temperature controlled oven, pressure transducer, feeding cell, toluene storage cell, and data acquisition equipment. The viscometer has various pistons, which were used depending on the viscosity range of the system under consideration. The pump can be operated at two different conditions at either constant flow rate or constant pressure depending on the requirements of the system. Figure 3-1 is a schematic diagram of the apparatus.

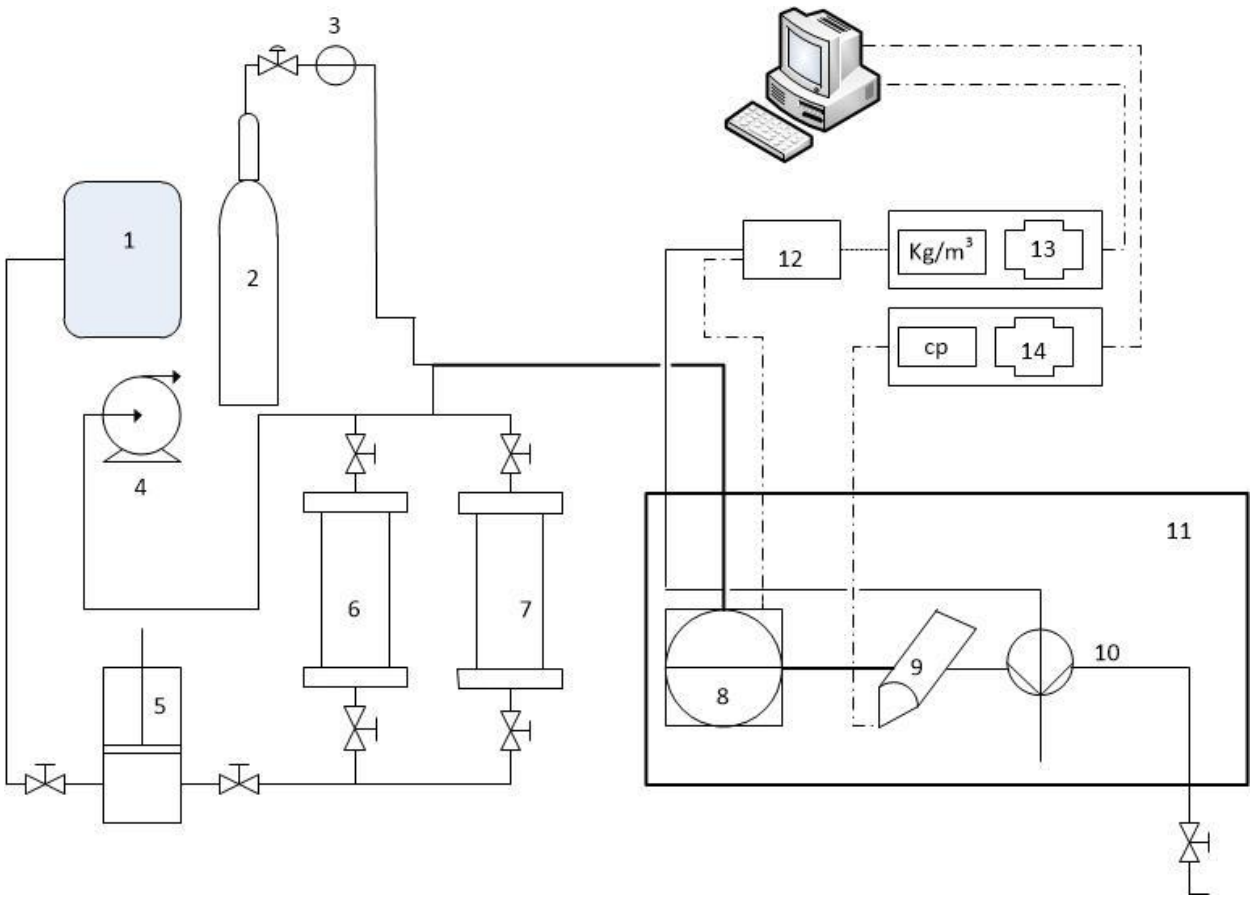

Figure 3-1: Experimental apparatus schematic diagram: (1) water storage tank, (2) nitrogen cylinder, (3) pressure gauge, (4) vacuum pump, (5) reciprocating pump, (6) sampling cell, (7) toluene cell, (8) density measuring cell, (9) viscometer, (10) pressure transducer, (11) temperature controlled oven, (12) interface module, (13) density evaluation unit, and (14) Viscopro 2000 unit.

3.1.1 Density Measuring Cell

The density-measuring cell DMA HPM is commonly used to measure the density of high viscosity fluids like bitumen, petrochemical residues, and polymers at high temperatures up to 200 °C and pressures up to 140 MPa. The density of bitumen or heavy oil at different pressures and temperatures can be measured and displayed when this cell is combined with the evaluation unit mPDS 2000V3. The features of the DHA HPM density-measuring cell can also be changed using this evaluation unit. The general features of the DMA HPM cell are presented in Table 3-1.

Table 3-1: Features of the density-measuring cell DMA HPM.

Density Measuring Range	0 to 3 g/cm^3
Temperature Range	263.15 to 473.15 K
Density Error	1 x 10^{-3} to 1 x 10^{-4} g/cm^3
Pressure Range	0 to 140 x 10^3 kPa
Density Resolution	1 x 10^{-5} g/cm^3
Sample Fluid Volume	2 mL

The density-measuring cell is based on the period of harmonic oscillation of the fluid under consideration, which vibrates in the U-shaped tube at a specific characteristic electronic frequency. The density of the sample can be exactly determined by measuring the characteristic frequency.

3.1.2 Cambridge Viscometer

A Cambridge viscometer was used to measure the viscosity of all of the samples of toluene, hexane, and bitumen. The viscometer consists of a solid piston that moves through the sample in the cylindrical chamber. The length of the travelling time of the piston determines the viscosity of the sample. The Cambridge viscometer also consists of platinum Resistance Temperature Detector (RTD) and two electronic coils. Once the sample is forced into the cylindrical chamber, the electronic coils move the magnetic piston back and forth and the longer the travelling time of the piston the greater the viscosity of the fluid.

This study involved both extremely light fluids and very heavy fluids so different pistons were used to accurately measure their viscosities. Each piston has a specific length and viscosity measuring range.

Table 3-2: VISCO Pro 2000 Specifications.

Sensor Model	Spc-372
Maximum Temperature	463.15 K
Maximum Recommended Pressure	1000 Psi
Electronics Model	BCC-323
Viscosity Accuracy	± 1.0 %

3.2 Experimental Procedure

The first step was cleaning the experimental apparatus by injecting toluene using the pump. Next, nitrogen was blown into the system to pump toluene and potential contaminants out of the system. This was followed by the removal of any remaining contaminants or toluene using a vacuum pump. The sample was prepared by mixing 300 g of bitumen with the desired mass of solvent using a Sartorius balance. The addition of the solvent was completed in several steps to ensure a more homogenous mixture. After the sample was prepared, it was transferred to the feeding cell and allowed to stabilize for 12 hours. The sample was then injected into the system at a flow rate of 7 ml/min for physical properties measurement at the desired temperature and pressure.

3.3 Evaluation of Calibration

3.3.1 Densitometer Calibration Evaluation

In this experimental study, a previously calibrated experimental apparatus was used to measure the densities of several fluids at different pressures and temperatures. The apparatus was shut down for several months before the start of this study so the density of pure toluene and hexane were measured along with the n-decane/bitumen system to evaluate the calibration of the density-measuring cell. The density results from this system were compared with the results

obtained from the (National Institute of Standards and Technology) for pure toluene and hexane. The results of bitumen/n-decane were compared with those obtained by (Nourozieh et al., 2013), as the same apparatus was used in their study.

The densities of toluene were determined from ambient temperature to 333 K over a pressure range of 1 to 10 MPa. Since pressure did not have a significant effect on the properties of the pure solvent, measurements were taken at 2 MPa pressure intervals. A comparison of the experimental results and densities of toluene and the densities taken from the NIST Web Book are presented in Table 3-3 and Figure 3-2. The symbols and solid lines represent the measured experimental and NIST densities, respectively

Table 3-3: Experimental measured and NIST density data comparison for pure toluene as a function of temperatures (T) and pressures (P).

Toluene				
Temperature (K)	**Pressure (MPa)**	**Measured Density (kg/m^3)**	**NIST Density (kg/m^3)**	**Error (%)**
297.9	1.002	864.3	863.3	0.1157
297.8	3.001	866.0	864.8	0.1386
297.8	5.004	867.6	866.4	0.1383
297.7	7.004	869.1	867.9	0.1381
297.7	10.004	871.4	870.1	0.1492
303.6	1.005	857.9	857.9	0.0000
303.6	3.005	859.6	859.5	0.0116
303.6	5.001	861.3	861.1	0.0232
303.6	7.004	862.9	862.6	0.0348
303.6	10.004	865.1	864.9	0.0231

318.5	1.003	843.0	843.9	0.1068
318.6	3.000	844.9	845.7	0.0947
318.5	5.004	846.7	847.5	0.0945
318.5	7.004	848.4	849.2	0.0943
318.5	10.004	850.8	851.6	0.0940
333.2	1.005	829.3	829.9	0.0724
333.3	3.003	831.4	831.9	0.0601
333.3	5.0045	833.3	833.8	0.0600
333.3	7.0044	835.2	835.6	0.0479
333.3	10.0047	837.9	838.4	0.0597

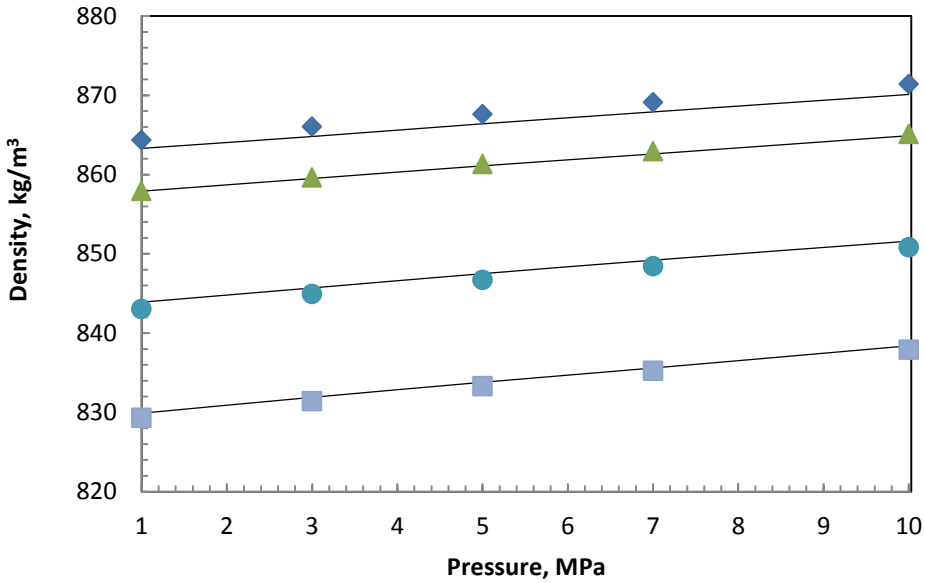

Figure 3-2: Density of pure toluene versus pressure, P, at different temperature, T; ■,●,▲,♦, measured densities; ■, T = 333.3 K; ●, T=318.5 K; ▲, T = 303.6 K, ♦, T = 297.8 K; − , NIST density data.

The density of pure hexane was also measured at room temperature over a pressure range of 1 to 10 MPa. A comparison of the experimental density data for hexane and the data taken from the NIST Web Book is presented in Table 3-4. The percent error in the case of hexane was

greater than the percent error in the case of toluene. This might have occurred if the experimental system was not clean enough. The densities of the pure solvents are very sensitive to impurities in the apparatus.

Table 3-4: Comparison of experimental measured and NIST density data for pure hexane as a function of temperatures, (T) and pressures (P).

Hexane				
Temperature (K)	**Pressure (MPa)**	**Measured Density (kg/m^3)**	**NIST Density (kg/m^3)**	**Error (%)**
297.4	1.001	658.0	656.50	0.2280
297.4	3.004	660.2	658.73	0.2227
297.4	5.005	662.4	660.89	0.2280
297.3	7.004	664.4	662.98	0.2137
297.3	10.004	667.4	666.02	0.2068

The density of the binary mixture of n-decane and bitumen was measured at ten pressures and five temperatures. This experimental study also considered the effect of solvent concentration on the properties of the binary mixture. Four different samples, consisting of 35, 40, 45, and 50 wt% of hexane with the remaining bitumen were prepared to evaluate the calibration of the densitometer. (Nourozieh et al., 2013) conducted the same experiments for an n-decane/bitumen binary system using the same experimental apparatus. Comparing the data obtained from this study with that of (Nourozieh et al., 2013)showed that the experimental apparatus is well calibrated. The experimental density results for the n-decane/bitumen system at different pressure and temperature conditions with n-decane mass compositions of 35%, 40%, 45% and 50 % are presented in Tables 3-5 to 3-8.

Table 3-5: Experimental measured density data of MacKay River bitumen/n-decane mixture as a function of temperatures (T) and pressures (P) at a constant mass fraction of n-decane (w_s = 0.35) in the binary mixture.

$W_S = 0.35$

P (MPa)	T (K)	ρ_m (kg/m^3)	P (MPa)	T (K)	ρ_m (kg/m^3)	P (MPa)	T (K)	ρ_m (kg/m^3)
1.002	333.2	864.9	4.003	313.3	880.6	7.004	296.1	896.5
1.002	323.5	871.6	4.003	303.1	888.7	8.001	333.2	870.4
1.002	313.3	878.5	4.003	296.2	894.6	8.001	323.5	876.5
1.002	303.1	886.8	5.005	333.3	868.0	8.001	313.4	883.2
1.002	296.5	892.6	5.005	323.5	874.5	8.001	303.1	891.3
2.005	333.2	865.7	5.005	313.3	881.3	8.001	296.1	897.1
2.005	323.5	872.3	5.005	303.1	889.4	9.003	333.2	871.0
2.005	313.3	879.2	5.005	296.3	895.1	9.003	323.5	877.2
2.005	303.1	887.4	6.000	333.3	868.8	9.003	313.4	883.8
2.005	296.4	893.3	6.000	323.5	875.2	9.003	303.1	891.9
3.003	333.2	866.6	6.000	313.4	881.9	9.003	296.2	897.6
3.003	323.5	873.0	6.000	303.1	890.0	10.003	333.2	871.7
3.003	313.3	879.9	6.000	296.2	895.9	10.003	323.5	877.8
3.003	303.1	888.1	7.004	333.2	869.6	10.003	313.4	884.5
3.003	296.2	894.0	7.004	323.5	875.8	10.003	303.1	892.5
4.003	333.2	867.2	7.004	313.4	882.6	10.003	296.2	898.2
4.003	323.5	873.8	7.004	303.1	890.6			

Table 3-6: Experimental measured density data of MacKay River bitumen/n-decane mixture as a function of temperatures (T) and pressures (P) at a constant mass fraction of n-decane (w_s = 0.40) in the binary mixture.

$W_S = 0.40$

P (MPa)	T (K)	ρ_m (kg/m^3)	P (MPa)	T (K)	ρ_m (kg/m^3)	P (MPa)	T (K)	ρ_m (kg/m^3)
1.004	333.4	849.4	4.005	313.3	865.2	7.004	297.6	880.1
1.004	323.5	855.9	4.005	303.2	874.0	8.004	333.4	854.8
1.004	313.2	862.6	4.005	297.4	878.3	8.004	323.5	860.8
1.004	303.1	872.0	5.005	333.4	852.5	8.004	313.2	867.9
1.004	297.3	876.3	5.005	323.5	858.7	8.004	303.2	876.6
2.001	333.4	850.1	5.005	313.3	866.0	8.004	297.6	880.7
2.001	323.5	856.6	5.005	303.2	874.6	9.005	333.4	855.4
2.001	313.3	863.7	5.005	297.5	878.9	9.005	323.5	861.6
2.001	303.1	872.7	6.001	333.4	853.2	9.005	313.3	868.5
2.001	297.3	877.0	6.001	323.5	859.4	9.005	303.2	877.2
3.003	333.4	850.9	6.001	313.3	866.6	9.005	297.6	881.3
3.003	323.5	857.3	6.001	303.2	875.3	10.005	333.4	856.2
3.003	313.3	864.3	6.001	297.5	879.5	10.005	323.5	862.2
3.003	303.1	873.3	7.004	333.4	853.9	10.005	313.3	869.2
3.003	297.4	877.6	7.004	323.5	860.2	10.005	303.2	877.8
4.005	333.4	851.7	7.004	313.3	867.3	10.005	297.7	881.8
4.005	323.5	858.1	7.004	303.2	875.9			

Table 3-7: Experimental measured density data of MacKay River bitumen/n-decane mixture as a function of temperatures (T) and pressures (P) at a constant mass fraction of n-decane (w_s = 0.45) in the binary mixture.

$W_S = 0.45$

P (MPa)	T (K)	ρ_m (kg/m^3)	P (MPa)	T (K)	ρ_m (kg/m^3)	P (MPa)	T (K)	ρ_m (kg/m^3)
1.004	333.5	834.9	4.005	313.5	851.0	7.004	297.2	866.2
1.004	323.6	841.6	4.005	303.3	860.0	8.004	333.4	840.3
1.004	313.5	848.8	4.005	297.3	864.2	8.004	323.8	846.7
1.004	303.3	857.9	5.005	333.5	838.0	8.004	313.5	853.9
1.004	297.2	862.1	5.005	323.7	844.6	8.004	303.3	862.7
2.001	333.5	835.7	5.005	313.5	851.7	8.004	297.2	866.7
2.001	323.6	842.4	5.005	303.3	860.7	9.005	333.5	840.9
2.001	313.5	849.6	5.005	297.2	864.9	9.005	323.8	847.4
2.001	303.3	858.6	6.001	333.5	838.7	9.005	313.6	854.6
2.001	297.3	862.8	6.001	323.8	845.2	9.005	303.3	863.3
3.003	333.5	836.5	6.001	313.5	852.5	9.005	297.3	867.3
3.003	323.7	843.1	6.001	303.3	861.4	10.005	333.4	841.7
3.003	313.5	850.4	6.001	297.2	865.6	10.005	323.8	848.0
3.003	303.3	859.3	7.004	333.5	839.5	10.005	313.6	855.2
3.003	297.3	863.4	7.004	323.8	846.0	10.005	303.3	863.9
4.005	333.5	837.3	7.004	313.5	853.2	10.005	297.4	867.9
4.005	323.7	843.8	7.004	303.3	862.0			

Table 3-8: Experimental measured density data of MacKay River bitumen/n-decane mixture as a function of temperature (T) and pressure (P) at a constant mass fraction of n-decane (w_s = 0. 50) in the binary mixture.

$W_S = 0.50$

P (MPa)	T (K)	ρ_m (kg/m^3)	P (MPa)	T (K)	ρ_m (kg/m^3)	P (MPa)	T (K)	ρ_m (kg/m^3)
1.006	333.5	820.7	4.005	313.6	836.8	7.004	297.2	852.5
1.006	323.2	827.8	4.005	303.3	846.2	8.004	333.5	826.3
1.006	313.6	834.6	4.005	297.2	850.5	8.004	323.2	833.1
1.006	303.2	844.1	5.005	333.5	823.9	8.004	313.6	839.6
1.006	297.0	848.5	5.005	323.2	830.9	8.004	303.3	848.9
2.004	333.5	821.5	5.005	313.6	837.5	8.004	297.2	853.1
2.004	323.2	828.6	5.005	303.3	846.9	9.004	333.5	827.1
2.004	313.6	835.4	5.005	297.2	851.2	9.004	323.2	833.8
2.004	303.2	844.9	6.001	333.5	824.7	9.004	313.6	840.3
2.004	297.1	849.2	6.001	323.2	831.6	9.004	303.3	849.6
3.003	333.4	822.4	6.001	313.6	838.2	9.004	297.2	853.7
3.003	323.2	829.4	6.001	303.3	847.6	10.004	333.5	827.8
3.003	313.6	836.1	6.001	297.2	851.8	10.004	323.3	834.5
3.003	303.2	845.5	7.004	333.4	825.5	10.004	313.6	840.9
3.003	297.1	849.8	7.004	323.2	832.3	10.004	303.2	850.2
4.005	333.4	823.2	7.004	313.6	838.9	10.004	297.2	854.4
4.005	323.2	830.1	7.004	303.3	848.3			

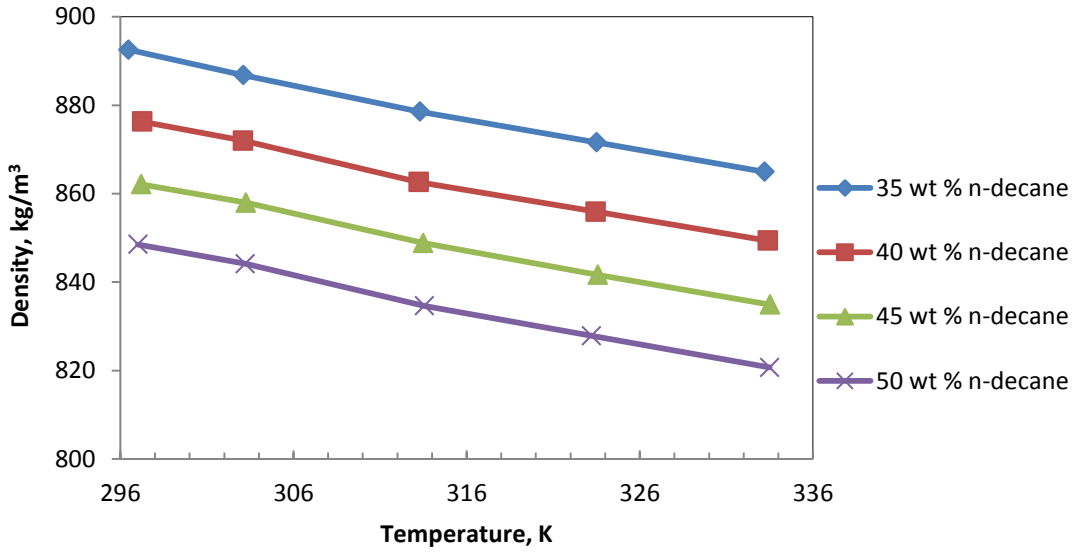

Figure 3-3: Density variation of bitumen/n-decane system with temperature, at different mass fractions of n-decane and at a constant pressure of 1 MPa.

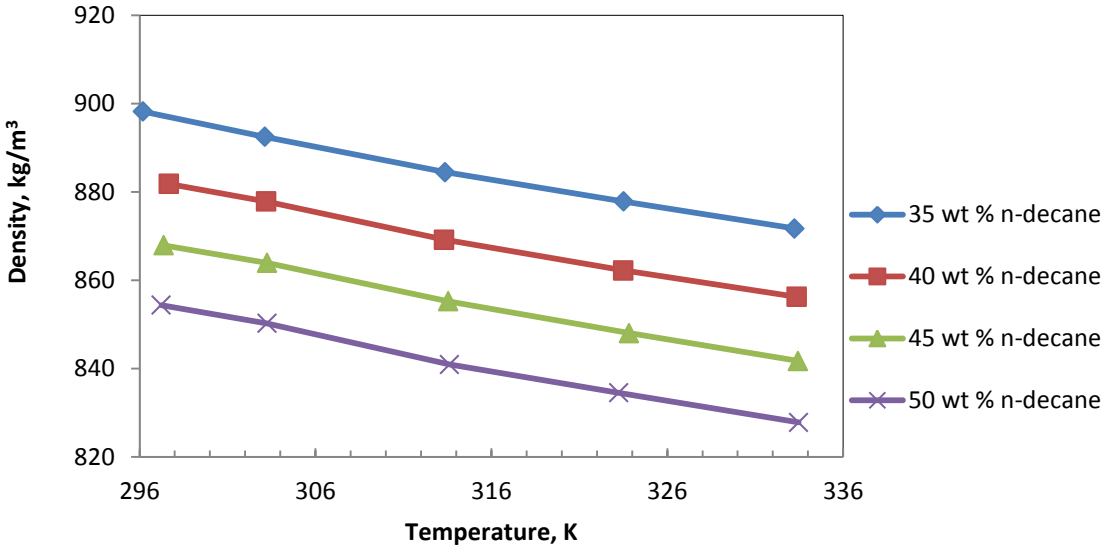

Figure 3-4: Density variation of bitumen/n-decane system with temperature, at different mass fractions of n-decane and at a constant pressure of 10 MPa.

3.3.2 Viscometer Calibration Evaluation

The viscosities of the various mixtures were measured at several temperatures and pressures using the viscometer. In this study, we used the same chemicals as were used in the densitometer calibration evaluation. The viscosities of hexane were determined from ambient temperature to 333.1 K over a pressure range of 1 to 10 MPa. The experimental results were compared with the viscosities of hexane from the NIST Web Book. A comparison of the results is presented in Table 3-9. A comparison of the viscosity data for toluene could not be performed because toluene viscosity data is not available in the NIST Web Book. The viscosity data for the n-decane diluted bitumen system was also measured using the same viscometer. The results obtained in this study are well matched with those obtained by (Nourozieh et al., 2013). The viscosity results for the n-decane diluted bitumen are presented in Tables 3-10 to 3-13 for 35, 40, 45 and 50 wt%, respectively.

Table 3-9: Comparison of experimental measured and NIST viscosity data for pure hexane as a function of temperature (T) and pressure (P).

Temperature (K)	**Hexane**			
	Pressure (MPa)	**Viscosity (cp)**	**NIST (cp)**	**Error (%)**
301.08	1.003	0.285	0.291	2.1
	3.002	0.281	0.300	6.8
	5.003	0.287	0.309	7.7
	7.004	0.293	0.318	8.5
	10.004	0.300	0.331	10.3

Table 3-10: Experimental viscosity data for a MacKay River bitumen/n-decane mixture as a function of temperature (T) and pressure (P) at a constant mass fraction of n-decane (w_s = 0.35) in the binary mixture.

$W_S = 0.35$

P (MPa)	T (K)	μ_m (cp)	P (MPa)	T (K)	μ_m (cp)	P (MPa)	T (K)	μ_m (cp)
1.002	344.2	8.64	4.003	321.3	20.07	7.004	301.1	52.29
1.002	333.0	12.37	4.003	311.8	29.17	8.001	344.2	9.90
1.002	321.2	18.94	4.003	301.1	48.78	8.001	333.0	14.17
1.002	311.8	27.58	5.005	344.3	9.33	8.001	321.3	21.73
1.002	301.2	45.75	5.005	333.0	13.32	8.001	311.8	31.60
2.005	344.3	8.72	5.005	321.3	20.48	8.001	301.1	53.46
2.005	333.0	12.60	5.005	311.8	29.73	9.003	344.2	10.18
2.005	321.2	19.26	5.005	301.4	49.28	9.003	333.0	14.52
2.005	311.9	28.10	6.000	344.2	9.49	9.003	321.3	22.22
2.005	301.1	46.73	6.000	333.0	13.62	9.003	311.8	32.62
3.003	344.4	8.88	6.000	321.3	20.87	9.003	301.2	54.89
3.003	333.0	12.85	6.000	311.8	30.39	10.003	344.2	10.42
3.003	321.3	19.68	6.000	301.1	50.99	10.003	333.0	14.89
3.003	311.8	28.54	7.004	344.2	9.66	10.003	321.3	22.77
3.003	300.9	48.05	7.004	333.0	13.91	10.003	311.8	33.40
4.003	344.3	9.13	7.004	321.3	21.28	10.003	301.3	56.07
4.003	333.0	13.06	7.004	311.8	30.88			

Table 3-11: Experimental measured viscosity data for a MacKay River bitumen/n-decane mixture as a function of temperature (T) and pressure (P) at a constant mass fraction of n-decane (w_s = 0.40) in the binary mixture.

$W_S = 0.40$

P (MPa)	T (K)	μ_m (cp)	P (MPa)	T (K)	μ_m (cp)	P (MPa)	T (K)	μ_m (cp)
1.002	344.1	5.47	4.003	321.3	11.88	7.004	302.8	25.34
1.002	332.7	7.78	4.003	312.0	16.44	8.001	344.0	6.15
1.002	321.5	11.26	4.003	302.6	24.12	8.001	332.8	8.76
1.002	311.9	15.73	5.005	344.0	5.88	8.001	321.1	12.82
1.002	302.2	23.49	5.005	332.9	8.24	8.001	312.0	17.81
2.005	344.2	5.52	5.005	321.0	12.22	8.001	302.8	25.93
2.005	332.8	7.86	5.005	312.0	16.70	9.003	344.5	6.17
2.005	321.5	11.42	5.005	302.7	24.34	9.003	332.6	9.01
2.005	311.9	15.92	6.000	344.0	5.90	9.003	321.4	12.98
2.005	302.5	23.56	6.000	332.7	8.44	9.003	312.0	18.22
3.003	344.2	5.63	6.000	321.2	12.36	9.003	302.8	26.37
3.003	332.7	8.00	6.000	312.0	17.02	10.003	343.7	6.50
3.003	321.2	11.68	6.000	302.7	24.84	10.003	332.8	9.14
3.003	312.0	16.19	7.004	344.4	5.95	10.003	321.1	13.39
3.003	302.5	23.85	7.004	332.6	8.64	10.003	312.0	18.63
4.003	344.0	5.77	7.004	321.1	12.64	10.003	302.9	26.92
4.003	332.7	8.14	7.004	312.0	17.43			

Table 3-12: Experimental measured viscosity data for a MacKay River bitumen/n-decane mixture as a function of temperature (T) and pressure (P) at a constant mass fraction of n-decane (w_s = 0.45) in the binary mixture.

$W_S = 0.45$

P (MPa)	T (K)	μ_m (cp)	P (MPa)	T (K)	μ_m (cp)	P (MPa)	T (K)	μ_m (cp)
1.002	344.6	3.54	4.003	321.5	7.56	7.004	302.3	15.95
1.002	333.3	4.96	4.003	312.0	10.44	8.001	344.3	4.10
1.002	321.5	7.22	4.003	302.2	15.01	8.001	333.3	5.57
1.002	312.1	9.94	5.005	344.6	3.80	8.001	321.6	8.20
1.002	302.3	14.35	5.005	333.3	5.30	8.001	312.0	11.30
2.005	344.6	3.59	5.005	321.5	7.69	8.001	302.5	16.06
2.005	333.3	5.03	5.005	312.0	10.62	9.003	344.5	4.19
2.005	321.6	7.30	5.005	302.2	15.31	9.003	333.4	5.69
2.005	312.0	10.09	6.000	344.6	3.88	9.003	321.6	8.34
2.005	302.6	14.41	6.000	333.3	5.39	9.003	312.0	11.52
3.003	344.6	3.63	6.000	321.6	7.82	9.003	302.6	16.39
3.003	333.3	5.10	6.000	312.0	10.83	10.003	344.2	4.33
3.003	321.6	7.42	6.000	302.2	15.63	10.003	333.4	5.83
3.003	312.0	10.26	7.004	344.4	4.02	10.003	321.6	8.52
3.003	302.5	14.69	7.004	333.3	5.46	10.003	312.0	11.79
4.003	344.6	3.73	7.004	321.6	7.99	10.003	302.6	16.76
4.003	333.3	5.21	7.004	312.0	11.07			

Table 3-13: Experimental measured viscosity data for a MacKay River bitumen/n-decane mixture as a function of temperature (T) and pressure (P) at a constant mass fraction of n-decane (w_s = 0.50) in the binary mixture.

$W_S = 0.50$

P (MPa)	T (K)	μ_m (cp)	P (MPa)	T (K)	μ_m (cp)	P (MPa)	T (K)	μ_m (cp)
1.002	344.1	2.38	4.003	321.5	5.05	7.004	302.3	10.21
1.002	332.5	3.44	4.003	312.0	6.83	8.001	344.4	2.74
1.002	321.5	4.79	4.003	302.3	9.65	8.001	332.5	3.90
1.002	311.9	6.55	5.005	344.4	2.57	8.001	321.5	5.42
1.002	302.2	9.26	5.005	332.5	3.65	8.001	311.9	7.42
2.005	344.2	2.42	5.005	321.5	5.15	8.001	302.3	10.45
2.005	332.4	3.49	5.005	312.0	6.96	9.003	344.4	2.83
2.005	321.5	4.88	5.005	302.3	9.84	9.003	332.5	3.97
2.005	312.0	6.65	6.000	344.3	2.64	9.003	321.5	5.55
2.005	302.3	9.35	6.000	332.5	3.73	9.003	311.9	7.59
3.003	344.2	2.48	6.000	321.5	5.24	9.003	302.4	10.63
3.003	332.4	3.54	6.000	312.0	7.11	10.003	344.4	2.90
3.003	321.5	4.94	6.000	302.4	10.05	10.003	332.6	4.07
3.003	312.0	6.72	7.004	344.4	2.71	10.003	321.5	5.68
3.003	302.3	9.51	7.004	332.5	3.80	10.003	311.9	7.74
4.003	344.3	2.52	7.004	321.5	5.33	10.003	302.3	10.87
4.003	332.5	3.61	7.004	311.9	7.26			

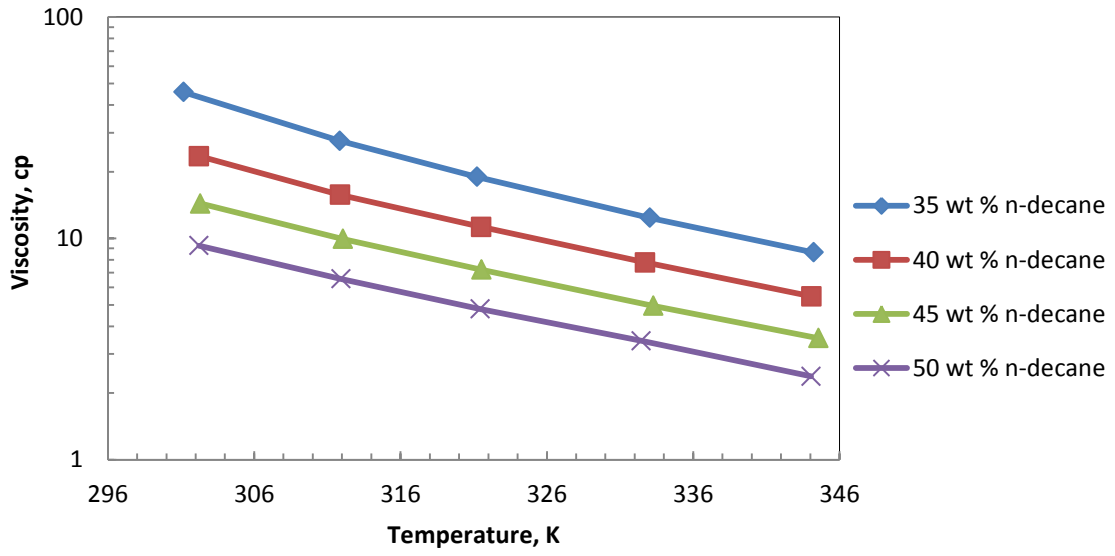

Figure 3-5: Viscosity variation of bitumen/n-decane systems with temperature, at different mass fractions of n-decane and a constant pressure of 1 MPa.

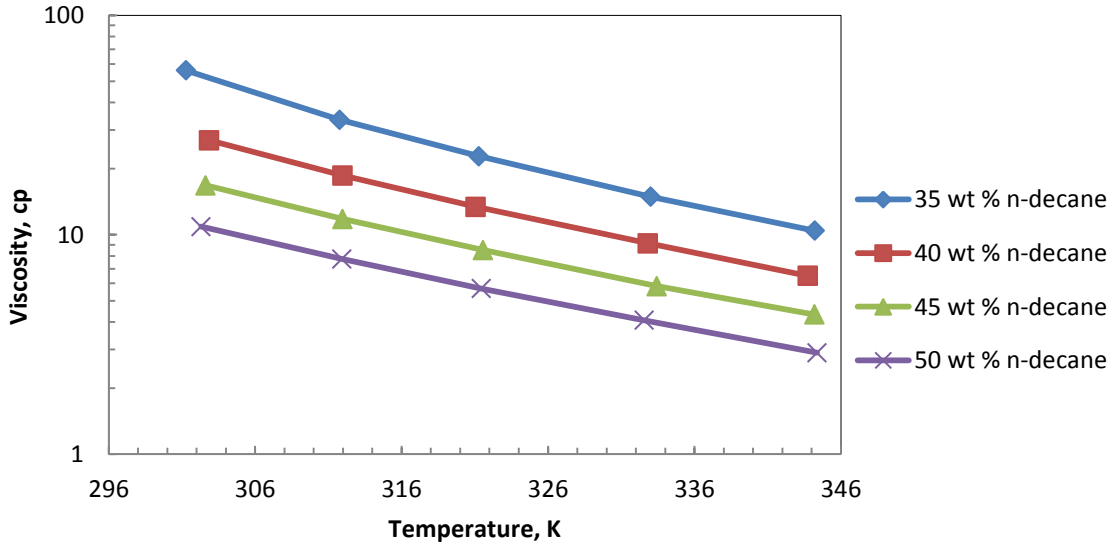

Figure 3-6: Viscosity variation of bitumen/n-decane systems with temperature, at different mass fractions of n-decane and a constant pressure of 10 MPa.

Chapter 4 Experimental Results

4.1 Measured Density and Viscosity Data of Pure Solvents

The experimental density data of the pure solvents (toluene and hexane) is summarized in Table 4-1. The measurements for toluene were performed over a wide range of pressures from 1 MPa to 10 MPa at 2 MPa intervals and at temperatures ranging from ambient to 333.1 K at 15 K intervals. The measurements for hexane were performed at the same pressures and at ambient temperature only. The temperature and pressure fluctuations were kept under 0.6 K and 0.008 MPa at each density value.

The measured viscosity data for the pure solvents (toluene and hexane) is summarized in Table 4-2. The viscosity measurements for both solvents were taken at pressure conditions similar to those in the density measurements over a different range of temperatures. The viscosity was measured at temperatures of 301, 308, 325 and 345 K for each pressure.

Table 4-1: Experimental measured density data of pure solvents (toluene and hexane) as a function of temperature (T) and pressure (P).

Toluene			**Hexane**		
Temperature (K)	**Pressure (MPa)**	**Density (kg/m^3)**	**Temperature (K)**	**Pressure (MPa)**	**Density (kg/m^3)**
297.9	1.002	864.3	297.4	1.001	658.0
297.8	3.001	866.0	297.4	3.004	660.2
297.8	5.004	867.6	297.4	5.005	662.4
297.7	7.004	869.1	297.3	7.004	664.4
297.7	10.004	871.4	297.3	10.004	667.4
303.6	1.005	857.9	------	-----	------
303.6	3.005	859.6	------	-----	------
303.6	5.001	861.3	------	-----	------
303.6	7.004	862.9	------	-----	------
303.6	10.004	865.1	------	-----	------
318.5	1.003	843.0	------	-----	------
318.6	3.000	844.9	------	-----	------
318.5	5.004	846.7	------	-----	------
318.5	7.004	848.4	------	-----	------
318.5	10.004	850.8	------	-----	------
333.2	1.005	829.3	------	-----	------
333.3	3.003	831.4	------	-----	------
333.3	5.0045	833.3			
333.3	7.0044	835.2			
333.3	10.0047	837.9			

Table 4-2: Experimental measured viscosity data of pure solvents (toluene and hexane) as a function of temperatures (T) and pressure (P).

Pressure (MPa)	Toluene		Hexane	
	Temperature (K)	Viscosity (cp)	Temperature (K)	Viscosity (cp)
1.003	343.0	0.307	------	-----
	325.9	0.366	------	-----
	308.8	0.451	------	-----
	301.5	0.494	301.08	0.285
3.002	342.9	0.304	------	-----
	325.9	0.364	------	-----
	308.8	0.448	------	-----
	301.6	0.495	301.10	0.281
5.003	342.9	0.303	------	-----
	325.7	0.363	------	-----
	308.8	0.448	------	-----
	301.6	0.491	301.04	0.287
7.004	342.9	0.304	------	-----
	325.7	0.364	------	-----
	308.8	0.447	------	-----
	301.6	0.493	301.02	0.293
10.004	342.9	0.304	------	-----
	325.9	0.364	------	-----
	308.9	0.449	------	-----
	301.6	0.496	300.95	0.300

4.2 Measured Density and Viscosity Data of Raw MacKay River Bitumen

Table 4-3 summaries the measured density data of raw MacKay River bitumen at different pressures and temperatures. At each temperature, the density was measured at five different pressures using the same stepwise intervals used for the pure solvents.

Table 4-3: Experimental measured density data of raw MacKay River bitumen as a function of temperature (T) and pressure (P).

Temperature (K)	Pressure (MPa)	Density (kg/m^3)	Temperature (K)	Pressure (MPa)	Density (kg/m^3)
303.3	1.002	1000.2	323.6	1.005	988.9
	3.003	1001.4		3.003	990.0
	5.001	1002.4		5.005	991.1
	7.003	1003.5		7.005	992.2
	10.002	1004.9		10.006	993.7
313.4	1.004	995.2	333.3	1.004	983.4
	3.003	996.3		3.005	984.6
	5.000	997.4		5.004	985.8
	6.999	998.4		7.006	986.9
	10.003	1000.0		10.006	988.5
318.1	1.002	993.1	———	-----	------
	3.004	994.2		-----	------
	5.003	995.4		-----	------
	7.005	996.4		-----	------
	10.006	998.4		-----	------

The data tabulated above is plotted in Figure 4-1, which shows the variations in measured density of MacKay River bitumen with various pressures at 303.3, 313.4, 318.1, 323.6 and 333.3 K. A linear relationship between bitumen density and pressure can be observed and the density is shown to decrease with increasing temperature at a specific pressure point.

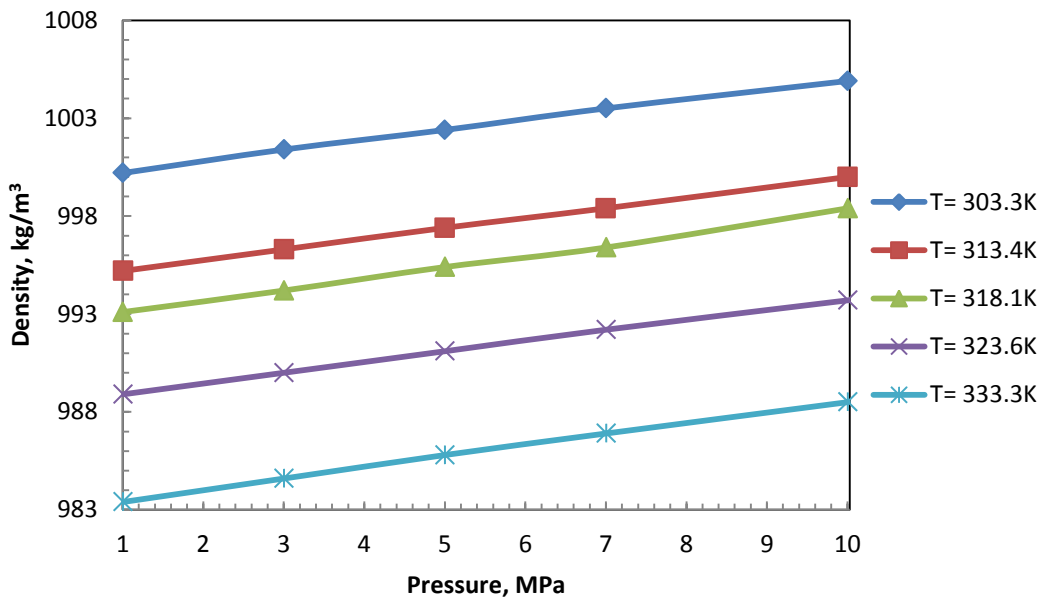

Figure 4-1: Raw MacKay River bitumen density dependence on pressure (P) and temperature (T).

The experimental viscosity data for raw MacKay River bitumen at different temperature and pressure conditions is summarized in Table 4-4. The viscosity values for all pressures at temperatures less than 321 K were more than the maximum viscometer piston ranges. For this reason, the viscosity data was measured at the following temperatures, 321.3, 325.9, 333.1 and 344.7 K.

Table 4-4: Experimental measured viscosity data for raw MacKay River bitumen as a function of temperature (T) and pressure (P).

Pressure (MPa)	Temperature (K)	Viscosity (cp)	Pressure (MPa)	Temperature (K)	Viscosity (cp)
1.004	344.7	1223	5.003	325.9	7704
1.005	333.0	3425	5.000	321.3	10103
1.002	326.0	6202	7.006	344.7	1600
1.004	321.3	8555	7.005	333.1	4502
3.005	344.7	1331	7.005	325.9	8308
3.003	333.1	3807	6.999	321.3	11422
3.004	326.0	6862	10.006	344.7	1830
3.003	321.3	9382	10.006	333.2	5181
5.004	344.7	1469	10.006	325.9	9642
5.005	333.1	4075	10.003	321.3	13330

4.3 Physical Properties of Toluene Diluted Bitumen Systems

4.3.1 Measured Viscosity Data of Toluene Diluted Bitumen Mixtures

The viscosity values for the bitumen/toluene binary mixtures at different pressures and temperatures were accurately measured. The viscosity was found to be dependent on the mass composition of toluene.

The measured viscosity data at similar previous pressure and temperature conditions for the binary mixture is summarized in Tables 4-5 to 4-10. In these tables, the mass compositions of toluene are 5%, 10%, 20%, 35%, 50% and 70%, respectively.

Table 4-5: Experimental measured viscosity data of MacKay River bitumen/toluene mixture as a function of temperature (T) and pressure (P) at constant mass fraction of toluene (w_s = 0.05) in the binary mixture.

$W_S = 0.05$

P (MPa)	T (K)	μ_m (cp)	P (MPa)	T (K)	μ_m (cp)
1.004	344.6	330.30	7.003	344.5	410.90
1.004	327.0	1070.3	7.003	327.0	1370.0
1.004	311.3	4362.5	7.003	311.3	5479.8
1.004	302.1	11028	7.003	302.2	14632
3.003	344.6	353.00	10.003	344.6	462.80
3.003	327.0	1156.0	10.003	327.0	1574.3
3.003	311.3	4693.1	10.003	311.3	6220.1
3.003	302.2	12217	10.003	302.2	16596
5.004	344.5	379.40	------	-----	------
5.004	327.0	1248.9	------	-----	------
5.004	311.3	5064.6	------	-----	------
5.004	302.2	13332	------	-----	------

Table 4-6: Experimental measured viscosity data of MacKay River bitumen/toluene mixture as a function of temperature (T) and pressure (P) at constant mass fraction of toluene (w_s = 0.1) in the binary mixture.

$W_S = 0.1$

P (MPa)	T (K)	μ_m (cp)	P (MPa)	T (K)	μ_m (cp)
1.004	345.6	106.9	7.003	345.6	129.8
1.004	327.7	292.3	7.003	327.7	352.4
1.004	313.0	768.7	7.003	312.9	961.3
1.004	301.8	2046.0	7.003	301.8	2515.3
3.003	345.6	113.2	10.003	345.5	147.9
3.003	327.7	308.8	10.003	327.7	397.3
3.003	312.9	823.1	10.003	312.9	1096.0
3.003	301.8	2151.4	10.003	301.8	2821.1
5.004	345.6	121.4	------	-----	------
5.004	327.7	328.2	------	-----	------
5.004	312.9	889.2	------	-----	------
5.004	301.8	2311.9	------	-----	------

Table 4-7: Experimental measured viscosity data of MacKay River bitumen/toluene mixture as a function of temperature (T) and pressure (P) at a constant mass fraction of toluene (w_s = 0.2) in the binary mixture.

$W_S = 0.2$

P (MPa)	T (K)	μ_m (cp)	P (MPa)	T (K)	μ_m (cp)
1.004	344.5	25.52	7.003	344.4	28.64
1.004	326.9	51.22	7.003	326.9	58.79
1.004	311.9	104.4	7.003	311.9	120.5
1.004	301.5	183.0	7.003	302.1	205.5
3.003	344.5	26.50	10.003	344.4	30.71
3.003	326.9	53.50	10.003	326.9	63.15
3.003	311.9	109.4	10.003	311.9	129.9
3.003	301.8	190.3	10.003	302.2	219.4
5.004	344.4	27.58	------	-----	------
5.004	326.9	55.99	------	-----	------
5.004	311.9	115.3	------	-----	------
5.004	302.0	196.3	------	-----	------

Table 4-8: Experimental measured viscosity data of MacKay River bitumen/toluene mixture as a function of temperature (T) and pressure (P) at a constant mass fraction of toluene (w_s = 0.35) in the binary mixture..

$W_S = 0.35$

P (MPa)	T (K)	μ_m (cp)	P (MPa)	T (K)	μ_m (cp)
1.004	344.0	5.172	7.003	344.0	5.878
1.004	327.1	8.652	7.003	327.1	9.562
1.004	312.0	13.93	7.003	312.0	15.44
1.004	301.7	20.32	7.003	301.7	22.67
3.003	344.0	5.477	10.003	344.0	6.293
3.003	327.1	8.912	10.003	327.1	10.25
3.003	312.0	14.40	10.003	312.0	16.54
3.003	301.7	21.06	10.003	301.7	24.22
5.004	344.0	5.666	------	-----	------
5.004	327.1	9.194	------	-----	------
5.004	312.0	14.98	------	-----	------
5.004	301.7	21.92	------	-----	------

Table 4-9: Experimental measured viscosity data of MacKay River bitumen/toluene mixture as a function of temperature (T) and pressure (P) at a constant mass fraction of toluene (w_s = 0.5) in the binary mixture..

$W_S = 0.5$

P (MPa)	T (K)	μ_m (cp)	P (MPa)	T (K)	μ_m (cp)
1.004	343.6	2.135	7.003	343.5	2.157
1.004	328.4	2.919	7.003	328.4	2.952
1.004	310.9	4.347	7.003	311.0	4.393
1.004	301.1	5.546	7.003	301.2	5.624
3.003	343.5	2.138	10.003	343.4	2.198
3.003	328.4	2.938	10.003	328.3	2.992
3.003	311.0	4.356	10.003	311.0	4.458
3.003	301.1	5.564	10.003	301.2	5.720
5.004	343.5	2.147	------	-----	------
5.004	328.4	2.944	------	-----	------
5.004	311.0	4.372	------	-----	------
5.004	301.2	5.585	------	-----	------

Table 4-10: Experimental measured viscosity data of MacKay River bitumen/toluene mixture as a function of temperature (T) and pressure (P) at a constant mass fraction of toluene (w_s = 0.7) in the binary mixture..

$W_S = 0.7$

P (MPa)	T (K)	μ_m (cp)	P (MPa)	T (K)	μ_m (cp)
1.004	343.3	0.826	7.003	343.3	0.824
1.004	326.2	1.055	7.003	326.3	1.051
1.004	311.1	1.345	7.003	311.1	1.333
1.004	300.4	1.614	7.003	300.5	1.618
3.003	343.3	0.821	10.003	343.3	0.831
3.003	326.2	1.047	10.003	326.3	1.061
3.003	311.1	1.338	10.003	311.0	1.348
3.003	300.4	1.614	10.003	300.6	1.629
5.004	343.3	0.822	------	-----	------
5.004	326.2	1.049	------	-----	------
5.004	311.1	1.333	------	-----	------
5.004	300.4	1.616	------	-----	------

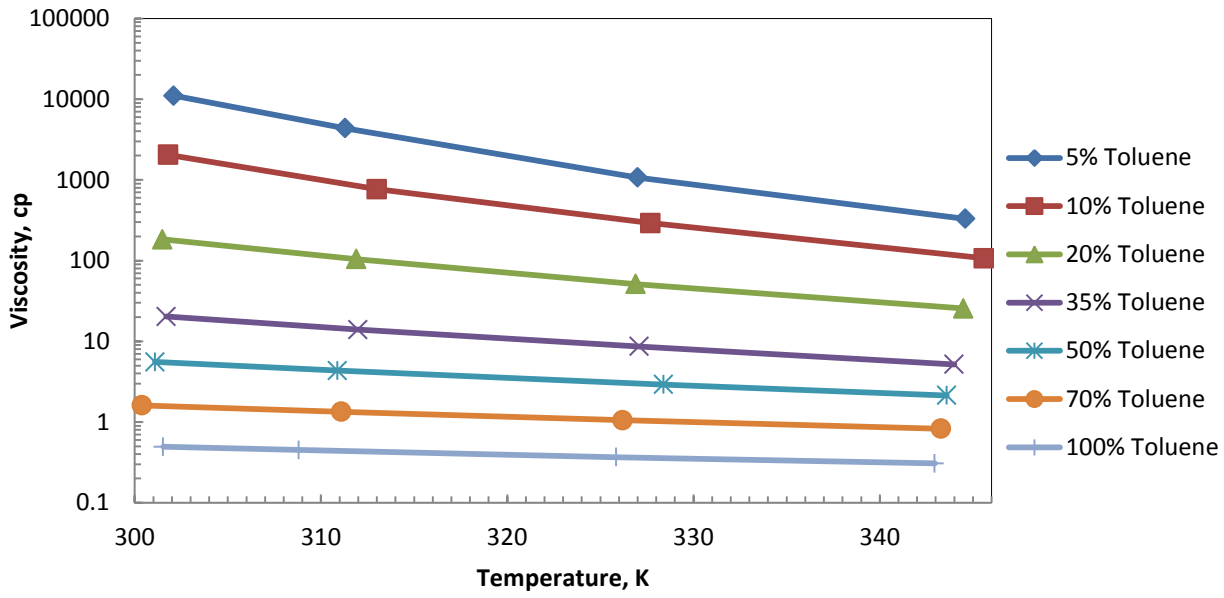

Figure 4-2: Calculated viscosity of the toluene-bitumen mixture versus temperature, at different mass fractions of toluene and at a constant pressure of 1 MPa.

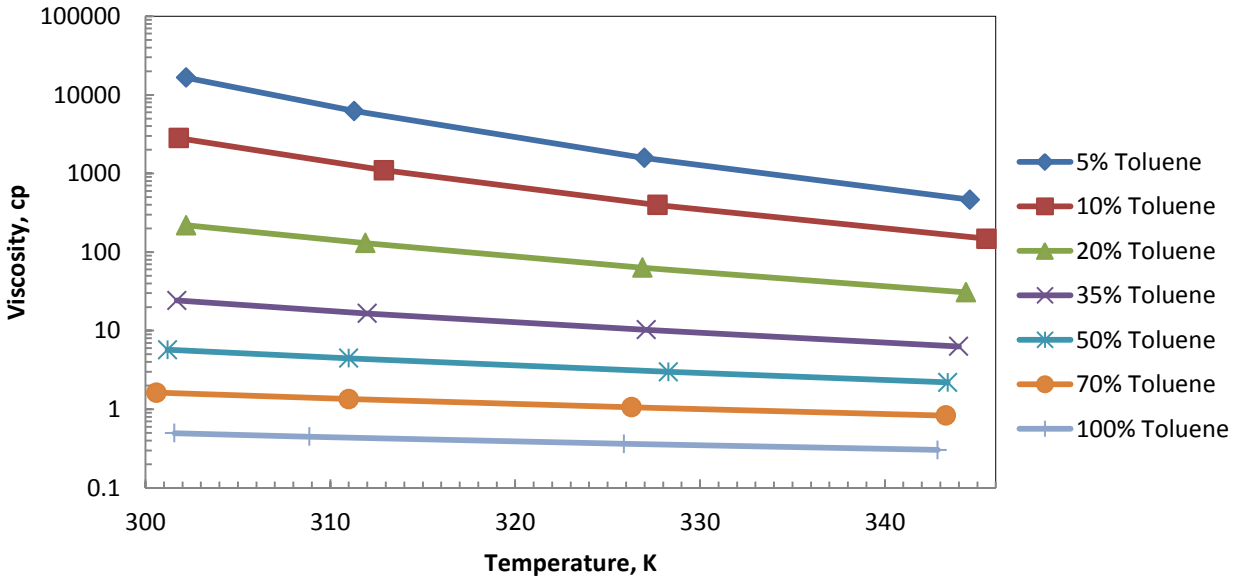

Figure 4-3: Calculated viscosity of the toluene-bitumen mixture versus temperature, at different mass fractions of toluene and at a constant pressure of 10 MPa.

4.3.2 Measured Density Data of Toluene Diluted Bitumen Mixtures

The density values of the bitumen/toluene binary mixtures at different pressures and temperatures were measured as a function of temperature and pressure. The density was dependent on the mass composition of the solvent i.e. toluene.

The density data measured for the binary mixture at similar pressure and temperature conditions is tabulated in Tables 4-11 through 4-16 at toluene mass compositions of 5%, 10%, 20%, 35%, 50% and 70%, respectively. The measurements were taken over a temperature range from ambient to 333 K and at pressures ranging from 1 to 10 MPa.

Table 4-11: Experimental measured density data of the MacKay River bitumen/toluene mixture as a function of temperature (T) and pressure (P) at a constant mass fraction of toluene (w_s = 0.05) in the binary mixture.

$W_S = 0.05$

P (MPa)	T (K)	ρ_m (kg/m^3)	P (MPa)	T (K)	ρ_m (kg/m^3)
1.004	297.6	996.4	7.003	297.6	999.5
1.004	303.2	992.5	7.003	303.3	995.7
1.004	318.0	984.6	7.003	318.0	988.0
1.004	333.1	974.8	7.003	333.2	978.4
3.003	297.6	997.5	10.003	297.6	1001.0
3.003	303.2	993.6	10.003	303.3	997.1
3.003	318.0	985.7	10.003	318.0	989.5
3.003	333.2	976.0	10.003	333.3	980.0
5.004	297.6	998.5	------	-----	------
5.004	303.3	994.6	------	-----	------
5.004	318.0	986.8	------	-----	------
5.004	333.2	977.2	------	-----	------

Table 4-12: Experimental measured density data for the MacKay River bitumen/toluene mixture as a function of temperature (T) and pressure (P) at a constant mass fraction of toluene (w_s = 0.1) in the binary mixture.

$W_S = 0.1$

P (MPa)	T (K)	ρ_m (kg/m^3)	P (MPa)	T (K)	ρ_m (kg/m^3)
1.004	296.3	992.0	7.003	296.3	995.6
1.004	303.2	987.7	7.003	303.2	991.0
1.004	318.2	975.7	7.003	318.2	979.2
1.004	333.4	965.8	7.003	333.5	969.6
3.003	296.3	993.4	10.003	296.3	997.1
3.003	303.2	988.9	10.003	303.2	992.6
3.003	318.2	976.9	10.003	318.2	980.8
3.003	333.5	967.2	10.003	333.6	971.3
5.004	296.3	994.5	------	-----	------
5.004	303.2	990.0	------	-----	------
5.004	318.2	978.1	------	-----	------
5.004	333.5	968.4	------	-----	------

Table 4-13: Experimental measured density data for the MacKay River bitumen/toluene mixture as a function of temperature (T) and pressure (P) at a constant mass fraction of toluene (w_s = 0.2) in the binary mixture.

$W_S = 0.2$

P (MPa)	T (K)	ρ_m (kg/m^3)	P (MPa)	T (K)	ρ_m (kg/m^3)
1.004	296.5	976.3	7.003	297.0	979.3
1.004	303.2	971.0	7.003	303.3	974.4
1.004	318.2	959.0	7.003	318.3	962.6
1.004	333.6	948.5	7.003	333.5	952.6
3.003	296.6	977.3	10.003	297.1	980.8
3.003	303.2	972.2	10.003	303.3	976.1
3.003	318.2	960.2	10.003	318.3	964.4
3.003	333.6	949.9	10.003	333.5	954.4
5.004	296.8	978.3	------	-----	------
5.004	303.3	973.3	------	-----	------
5.004	318.3	961.4	------	-----	------
5.004	333.6	951.2	------	-----	------

Table 4-14: Experimental measured density data for the MacKay River bitumen/toluene mixture as a function of temperature (T) and pressure (P) at a constant mass fraction of toluene (w_s = 0.35) in the binary mixture.

$W_S = 0.35$

P (MPa)	T (K)	ρ_m (kg/m^3)	P (MPa)	T (K)	ρ_m (kg/m^3)
1.004	297.0	951.9	7.003	296.8	955.7
1.004	303.3	947.4	7.003	303.4	951.2
1.004	318.4	934.3	7.003	318.5	938.3
1.004	333.2	923.8	7.003	333.2	928.2
3.003	296.9	953.2	10.003	296.8	957.4
3.003	303.4	948.7	10.003	303.4	953.0
3.003	318.5	935.7	10.003	318.5	940.2
3.003	333.2	925.3	10.003	333.2	930.2
5.004	296.9	954.4	------	-----	------
5.004	303.4	949.9	------	-----	------
5.004	318.5	937.0	------	-----	------
5.004	333.2	926.8	------	-----	------

Table 4-15: Experimental measured density data for the MacKay River bitumen/toluene mixture as a function of temperature (T) and pressure (P) at a constant mass fraction of toluene (w_s = 0.5) in the binary mixture.

$W_S = 0.5$

P (MPa)	T (K)	ρ_m (kg/m^3)	P (MPa)	T (K)	ρ_m (kg/m^3)
1.004	296.8	931.4	7.003	296.9	935.3
1.004	303.3	926.1	7.003	303.4	930.1
1.004	318.5	912.4	7.003	318.4	916.7
1.004	333.5	900.7	7.003	333.5	905.5
3.003	296.9	932.7	10.003	296.9	937.1
3.003	303.3	927.5	10.003	303.4	932.0
3.003	318.5	913.9	10.003	318.4	918.8
3.003	333.5	902.3	10.003	333.4	907.7
5.004	296.9	934.0	------	-----	------
5.004	303.3	928.8	------	-----	------
5.004	318.5	915.3	------	-----	------
5.004	333.5	903.9	------	-----	------

Table 4-16: Experimental measured density data for the MacKay River bitumen/toluene mixture as a function of temperature (T) and pressure (P) at a constant mass fraction of toluene (w_s = 0.7) in the binary mixture.

$W_S = 0.7$

P (MPa)	T (K)	ρ_m (kg/m^3)	P (MPa)	T (K)	ρ_m (kg/m^3)
1.004	296.1	904.0	7.003	296.2	908.2
1.004	303.4	897.7	7.003	303.4	902.1
1.004	318.5	883.5	7.003	318.5	888.2
1.004	333.3	871.1	7.003	333.3	876.3
3.003	296.1	905.5	10.003	296.2	910.1
3.003	303.4	899.3	10.003	303.4	904.2
3.003	318.4	885.1	10.003	318.5	890.4
3.003	333.3	872.9	10.003	333.3	878.6
5.004	296.1	906.8	------	-----	------
5.004	303.4	900.7	------	-----	------
5.004	318.5	886.7	------	-----	------
5.004	333.3	874.6	------	-----	------

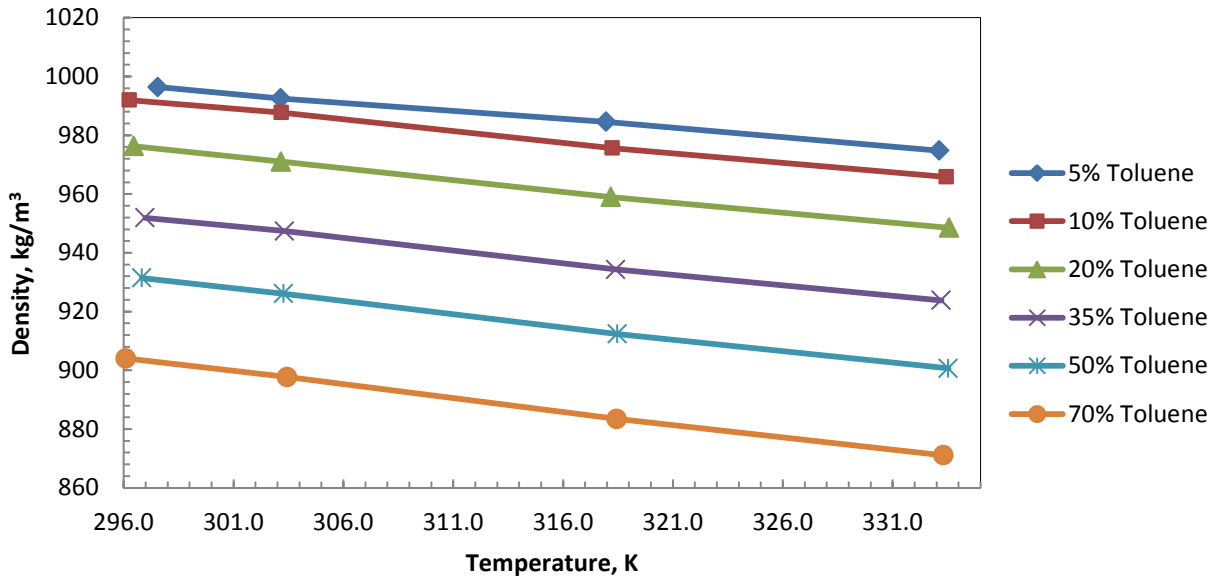

Figure 4-4: Density variation of the toluene-bitumen mixture with temperature, at different mass fractions of toluene and a constant pressure of 1 MPa.

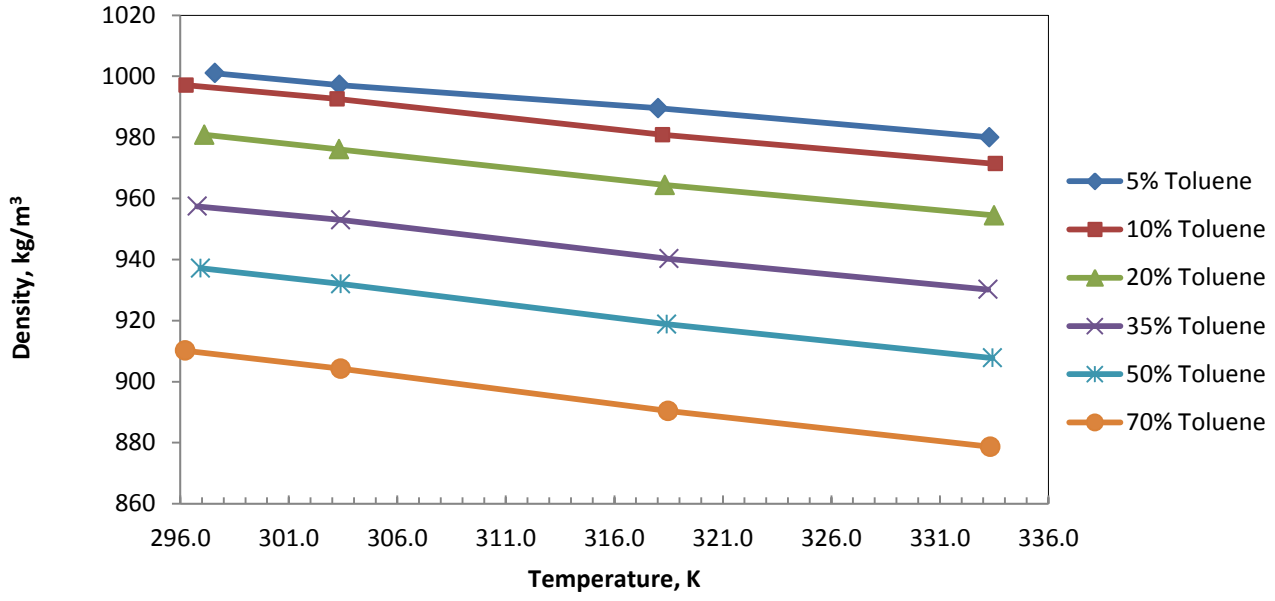

Figure 4-5: Density variation of the toluene-bitumen mixture with temperature, at different mass fractions of toluene and a constant pressure of 10 MPa.

4.4 Physical Properties of Hexane Diluted Bitumen Systems

4.4.1 Measured Viscosity Data of Hexane Diluted Bitumen Mixtures

The viscosity of the hexane diluted bitumen mixtures was measured at various pressures and temperature similar to those measured for the bitumen/toluene mixtures. The viscosity of these mixtures was also found to be dependent on pressure, temperature, and the mass composition of hexane in the mixture.

The viscosity data for the hexane bitumen binary mixture at different pressure and temperature conditions is summarized in Tables 4-17 to 4-22. The data in Tables 4-17 to 4-22 represents the measured viscosity at hexane mass compositions of 5%, 10%, 20%, 35%, 50%, and 70%.

Table 4-17: Experimental measured viscosity data of the MacKay River bitumen/hexane mixture as a function of temperature (T) and pressure (P) at constant hexane mass fraction (w_s = 0.05) in the binary mixture.

$W_S = 0.05$

P (MPa)	T (K)	μ_m (cp)	P (MPa)	T (K)	μ_m (cp)
1.003	344.6	267.7	7.004	344.7	324.0
1.003	327.8	808.3	7.004	328.0	997.1
1.003	311.4	3195.3	7.004	311.3	4170.9
1.003	300.9	9230	7.004	300.8	12476
3.003	344.5	285.5	10.004	344.6	365.4
3.003	327.9	858.3	10.004	328.0	1133.7
3.003	311.3	3496.4	10.004	311.2	4709.9
3.003	300.9	10330	10.004	300.8	14365
5.004	344.6	303.6	------	-----	------
5.004	328.0	919.7	------	-----	------
5.004	311.3	3808.1	------	-----	------
5.004	300.9	11301	------	-----	------

Table 4-18: Experimental measured viscosity data of the MacKay River bitumen/hexane mixture as a function of temperature (T) and pressure (P) at constant hexane mass fraction (w_s = 0.1) in the binary mixture.

$W_S = 0.1$

P (MPa)	T (K)	μ_m (cp)	P (MPa)	T (K)	μ_m (cp)
1.004	345.7	75.4	7.003	345.6	88.5
1.004	327.9	197.8	7.003	327.8	236.7
1.004	312.9	501.7	7.003	312.9	602.6
1.004	300.2	1361.1	7.003	300.4	1644.8
3.003	345.7	78.8	10.003	345.6	99.8
3.003	327.9	209.1	10.003	327.8	264.2
3.003	312.9	531.3	10.003	312.9	674.1
3.003	300.2	1452.6	10.003	300.5	1830.3
5.004	345.7	83.3	------	-----	------
5.004	327.8	221.5	------	-----	------
5.004	312.9	563.5	------	-----	------
5.004	300.2	1545.8	------	-----	------

Table 4-19: Experimental measured viscosity data of the MacKay River bitumen/hexane mixture as a function of temperature (T) and pressure (P) at constant hexane mass fraction (w_s = 0.2) in the binary mixture.

$W_S = 0.2$

P (MPa)	T (K)	μ_m (cp)	P (MPa)	T (K)	μ_m (cp)
1.004	344.2	10.60	7.003	344.2	12.13
1.004	327.2	20.04	7.003	327.1	22.66
1.004	312.1	37.29	7.003	311.9	43.35
1.004	300.5	68.80	7.003	300.5	79.12
3.003	344.2	11.10	10.003	344.2	13.06
3.003	327.2	20.78	10.003	327.1	24.48
3.003	312.1	39.15	10.003	311.9	47.44
3.003	300.6	71.67	10.003	300.6	85.82
5.004	344.2	11.62	------	-----	------
5.004	327.2	21.68	------	-----	------
5.004	312.0	41.04	------	-----	------
5.004	300.5	75.43	------	-----	------

Table 4-20: Experimental measured viscosity data of the MacKay River bitumen/hexane mixture as a function of temperature (T) and pressure (P) at constant hexane mass fraction (w_s = 0.35) in the binary mixture.

$W_S = 0.35$

P (MPa)	T (K)	μ_m (cp)	P (MPa)	T (K)	μ_m (cp)
1.004	344.0	3.54	7.003	343.8	3.67
1.004	327.3	5.32	7.003	327.3	6.05
1.004	311.5	8.65	7.003	311.6	9.77
1.004	299.8	13.25	7.003	299.9	14.97
3.003	344.1	3.56	10.003	343.8	3.74
3.003	327.3	5.54	10.003	327.2	6.55
3.003	311.6	8.99	10.003	311.6	10.49
3.003	299.8	13.80	10.003	300.0	16.00
5.004	343.9	3.63	------	-----	------
5.004	327.3	5.77	------	-----	------
5.004	311.6	9.35	------	-----	------
5.004	299.8	14.31	------	-----	------

Table 4-21: Experimental measured viscosity data of the MacKay River bitumen/hexane mixture as a function of temperature (T) and pressure (P) at constant hexane mass fraction (w_s = 0.5) in the binary mixture.

$W_S = 0.5$

P (MPa)	**T (K)**	**μ_m (cp)**	**P (MPa)**	**T (K)**	**μ_m (cp)**
1.004	343.8	1.292	7.003	343.8	1.325
1.004	326.2	1.614	7.003	326.2	1.644
1.004	310.6	2.281	7.003	310.6	2.324
1.004	299.7	3.029	7.003	299.7	3.087
3.003	343.9	1.317	10.003	343.9	1.343
3.003	326.2	1.626	10.003	326.2	1.677
3.003	310.6	2.297	10.003	310.6	2.369
3.003	299.7	3.038	10.003	299.7	3.139
5.004	344.0	1.319	------	-----	------
5.004	326.2	1.632	------	-----	------
5.004	310.6	2.313	------	-----	------
5.004	299.7	3.068	------	-----	------

Table 4-22: Experimental measured viscosity data of the MacKay River bitumen/hexane mixture as a function of temperature (T) and pressure (P) at constant hexane mass fraction (w_s = 0.7) in the binary mixture.

$W_S = 0.7$

P (MPa)	T (K)	μ_m (cp)	P (MPa)	T (K)	μ_m (cp)
1.004	343.0	0.370	7.003	343.0	0.378
1.004	326.1	0.462	7.003	326.0	0.470
1.004	308.9	0.595	7.003	308.9	0.602
1.004	298.8	0.683	7.003	298.7	0.691
3.003	343.0	0.372	10.003	343.0	0.384
3.003	326.1	0.464	10.003	326.0	0.477
3.003	308.9	0.594	10.003	308.9	0.610
3.003	298.9	0.683	10.003	298.8	0.702
5.004	343.0	0.374	------	-----	------
5.004	326.0	0.467	------	-----	------
5.004	308.9	0.600	------	-----	------
5.004	298.6	0.690	------	-----	------

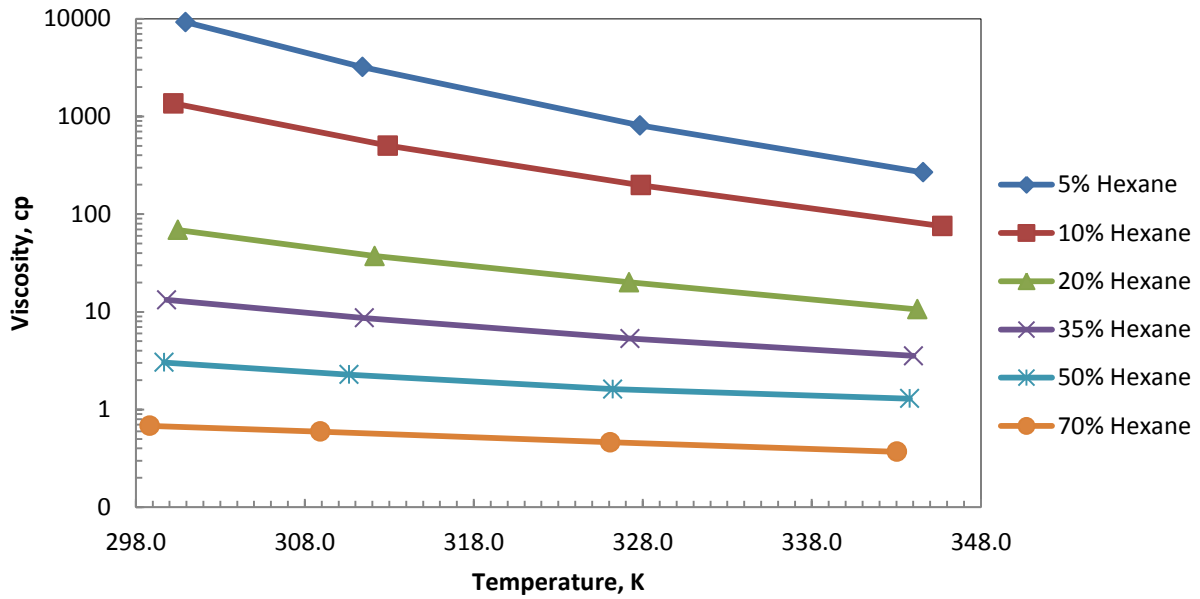

Figure 4-6: Viscosity variation of hexane-bitumen mixtures with temperature, at different mass fractions of hexane and a constant pressure of 1 MPa.

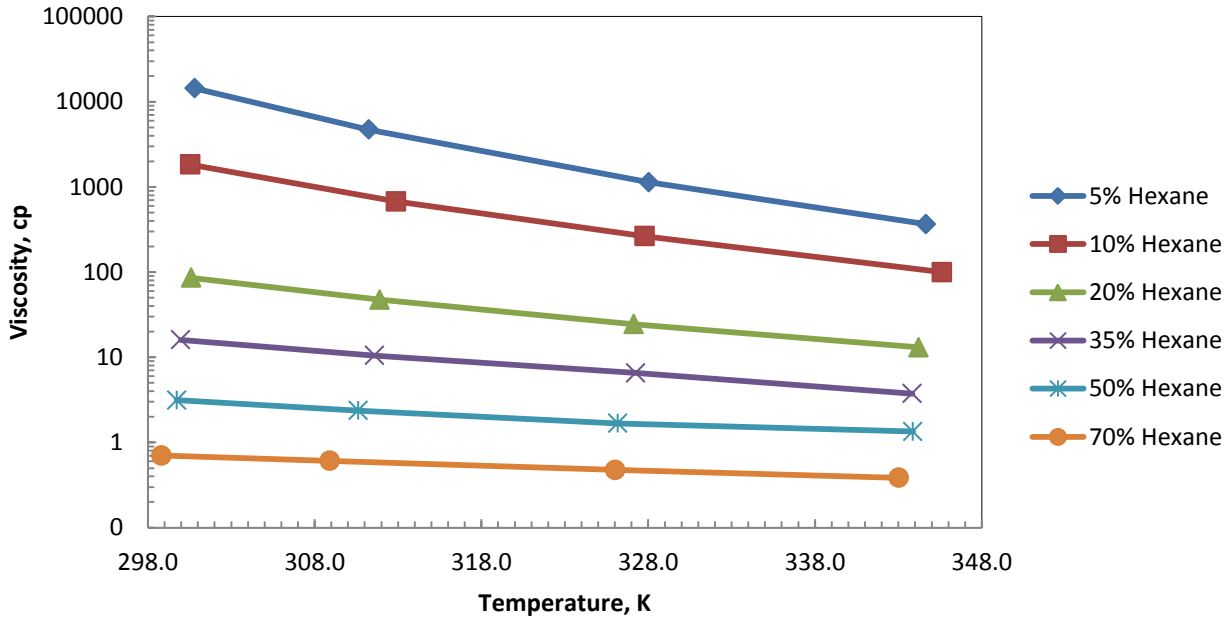

Figure 4-7: Viscosity variation of hexane-bitumen mixtures with temperature, at different mass fractions of hexane and a constant pressure of 10 MPa.

4.4.2 Measured Density Data of Hexane Diluted Bitumen Mixtures

The same procedure used for the bitumen-toluene density measurement was followed to measure the density of hexane-diluted mixtures. The measurements were taken at temperatures from 294 K to 333 K and pressures from 1 to 10 MPa. The density of the mixtures was determined to be dependent on pressure, temperature, and the mass composition of hexane in the mixture.

Tables 4-23 to 4-28 summarize the density of the binary mixture at different pressure and temperature conditions. The mass fractions of hexane from were 5%, 10%, 20%, 35%, 50% and 70%.

Table 4-23: Experimental measured density data of the MacKay River bitumen/hexane mixture as a function of temperature (T) and pressure (P) at a constant mass fraction of hexane (w_s = 0.05) in the binary mixture.

W_S = 0.05

P (MPa)	T (K)	ρ_m (kg/m^3)	P (MPa)	T (K)	ρ_m (kg/m^3)
1.003	333.2	959.7	7.004	333.2	963.4
1.003	318.4	969.2	7.004	318.7	972.6
1.003	303.4	977.5	7.004	303.3	980.9
1.003	296.4	982.2	7.004	296.4	985.5
3.003	333.2	961.0	10.004	333.2	965.1
3.003	318.5	970.4	10.004	318.7	974.2
3.003	303.3	978.6	10.004	303.3	982.4
3.003	296.4	983.3	10.004	296.4	987.0
5.004	333.2	962.3	------	-----	------
5.004	318.6	971.5	------	-----	------
5.004	303.3	979.8	------	-----	------
5.004	296.4	984.4	------	-----	------

Table 4-24: Experimental measured density data of the MacKay River bitumen/hexane mixture as a function of temperature (T) and pressure (P) at a constant mass fraction of hexane (w_s = 0.1) in the binary mixture.

$W_S = 0.1$

P (MPa)	T (K)	ρ_m (kg/m^3)	P (MPa)	T (K)	ρ_m (kg/m^3)
1.004	333.5	934.6	7.003	333.5	938.7
1.004	318.4	944.6	7.003	318.3	948.4
1.004	303.3	956.0	7.003	303.1	959.7
1.004	295.2	962.4	7.003	294.9	965.9
3.003	333.6	936.1	10.003	333.5	940.6
3.003	318.4	945.9	10.003	318.3	950.2
3.003	303.2	957.3	10.003	303.1	961.4
3.003	295.0	963.7	10.003	294.9	967.4
5.004	333.5	937.4	------	-----	------
5.004	318.4	947.2	------	-----	------
5.004	303.2	958.5	------	-----	------
5.004	294.9	964.8	------	-----	------

Table 4-25: Experimental measured density data of the MacKay River bitumen/hexane mixture as a function of temperature (T) and pressure (P) at a constant mass fraction of hexane (w_s = 0.2) in the binary mixture.

$W_S = 0.2$

P (MPa)	T (K)	ρ_m (kg/m^3)	P (MPa)	T (K)	ρ_m (kg/m^3)
1.004	333.2	876.0	7.003	333.2	880.6
1.004	318.2	886.3	7.003	318.3	890.8
1.004	303.1	898.4	7.003	303.2	903.4
1.004	295.4	905.4	7.003	295.5	909.9
3.003	333.2	877.6	10.003	333.2	882.8
3.003	318.3	887.8	10.003	318.3	892.9
3.003	303.2	900.2	10.003	303.2	905.4
3.003	295.5	907.1	10.003	295.6	911.7
5.004	333.2	879.1	------	-----	------
5.004	318.3	889.3	------	-----	------
5.004	303.2	902.0	------	-----	------
5.004	295.5	908.6	------	-----	------

Table 4-26: Experimental measured density data of the MacKay River bitumen/hexane mixture as a function of temperature (T) and pressure (P) at a constant mass fraction of hexane (w_s = 0.35) in the binary mixture.

$W_S = 0.35$

P (MPa)	T (K)	ρ_m (kg/m^3)	P (MPa)	T (K)	ρ_m (kg/m^3)
1.004	333.4	827.3	7.003	333.5	832.6
1.004	318.5	838.3	7.003	318.6	843.2
1.004	303.1	851.2	7.003	303.0	855.9
1.004	296.1	857.8	7.003	295.5	862.4
3.003	333.5	829.1	10.003	333.5	834.9
3.003	318.5	840.0	10.003	318.6	845.5
3.003	303.1	852.8	10.003	303.0	858.0
3.003	295.8	859.4	10.003	295.4	864.5
5.004	333.6	830.9	------	-----	------
5.004	318.5	841.6	------	-----	------
5.004	303.0	854.4	------	-----	------
5.004	295.6	861.0	------	-----	------

Table 4-27: Experimental measured density data of the MacKay River bitumen/hexane mixture as a function of temperature (T) and pressure (P) at a constant mass fraction of hexane (w_s = 0.5) in the binary mixture.

$W_S = 0.5$

P (MPa)	T (K)	ρ_m (kg/m^3)	P (MPa)	T (K)	ρ_m (kg/m^3)
1.004	333.5	770.7	7.003	333.6	777.4
1.004	318.2	783.1	7.003	318.3	788.8
1.004	302.9	797.1	7.003	303.0	801.6
1.004	295.4	804.0	7.003	295.5	808.9
3.003	333.5	772.7	10.003	333.6	780.3
3.003	318.2	785.0	10.003	318.3	791.4
3.003	302.9	798.7	10.003	303.0	804.3
3.003	295.5	805.7	10.003	295.5	811.1
5.004	333.6	775.1	------	-----	------
5.004	318.3	786.9	------	-----	------
5.004	302.9	800.2	------	-----	------
5.004	295.5	807.3	------	-----	------

Table 4-28: Experimental measured density data of the MacKay River bitumen/hexane mixture as a function of temperature (T) and pressure (P) at a constant mass fraction of hexane (w_s = 0.7) in the binary mixture.

$W_S = 0.7$

P (MPa)	T (K)	ρ_m (kg/m^3)	P (MPa)	T (K)	ρ_m (kg/m^3)
1.004	333.1	698.4	7.003	333.2	705.4
1.004	318.2	711.4	7.003	318.3	717.7
1.004	303.2	725.8	7.003	303.2	731.6
1.004	294.6	733.7	7.003	294.4	739.4
3.003	333.2	700.8	10.003	333.2	708.6
3.003	318.2	713.6	10.003	318.3	720.6
3.003	303.2	727.8	10.003	303.3	734.3
3.003	294.7	735.6	10.003	294.5	741.9
5.004	333.2	703.1	------	-----	------
5.004	318.3	715.7	------	-----	------
5.004	303.2	729.7	------	-----	------
5.004	294.4	737.7	------	-----	------

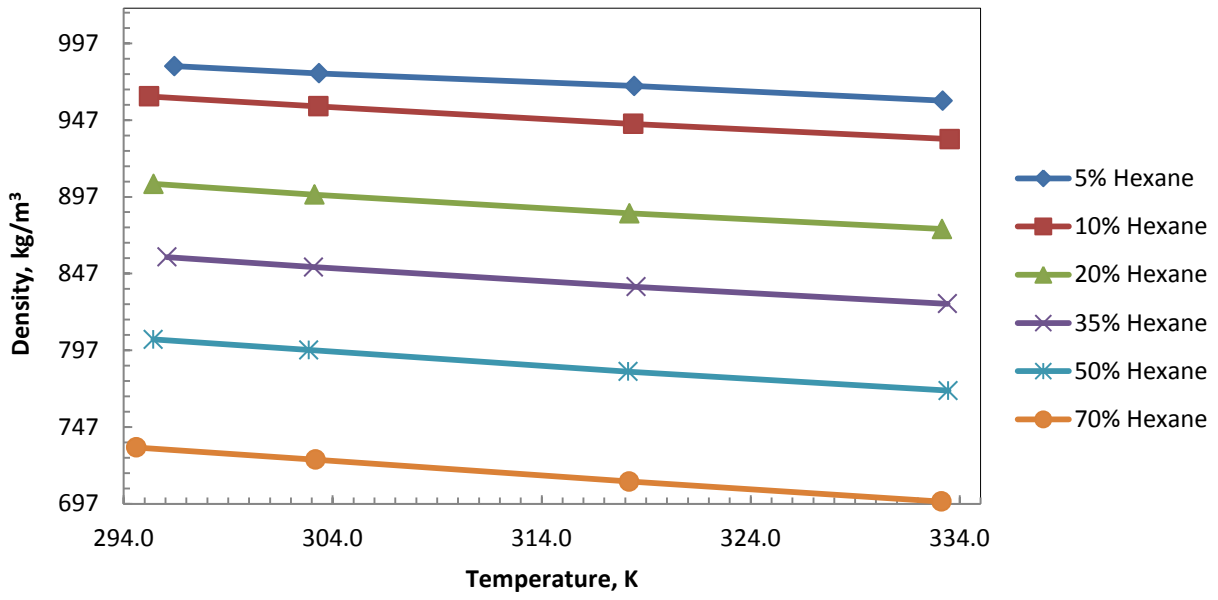

Figure 4-8: Density variation of hexane-bitumen mixtures with temperature, at different mass fractions of hexane and at a constant pressure of 1 MPa.

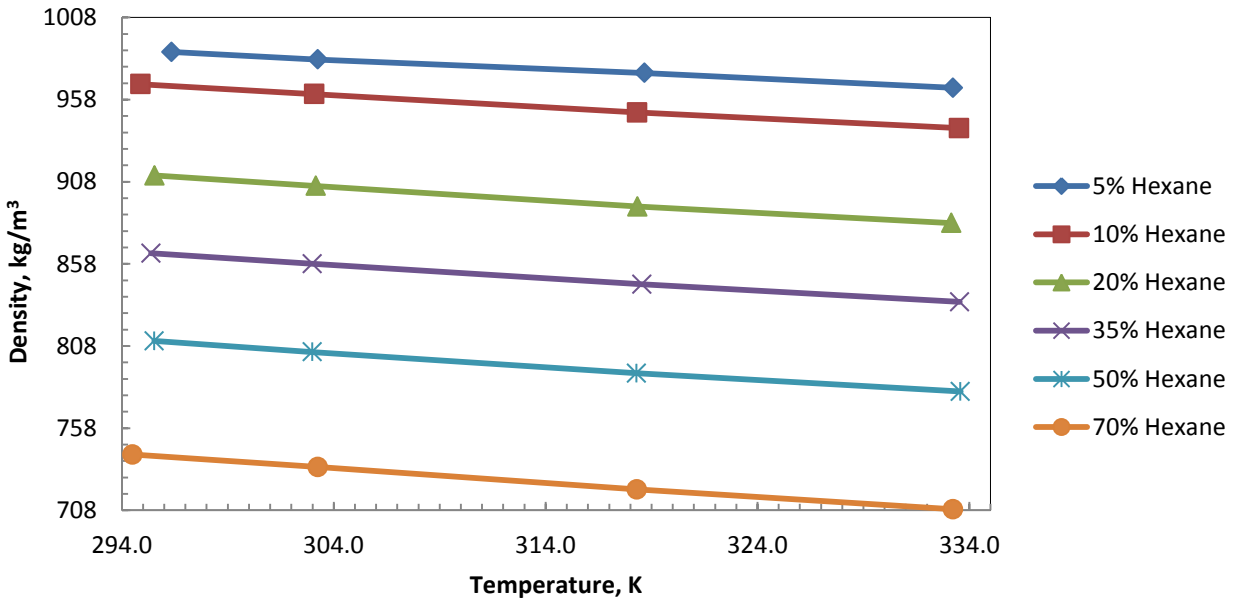

Figure 4-9: Density variation of hexane-bitumen mixtures with temperature at different hexane mass fractions at a constant 10MPa of pressure.

4.5 Physical Properties of Pure Mixtures of Toluene and Hexane

Three mixtures of hexane with toluene were prepared for these measurements. The mass fractions of hexane were 25%, 50%, and 75%. To prepare each mixture, the hexane was transferred to a weighed flask and toluene was carefully added up to the required mass fraction. A total of three different mixtures; mixture 1 (hexane 75% - toluene 25%), mixture 2 (hexane 50% - toluene 50%), and mixture 3 (hexane 25% - toluene 75%) were formed.

The density and viscosity measurements for the pure hexane-toluene (solvent) mixtures were completed at various temperatures and pressures after thoroughly cleaning the equipment. The data is presented in Tables 4-29 to 4-31 for mixtures 1, 2, and 3, respectively. The density data was acquired up to a maximum temperature of 333 K and maximum viscosity of 343 K at pressures from 1 to 10 MPa.

Table 4-29: Experimental measured density and viscosity data for pure mixture 1 (hexane 75%-toluene 25%) as a function of temperature (T) and pressure (P).

Pressure (MPa)	Mixture 1 (hexane 75%-toluene 25%)			
	Temperature (K)	Density (kg/m^3)	Temperature (K)	Viscosity (cp)
1.003	333.3	667.1	343.5	0.1829
1.003	318.3	681.2	325.6	0.2218
1.003	303.2	696.1	310.2	0.2920
1.003	294.6	705.1	298.3	0.3258
3.002	333.4	669.7	343.5	0.1830
3.002	318.3	683.6	325.7	0.2180
3.002	303.1	698.4	310.2	0.2864
3.002	294.6	707.3	298.3	0.3243
5.005	333.5	672.3	343.5	0.1843
5.005	318.3	685.9	325.7	0.2204
5.005	303.1	700.6	310.2	0.2779
5.005	294.6	709.4	298.3	0.3236
7.004	333.5	674.8	343.4	0.1860
7.004	318.3	688.1	325.7	0.2224
7.004	303.0	702.8	310.1	0.2770
7.004	294.5	711.3	298.3	0.3239
10.002	333.6	678.2	343.5	0.1897
10.002	318.3	691.3	325.7	0.2263
10.002	303.0	705.8	310.1	0.2783
10.002	294.5	714.0	298.3	0.3209

Table 4-30: Experimental measured density and viscosity data of pure mixture 2 (hexane 50%-toluene 50%) as a function of temperature (T) and pressure (P).

Pressure (MPa)	Mixture 2 (hexane 50%-toluene 50%)			
	Temperature (K)	Density (kg/m^3)	Temperature (K)	Viscosity (cp)
1.002	333.4	718.2	342.8	0.2170
1.002	318.2	732.7	325.3	0.2566
1.002	303.1	747.8	310.3	0.2967
1.002	296.4	754.6	300.3	0.3360
3.003	333.4	720.7	342.7	0.2151
3.003	318.2	734.9	325.3	0.2563
3.003	303.1	749.7	310.3	0.2981
3.003	296.4	756.5	300.3	0.3326
5.004	333.4	723.1	342.7	0.2174
5.004	318.1	737.4	325.2	0.2563
5.004	303.1	751.7	310.3	0.2959
5.004	296.4	758.4	300.3	0.3327
7.004	333.4	725.4	342.7	0.2183
7.004	318.1	738.6	325.0	0.2569
7.004	303.1	753.6	310.3	0.2964
7.004	296.4	760.2	300.4	0.3330
10.004	333.4	728.8	342.7	0.2220
10.004	317.9	742.5	325.0	0.2606
10.004	303.1	756.4	310.3	0.2980
10.004	296.4	762.8	300.4	0.3349

Table 4-31: Experimental measured density and viscosity data of pure mixture 3 (hexane 25%-toluene 75%) as a function of temperature, (T) and pressure (P).

Pressure (MPa)	Mixture 3 (hexane 25%-toluene 75%)			
	Temperature (K)	Density (kg/m^3)	Temperature (K)	Viscosity (cp)
1.002	332.9	770.3	342.4	0.2434
1.002	318.0	784.2	325.2	0.2903
1.002	303.1	799.0	310.4	0.3421
1.002	295.6	806.8	299.6	0.3920
3.002	332.9	772.5	342.4	0.2407
3.002	318.0	786.2	325.2	0.2883
3.002	303.1	800.8	310.4	0.3401
3.002	295.7	808.5	299.7	0.3903
5.004	332.9	774.7	342.4	0.2426
5.004	317.9	788.2	325.1	0.2890
5.004	303.2	802.7	310.5	0.3404
5.004	295.7	810.2	299.7	0.3891
7.003	332.8	776.8	342.4	0.2439
7.003	317.9	790.1	325.1	0.2904
7.003	303.2	804.4	310.4	0.3410
7.003	295.7	811.8	299.7	0.3906
10.004	332.8	779.9	342.3	0.2464
10.004	317.9	792.9	325.1	0.2943
10.004	303.2	806.9	310.4	0.3457
10.004	295.8	814.2	299.8	0.3939

4.6 Physical Properties of Bitumen/Mixture 1 (Hexane 75%-Toluene 25%)

4.6.1 Measured Viscosity Data of Mixture 1 Diluted Bitumen

The viscosity of the considered mixture was measured at various pressures and temperatures with the same technique used in the previous experiments. The dependence of the viscosity of the mixture on the pressure, temperature, and composition of the solvent mixture was measured.

Tables 4-32 to 4-38 summarize the viscosity of the mixture at various temperatures and pressures. The mixture 1 mass compositions were 5%, 10%, 20%, 35%, 50%, 70%, and 80 %. Measurements for this mixture were completed up to 80% mass composition of mixture 1in order to observe asphaltene precipitation.

Table 4-32: Experimental measured viscosity data for bitumen diluted with mixture 1 as a function of temperature (T) and pressure (P) with a constant mass fraction of mixture 1 (w_s = 0.05) in the mixture.

$W_S = 0.05$

P (MPa)	T (K)	μ_m (cp)	P (MPa)	T (K)	μ_m (cp)
1.003	344.8	274.3	7.003	344.7	355.1
1.003	327.1	890.9	7.003	327.1	1125.2
1.003	311.2	3362.4	7.003	311.2	4353.0
1.003	302.7	7896.3	7.003	302.9	10312
3.004	344.8	295.6	10.004	344.7	403.4
3.004	327.1	957.5	10.004	327.1	1278.7
3.004	311.2	3675.3	10.004	311.2	4939
3.004	302.7	8715	10.004	303.0	11702
5.003	344.8	321.7	------	-----	------
5.003	327.1	1036.3	------	-----	------
5.003	311.2	4012.7	------	-----	------
5.003	302.7	9487	------	-----	------

Table 4-33: Experimental measured viscosity data for bitumen diluted with mixture 1 as a function of temperature (T) and pressure (P) with a constant mass fraction of mixture 1 (w_s = 0.1) in the mixture.

$W_S = 0.1$

P (MPa)	T (K)	μ_m (cp)	P (MPa)	T (K)	μ_m (cp)
1.003	345.4	78.2	7.003	345.4	94.5
1.003	327.8	203.4	7.003	327.8	245.0
1.003	312.4	528.8	7.003	312.6	636.2
1.003	299.5	1482.1	7.003	299.6	1830.3
3.004	345.4	82.4	10.004	345.4	106.2
3.004	327.8	214.5	10.004	327.8	276.3
3.004	312.5	558.3	10.004	312.6	719.3
3.004	299.5	1588.1	10.004	299.8	2032.3
5.003	345.4	87.6	------	-----	------
5.003	327.8	228.0	------	-----	------
5.003	312.5	593.1	------	-----	------
5.003	299.5	1695.1	------	-----	------

Table 4-34: Experimental measured viscosity data for bitumen diluted with mixture 1 as a function of temperature (T) and pressure (P) with a constant mass fraction of mixture 1 (w_s = 0.2) in the mixture.

$W_S = 0.2$

P (MPa)	T (K)	μ_m (cp)	P (MPa)	T (K)	μ_m (cp)
1.003	344.0	18.41	7.003	343.9	20.60
1.003	326.8	33.88	7.003	326.8	39.00
1.003	311.9	75.75	7.003	312.0	85.16
1.003	299.6	155.68	7.003	299.6	173.43
3.004	344.0	18.98	10.004	343.9	22.14
3.004	326.8	35.56	10.004	326.8	42.28
3.004	311.9	79.01	10.004	311.8	89.79
3.004	299.6	159.13	10.004	299.6	184.97
5.003	344.0	19.81	------	-----	------
5.003	326.8	37.04	------	-----	------
5.003	311.9	82.74	------	-----	------
5.003	299.6	166.30	------	-----	------

Table 4-35: Experimental measured viscosity data for bitumen diluted with mixture 1 as a function of temperature (T) and pressure (P) with a constant mass fraction of mixture 1 (w_s = 0.35) in the mixture.

$W_S = 0.35$

P (MPa)	T (K)	μ_m (cp)	P (MPa)	T (K)	μ_m (cp)
1.003	343.4	3.894	7.003	343.4	3.977
1.003	326.6	5.382	7.003	326.7	6.233
1.003	312.1	8.462	7.003	312.1	9.714
1.003	300.2	13.045	7.003	300.4	14.860
3.004	343.4	3.909	10.004	343.5	4.078
3.004	326.6	5.636	10.004	326.7	6.721
3.004	312.1	8.919	10.004	312.1	10.396
3.004	300.3	13.636	10.004	300.4	15.901
5.003	343.4	3.936	------	-----	------
5.003	326.7	5.868	------	-----	------
5.003	312.1	9.284	------	-----	------
5.003	300.4	14.239	------	-----	------

Table 4-36: Experimental measured viscosity data for bitumen diluted with mixture 1 as a function of temperature (T) and pressure (P) with a constant mass fraction of mixture 1 (w_s = 0.5) in the mixture.

$W_S = 0.5$

P (MPa)	T (K)	μ_m (cp)	P (MPa)	T (K)	μ_m (cp)
1.003	343.2	1.296	7.003	343.3	1.316
1.003	326.3	1.764	7.003	326.1	1.786
1.003	310.6	2.477	7.003	310.5	2.518
1.003	298.8	3.304	7.003	298.9	3.344
3.004	343.2	1.301	10.004	343.3	1.340
3.004	326.2	1.770	10.004	326.1	1.818
3.004	310.6	2.484	10.004	310.5	2.568
3.004	298.8	3.302	10.004	299.1	3.389
5.003	343.2	1.305	------	-----	------
5.003	326.2	1.777	------	-----	------
5.003	310.5	2.497	------	-----	------
5.003	298.8	3.320	------	-----	------

Table 4-37: Experimental measured viscosity data for bitumen diluted with mixture 1 as a function of temperature (T) and pressure (P) with a constant mass fraction of mixture 1 (w_s = 0.7) in the mixture.

$W_S = 0.7$

P (MPa)	T (K)	μ_m (cp)	P (MPa)	T (K)	μ_m (cp)
1.003	343.0	0.4881	7.003	343.0	0.4958
1.003	326.3	0.6107	7.003	326.3	0.6160
1.003	310.9	0.7644	7.003	310.9	0.7671
1.003	299.9	0.9144	7.003	299.7	0.9164
3.004	343.0	0.4891	10.004	343.0	0.5024
3.004	326.3	0.6106	10.004	326.1	0.6267
3.004	310.9	0.7631	10.004	310.9	0.7784
3.004	299.6	0.9143	10.004	299.9	0.9270
5.003	343.0	0.4920	------	-----	------
5.003	326.3	0.6134	------	-----	------
5.003	310.9	0.7629	------	-----	------
5.003	299.7	0.9149	------	-----	------

Table 4-38: Experimental measured viscosity data for bitumen diluted with mixture 1 as a function of temperature (T) and pressure (P) with a constant mass fraction of mixture 1 (w_s = 0.8) in the mixture.

$W_S = 0.8$

P (MPa)	T (K)	μ_m (cp)	P (MPa)	T (K)	μ_m (cp)
1.003	343.1	0.3395	7.003	342.9	0.3410
1.003	325.3	0.4234	7.003	325.3	0.4228
1.003	310.9	0.5110	7.003	310.8	0.5117
1.003	299.9	0.5959	7.003	300.0	0.5949
3.004	343.0	0.3381	10.004	342.9	0.3479
3.004	325.3	0.4219	10.004	325.3	0.4313
3.004	310.9	0.5067	10.004	310.9	0.5199
3.004	300.0	0.5931	10.004	300.0	0.6030
5.003	343.0	0.3396	------	-----	------
5.003	325.3	0.4220	------	-----	------
5.003	310.8	0.5083	------	-----	------
5.003	300.0	0.5910	------	-----	------

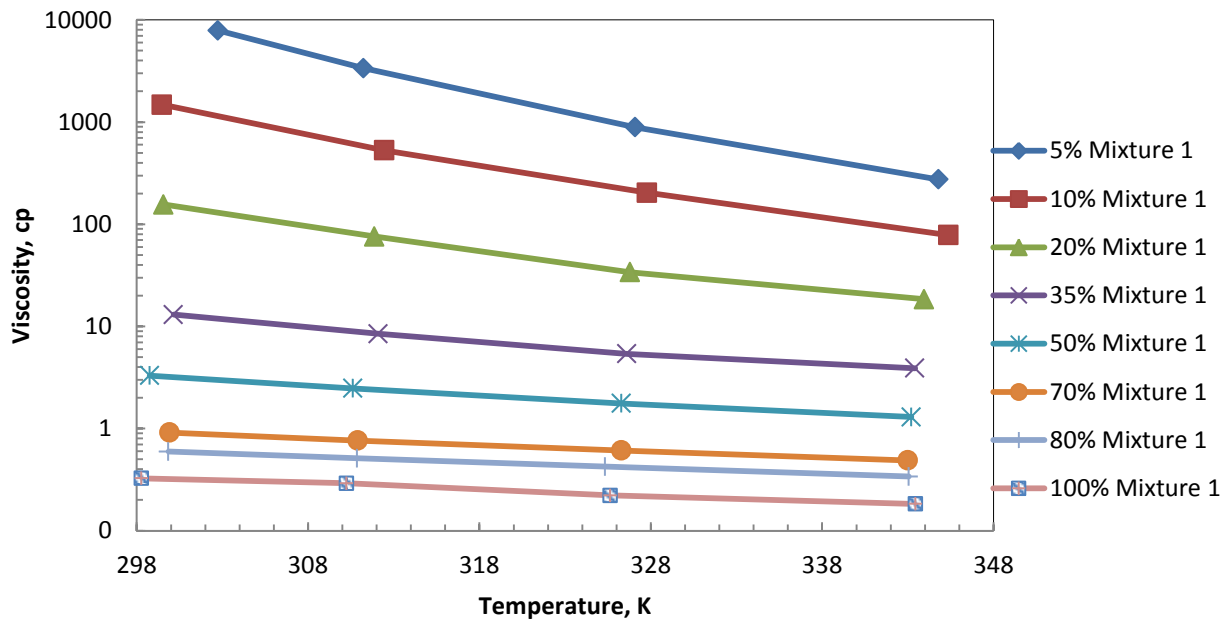

Figure 4-10: Viscosity variations of mixture 1 and bitumen with temperature, at different mass fractions of mixture 1 and 1 MPa constant pressure.

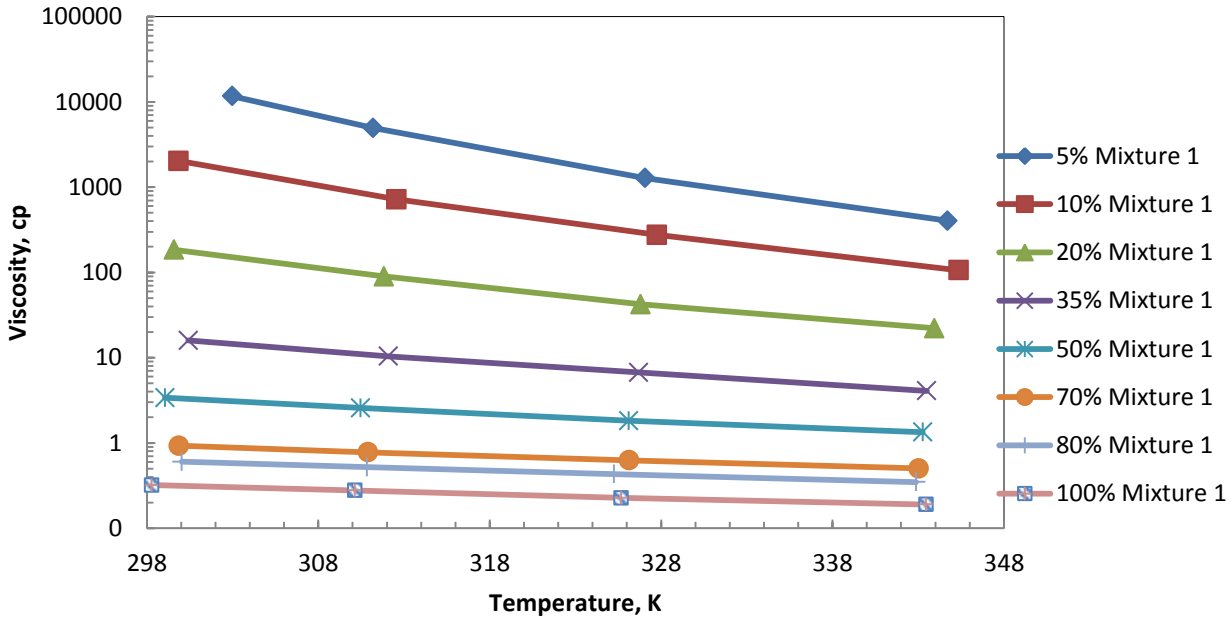

Figure 4-11: Viscosity variations of mixture 1/ bitumen with temperature, at different mass fractions of mixture 1 at constant pressure of 10 MPa.

4.6.2 Measured Density Data of Mixture 1 Diluted Bitumen

The density of the considered mixture was measured at various pressures and temperatures using the same method as the previous experiments. We measured the dependence of the mixture density on pressure, temperature, and the composition of the solvent mixture.

The density data for the mixture is tabulated in Tables 4-39 to 4-45 up to a maximum temperature of 333 K and pressure of 10 MPa. The mass compositions of Mixture 1 were 5%, 10%, 20%, 35%, 50%, 70%, and 80 %.

Table 4-39: Experimental measured density data for bitumen diluted with mixture 1 as a function of temperature (T) and pressure (P) at a constant mass fraction of mixture 1 (w_s = 0.05) in the mixture.

W_S = 0.05

P (MPa)	T (K)	ρ_m (kg/m^3)	P (MPa)	T (K)	ρ_m (kg/m^3)
1.003	333.5	963.5	7.003	333.5	967.2
1.003	318.1	973.4	7.003	318.2	976.9
1.003	303.1	981.5	7.003	303.3	984.7
1.003	298.2	984.8	7.003	298.2	988.0
3.004	333.5	964.8	10.004	333.6	968.9
3.004	318.2	974.7	10.004	318.2	978.6
3.004	303.2	982.6	10.004	303.3	986.3
3.004	298.2	986.0	10.004	298.3	989.5
5.003	333.5	966.0	------	-----	------
5.003	318.2	975.8	------	-----	------
5.003	303.2	983.7	------	-----	------
5.003	298.2	987.0	------	-----	------

Table 4-40: Experimental measured density data for bitumen diluted with mixture 1 as a function of temperature (T) and pressure (P) at a constant mass fraction of mixture 1 (w_s = 0.1) in the mixture.

$W_S = 0.1$

P (MPa)	T (K)	ρ_m (kg/m^3)	P (MPa)	T (K)	ρ_m (kg/m^3)
1.003	333.1	942.2	7.003	333.3	946.1
1.003	318.3	951.9	7.003	318.3	955.6
1.003	303.2	963.6	7.003	303.0	967.2
1.003	294.5	969.8	7.003	294.2	973.2
3.004	333.2	943.6	10.004	333.4	947.9
3.004	318.3	953.2	10.004	318.3	957.4
3.004	303.1	964.8	10.004	303.0	968.8
3.004	294.3	971.0	10.004	294.3	974.7
5.003	333.3	944.8	------	-----	------
5.003	318.3	954.4	------	-----	------
5.003	303.0	966.0	------	-----	------
5.003	294.2	972.2	------	-----	------

Table 4-41: Experimental measured density data for bitumen diluted with mixture 1 as a function of temperature (T) and pressure (P) at a constant mass fraction of mixture 1 (w_s = 0.2) in the mixture.

$W_S = 0.2$

P (MPa)	T (K)	ρ_m (kg/m^3)	P (MPa)	T (K)	ρ_m (kg/m^3)
1.003	333.0	904.8	7.003	333.0	909.2
1.003	318.0	915.2	7.003	318.0	919.2
1.003	303.1	927.3	7.003	303.1	930.7
1.003	294.7	933.5	7.003	294.8	937.1
3.004	333.0	906.3	10.004	333.0	911.3
3.004	318.0	916.5	10.004	318.1	921.1
3.004	303.1	928.3	10.004	303.1	932.6
3.004	294.7	934.7	10.004	294.8	938.8
5.003	333.0	907.8	------	-----	------
5.003	318.0	917.9	------	-----	------
5.003	303.1	929.5	------	-----	------
5.003	294.8	935.9	------	-----	------

Table 4-42: Experimental measured density data for bitumen diluted with mixture 1 as a function of temperature (T) and pressure (P) at a constant mass fraction of mixture 1 (w_s = 0.35) in the mixture.

$W_S = 0.35$

P (MPa)	T (K)	ρ_m (kg/m^3)	P (MPa)	T (K)	ρ_m (kg/m^3)
1.003	333.4	851.3	7.003	333.3	856.3
1.003	317.9	863.1	7.003	318.0	867.6
1.003	303.3	875.5	7.003	303.2	880.0
1.003	295.1	882.2	7.003	295.3	886.1
3.004	333.3	853.0	10.004	333.3	858.6
3.004	317.9	864.6	10.004	318.0	869.8
3.004	303.1	877.2	10.004	303.2	882.0
3.004	295.2	883.5	10.004	295.4	888.0
5.003	333.3	854.7	------	-----	------
5.003	317.9	866.2	------	-----	------
5.003	303.2	878.6	------	-----	------
5.003	295.3	884.8	------	-----	------

Table 4-43: Experimental measured density data for bitumen diluted with mixture 1 as a function of temperature (T) and pressure (P) at a constant mass fraction of mixture 1 (w_s = 0.5) in the mixture.

$W_S = 0.5$

P (MPa)	T (K)	ρ_m (kg/m^3)	P (MPa)	T (K)	ρ_m (kg/m^3)
1.003	333.2	801.8	7.003	333.2	807.6
1.003	318.3	813.8	7.003	318.3	819.0
1.003	303.2	826.7	7.003	303.1	831.6
1.003	294.7	834.7	7.003	294.8	839.2
3.004	333.2	803.8	10.004	333.2	810.1
3.004	318.3	815.6	10.004	318.3	821.4
3.004	303.2	828.3	10.004	303.0	833.9
3.004	294.7	836.3	10.004	294.8	841.3
5.003	333.2	805.7	------	-----	------
5.003	318.3	817.3	------	-----	------
5.003	303.1	830.0	------	-----	------
5.003	294.7	837.8	------	-----	------

Table 4-44: Experimental measured density data for bitumen diluted with mixture 1 as a function of temperature (T) and pressure (P) at a constant mass fraction of mixture 1 (w_s = 0.7) in the mixture.

$W_S = 0.7$

P (MPa)	T (K)	ρ_m (kg/m^3)	P (MPa)	T (K)	ρ_m (kg/m^3)
1.003	333.2	744.0	7.003	333.2	750.6
1.003	318.5	756.5	7.003	318.6	762.4
1.003	303.3	769.8	7.003	303.4	775.4
1.003	295.7	777.9	7.003	295.6	783.3
3.004	333.2	746.3	10.004	333.2	753.5
3.004	318.5	758.6	10.004	318.6	765.1
3.004	303.3	771.8	10.004	303.4	778.0
3.004	295.5	779.9	10.004	295.6	785.7
5.003	333.2	748.5	------	-----	------
5.003	318.6	760.5	------	-----	------
5.003	303.4	773.6	------	-----	------
5.003	295.5	781.6	------	-----	------

Table 4-45: Experimental measured density data for bitumen diluted with mixture 1 as a function of temperature (T) and pressure (P) at a constant mass fraction of mixture 1 (w_s = 0.8) in the mixture.

$W_S = 0.8$

P (MPa)	T (K)	ρ_m (kg/m^3)	P (MPa)	T (K)	ρ_m (kg/m^3)
1.003	333.4	716.3	7.003	333.4	723.4
1.003	318.2	729.9	7.003	318.1	736.4
1.003	303.5	743.1	7.003	303.5	749.2
1.003	295.7	751.4	7.003	295.9	756.8
3.004	333.4	718.8	10.004	333.4	727.1
3.004	318.2	732.2	10.004	318.0	739.3
3.004	303.5	745.1	10.004	303.5	752.1
3.004	295.7	753.3	10.004	295.9	759.3
5.003	333.4	721.1	------	-----	------
5.003	318.1	734.3	------	-----	------
5.003	303.5	747.2	------	-----	------
5.003	295.8	755.0	------	-----	------

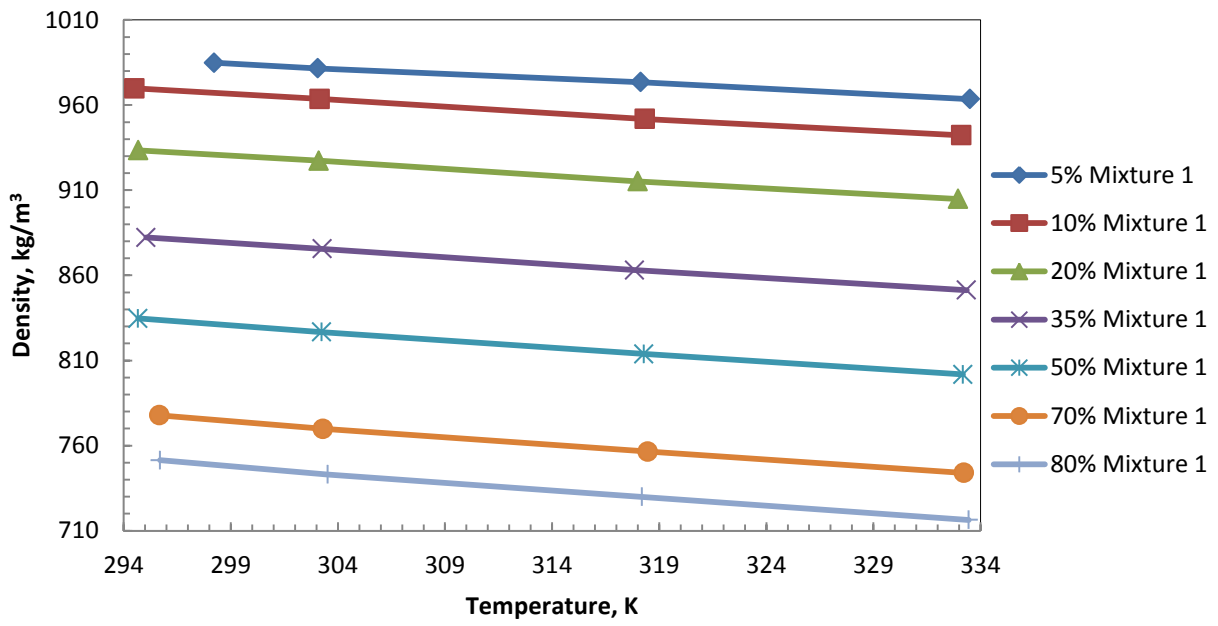

Figure 4-12: Density variations of mixture 1/ bitumen with temperature, at different mass fractions of mixture 1 at a constant pressure of 1 MPa.

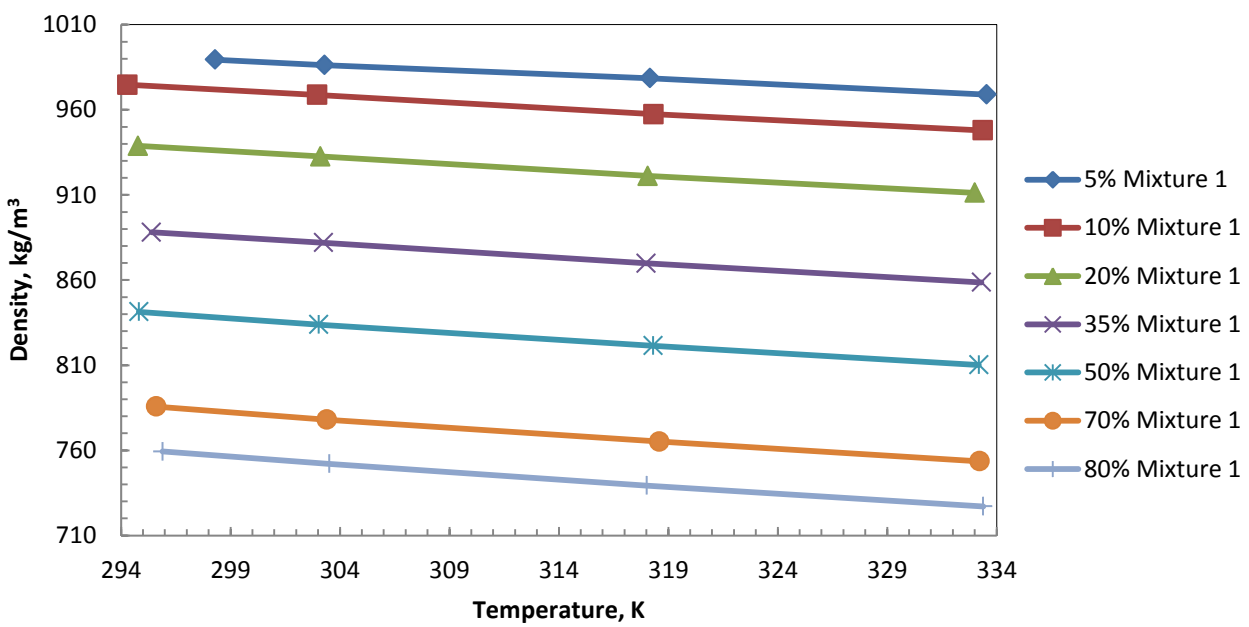

Figure 4-13: Density variations of mixture 1/ bitumen with temperature, at different mass fractions of mixture 1 at a constant pressure of 10 MPa.

4.7 Physical Properties of Bitumen/Mixture 2 (Hexane 50%-Toluene 50%)

4.7.1 Measured Viscosity Data of Mixture 2 Diluted Bitumen

The viscosity of the mixture 2 was measured at pressures and temperatures similar to those for mixture 1. The viscosity was determined to be dependent on the pressure, temperature, and composition of solvent mixture.

Tables 4-46 to 4-52 summarize the viscosity data for the mixtures at various temperatures and pressures. In Tables 4-46 to 4-52, the mass compositions of mixture 2 are 5%, 10%, 20%, 35%, 50%, 70%, and 80 %, respectively.

Table 4-46: Experimental measured viscosity data for bitumen diluted with mixture 2 as a function of temperature (T) and pressure (P) at constant mass fraction of mixture 2 (w_s = 0.05) in the mixture.

W_S = 0.05

P (MPa)	T (K)	μ_m (cp)	P (MPa)	T (K)	μ_m (cp)
1.003	344.7	300.9	7.004	344.6	363.6
1.003	326.9	965.6	7.004	327.0	1208.6
1.003	311.3	3443.3	7.004	311.3	4379.3
1.003	302.3	8690.9	7.004	301.8	12032.7
3.005	344.7	318.5	10.004	344.6	412.4
3.005	326.9	1038.7	10.004	327.0	1378.3
3.005	311.3	3734.4	10.004	311.3	4985.0
3.005	302.1	9797.7	10.004	301.7	14112.1
5.004	344.7	339.5	------	-----	------
5.004	327.0	1117.0	------	-----	------
5.004	311.3	4049.3	------	-----	------
5.004	302.0	10867.1	------	-----	------

Table 4-47: Experimental measured viscosity data for bitumen diluted with mixture 2 as a function of temperature (T) and pressure (P) at constant mass fraction of mixture 2 (w_s = 0.1) in the mixture.

$W_S = 0.1$

P (MPa)	T (K)	μ_m (cp)	P (MPa)	T (K)	μ_m (cp)
1.003	344.8	100.1	7.004	344.8	119.0
1.003	327.2	264.1	7.004	327.2	317.9
1.003	312.9	659.5	7.004	312.8	822.2
1.003	302.1	1590.2	7.004	302.1	1963.9
3.005	344.8	106.0	10.004	344.8	134.2
3.005	327.2	275.7	10.004	327.2	355.4
3.005	312.8	701.2	10.004	312.8	942.2
3.005	302.1	1699.7	10.004	302.1	2244.9
5.004	344.8	111.9	------	-----	------
5.004	327.2	294.1	------	-----	------
5.004	312.8	754.8	------	-----	------
5.004	302.1	1826.4	------	-----	------

Table 4-48: Experimental measured viscosity data for bitumen diluted with mixture 2 as a function of temperature (T) and pressure (P) at constant mass fraction of mixture 2 (w_s = 0.2) in the mixture.

$W_S = 0.2$

P (MPa)	T (K)	μ_m (cp)	P (MPa)	T (K)	μ_m (cp)
1.003	344.3	21.54	7.004	344.2	24.48
1.003	326.5	39.52	7.004	326.4	45.58
1.003	311.9	79.59	7.004	311.8	92.17
1.003	301.8	142.34	7.004	302.0	172.30
3.005	344.3	22.40	10.004	344.2	26.48
3.005	326.4	41.24	10.004	326.4	50.17
3.005	311.9	82.93	10.004	311.8	99.55
3.005	302.0	149.27	10.004	302.1	192.83
5.004	344.2	23.39	------	-----	------
5.004	326.4	43.31	------	-----	------
5.004	311.8	87.30	------	-----	------
5.004	302.0	160.26	------	-----	------

Table 4-49: Experimental measured viscosity data for bitumen diluted with mixture 2 as a function of temperature (T) and pressure (P) at constant mass fraction of mixture 2 (w_s = 0.35) in the mixture.

$W_S = 0.35$

P (MPa)	T (K)	μ_m (cp)	P (MPa)	T (K)	μ_m (cp)
1.003	343.0	4.499	7.004	343.0	4.619
1.003	326.4	6.233	7.004	326.4	7.149
1.003	312.0	10.067	7.004	311.9	11.594
1.003	300.7	15.159	7.004	300.8	17.333
3.005	343.0	4.525	10.004	343.0	4.715
3.005	326.4	6.564	10.004	326.4	7.788
3.005	311.9	10.534	10.004	311.8	12.469
3.005	300.8	15.741	10.004	300.8	18.499
5.004	343.0	4.567	------	-----	------
5.004	326.4	6.818	------	-----	------
5.004	311.9	11.093	------	-----	------
5.004	300.8	16.537	------	-----	------

Table 4-50: Experimental measured viscosity data for bitumen diluted with mixture 2 as a function of temperature (T) and pressure (P) at constant mass fraction of mixture 2 (w_s = 0.5) in the mixture.

$W_S = 0.5$

P (MPa)	T (K)	μ_m (cp)	P (MPa)	T (K)	μ_m (cp)
1.003	343.1	1.538	7.004	343.2	1.564
1.003	326.1	2.117	7.004	326.2	2.145
1.003	310.6	2.969	7.004	310.5	3.031
1.003	299.8	3.847	7.004	299.8	3.900
3.005	343.1	1.539	10.004	343.2	1.586
3.005	326.1	2.119	10.004	326.2	2.193
3.005	310.6	2.982	10.004	310.5	3.085
3.005	299.8	3.855	10.004	299.8	3.996
5.004	343.2	1.558	------	-----	------
5.004	326.1	2.126	------	-----	------
5.004	310.5	3.001	------	-----	------
5.004	299.7	3.894	------	-----	------

Table 4-51: Experimental measured viscosity data for bitumen diluted with mixture 2 as a function of temperature (T) and pressure (P) at constant mass fraction of mixture 2 (w_s = 0.7) in the mixture.

$W_S = 0.7$

P (MPa)	T (K)	μ_m (cp)	P (MPa)	T (K)	μ_m (cp)
1.003	342.8	0.576	7.004	342.9	0.576
1.003	325.5	0.734	7.004	325.4	0.738
1.003	310.7	0.915	7.004	310.7	0.914
1.003	300.1	1.083	7.004	299.9	1.091
3.005	342.8	0.573	10.004	343.0	0.583
3.005	325.5	0.730	10.004	325.4	0.748
3.005	310.7	0.908	10.004	310.6	0.923
3.005	300.1	1.085	10.004	299.7	1.108
5.004	343.0	0.574	------	-----	------
5.004	325.5	0.732	------	-----	------
5.004	310.7	0.910	------	-----	------
5.004	300.0	1.085	------	-----	------

Table 4-52: Experimental measured viscosity data for bitumen diluted with mixture 2 as a function of temperature (T) and pressure (P) at constant mass fraction of mixture 2 (w_s = 0.8) in the mixture.

$W_S = 0.8$

P (MPa)	T (K)	μ_m (cp)	P (MPa)	T (K)	μ_m (cp)
1.003	342.8	0.391	7.004	342.9	0.391
1.003	325.4	0.480	7.004	325.4	0.485
1.003	310.6	0.581	7.004	310.6	0.582
1.003	299.9	0.679	7.004	300.0	0.679
3.005	342.8	0.390	10.004	342.9	0.396
3.005	325.4	0.476	10.004	325.4	0.490
3.005	310.6	0.579	10.004	310.7	0.590
3.005	300.0	0.677	10.004	300.0	0.685
5.004	342.9	0.389	------	-----	------
5.004	325.4	0.479	------	-----	------
5.004	310.6	0.581	------	-----	------
5.004	300.0	0.676	------	-----	------

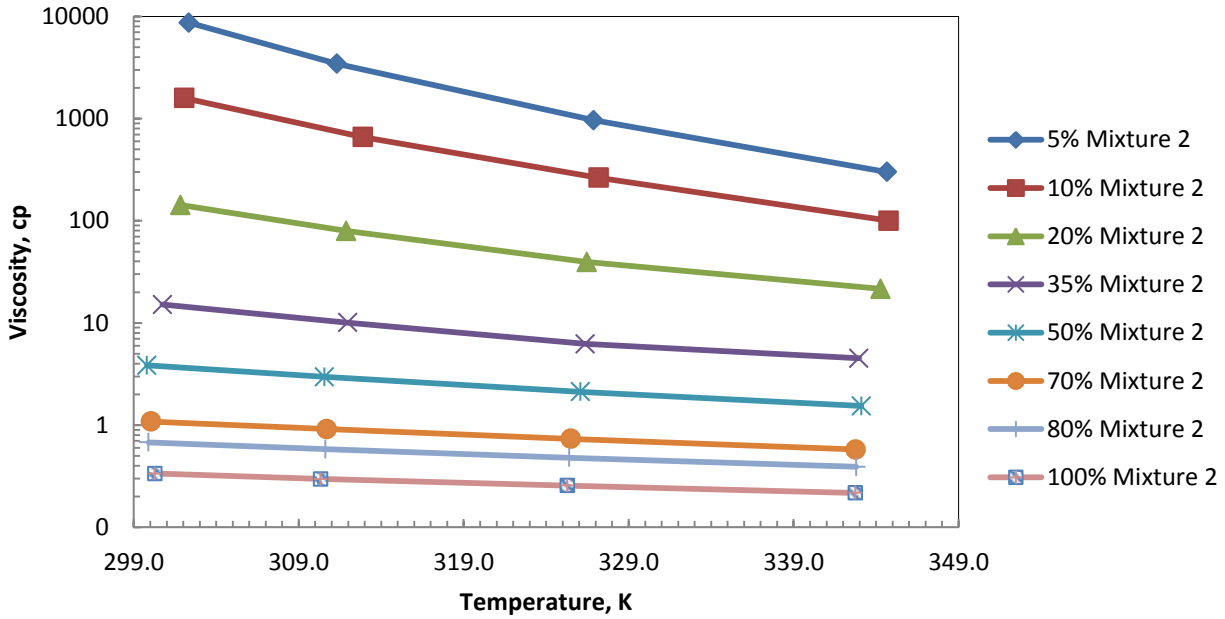

Figure 4-14: Viscosity variations of mixture 2/ bitumen with temperature, at different mass fractions of mixture 2 at a constant pressure of 1MPa.

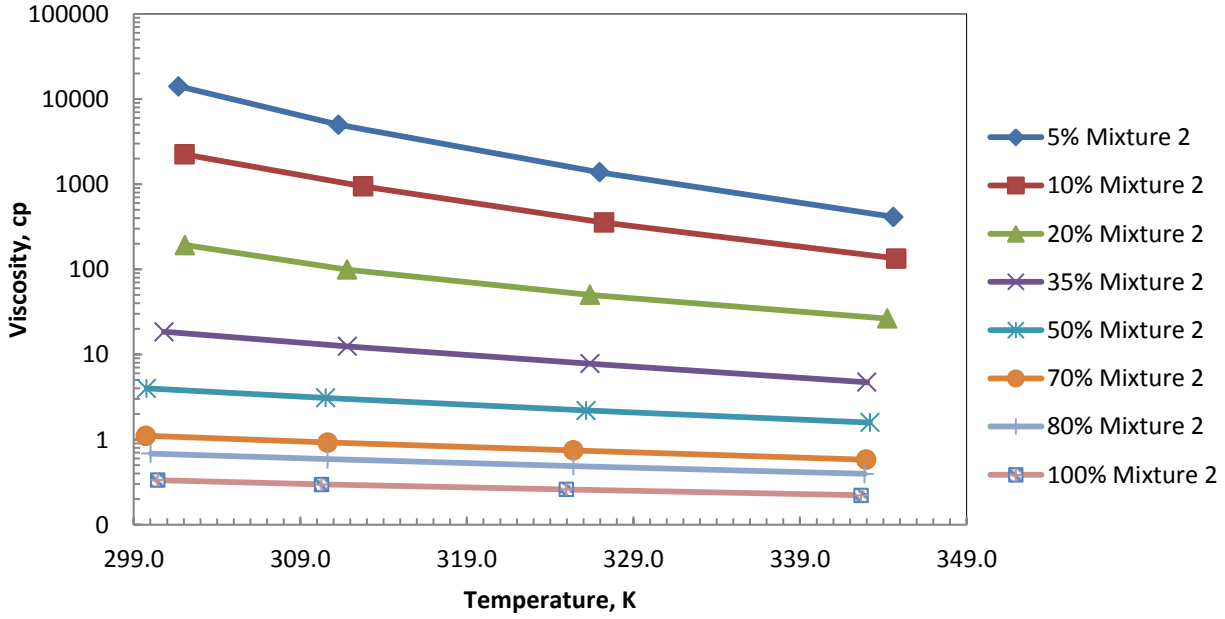

Figure 4-15: Viscosity variations of mixture 2/ bitumen with temperature, at different mass fractions of mixture 2 at a constant pressure of 10 MPa.

4.7.2 Measured Density Data of Mixture 2 Diluted Bitumen

The density of the mixture was measured at various pressures and temperatures with a similar method to the previous experiments. We measured the dependence of the density of the mixture on pressure, temperature, and the composition of the solvent mixture.

The density data of mixture is tabulated in Tables 4-53 to 4-59 up to a maximum temperature and pressure of 333 K and 10 MPa, respectively. The mass compositions of mixture 2 were 5%, 10%, 20%, 35%, 50%, 70%, and 80 %, respectively.

Table 4-53: Experimental measured density data of bitumen diluted with mixture 2 as a function of temperature (T) and pressure (P) at a constant mass fraction of mixture 2 (w_s = 0.05) in the mixture.

W_S = 0.05

P (MPa)	T (K)	ρ_m (kg/m^3)	P (MPa)	T (K)	ρ_m (kg/m^3)
1.003	333.3	967.3	7.004	333.4	971.0
1.003	318.1	977.2	7.004	318.0	980.7
1.003	303.3	985.1	7.004	303.3	988.4
1.003	297.7	988.9	7.004	297.5	992.3
3.005	333.3	968.6	10.004	333.4	972.7
3.005	318.0	978.5	10.004	318.0	982.3
3.005	303.3	986.2	10.004	303.3	989.9
3.005	297.6	990.1	10.004	297.3	993.9
5.004	333.3	969.8	------	-----	------
5.004	318.0	979.5	------	-----	------
5.004	303.3	987.3	------	-----	------
5.004	297.6	991.2	------	-----	------

Table 4-54: Experimental measured density data of bitumen diluted with mixture 2 as a function of temperature (T) and pressure (P) at a constant mass fraction of mixture 2 (w_s = 0.1) in the mixture.

$W_S = 0.1$

P (MPa)	T (K)	ρ_m (kg/m^3)	P (MPa)	T (K)	μ_m (cp)
1.003	333.2	951.6	7.004	333.2	955.5
1.003	318.0	961.5	7.004	318.1	965.1
1.003	303.1	973.0	7.004	303.2	976.4
1.003	296.5	977.6	7.004	296.5	980.9
3.005	333.2	952.9	10.004	333.2	957.3
3.005	318.0	962.7	10.004	318.1	966.8
3.005	303.2	974.1	10.004	303.3	978.0
3.005	296.5	978.8	10.004	296.6	982.5
5.004	333.2	954.2	------	-----	------
5.004	318.1	963.9	------	-----	------
5.004	303.2	975.3	------	-----	------
5.004	296.5	979.9	------	-----	------

Table 4-55: Experimental measured density data of bitumen diluted with mixture 2 as a function of temperature (T) and pressure (P) at a constant mass fraction of mixture 2 (w_s = 0.2) in the mixture.

$W_S = 0.2$

P (MPa)	T (K)	ρ_m (kg/m^3)	P (MPa)	T (K)	ρ_m (kg/m^3)
1.003	333.2	920.2	7.004	333.3	924.3
1.003	318.0	930.8	7.004	318.0	934.8
1.003	303.1	942.7	7.004	303.2	946.4
1.003	296.3	948.0	7.004	296.5	951.4
3.005	333.3	921.6	10.004	333.3	926.3
3.005	318.0	932.2	10.004	318.0	936.7
3.005	303.1	943.9	10.004	303.3	948.1
3.005	296.3	949.2	10.004	296.5	953.1
5.004	333.3	923.0	------	-----	------
5.004	318.0	933.5	------	-----	------
5.004	303.2	945.2	------	-----	------
5.004	296.4	950.3	------	-----	------

Table 4-56: Experimental measured density data of bitumen diluted with mixture 2 as a function of temperature (T) and pressure (P) at a constant mass fraction of mixture 2 (w_s = 0.35) in the mixture.

$W_S = 0.35$

P (MPa)	T (K)	ρ_m (kg/m^3)	P (MPa)	T (K)	ρ_m (kg/m^3)
1.003	333.0	877.2	7.004	333.1	881.9
1.003	318.0	888.3	7.004	317.9	892.7
1.003	303.3	900.6	7.004	303.3	904.9
1.003	295.9	907.1	7.004	295.9	911.0
3.005	333.0	878.8	10.004	333.1	884.1
3.005	317.9	889.8	10.004	318.0	894.7
3.005	303.3	902.1	10.004	303.3	906.9
3.005	295.9	908.4	10.004	296.0	912.9
5.004	333.1	880.4	------	-----	------
5.004	317.9	891.2	------	-----	------
5.004	303.3	903.5	------	-----	------
5.004	295.9	909.7	------	-----	------

Table 4-57: Experimental measured density data of bitumen diluted with mixture 2 as a function of temperature (T) and pressure (P) at a constant mass fraction of mixture 2 (w_s = 0.5) in the mixture.

W_S = 0.5

P (MPa)	T (K)	ρ_m (kg/m^3)	P (MPa)	T (K)	ρ_m (kg/m^3)
1.003	332.9	836.7	7.004	333.1	841.4
1.003	318.1	848.2	7.004	318.2	853.1
1.003	303.2	861.6	7.004	303.1	866.2
1.003	295.5	867.8	7.004	295.6	872.2
3.005	332.9	838.5	10.004	333.1	844.0
3.005	318.1	849.9	10.004	318.3	855.4
3.005	303.1	863.1	10.004	303.1	868.3
3.005	295.6	869.3	10.004	295.7	874.3
5.004	333.0	839.9	------	-----	------
5.004	318.2	851.5	------	-----	------
5.004	303.1	864.7	------	-----	------
5.004	295.6	870.8	------	-----	------

Table 4-58: Experimental measured density data of bitumen diluted with mixture 2 as a function of temperature (T) and pressure (P) at a constant mass fraction of mixture 2 (w_s = 0.7) in the mixture.

W_S = 0.7

P (MPa)	T (K)	ρ_m (kg/m^3)	P (MPa)	T (K)	ρ_m (kg/m^3)
1.003	333.0	786.2	7.004	333.1	792.2
1.003	318.1	798.9	7.004	318.0	804.5
1.003	303.2	812.0	7.004	303.2	817.2
1.003	296.0	819.6	7.004	295.9	824.7
3.005	333.0	788.1	10.004	333.1	794.9
3.005	318.0	800.9	10.004	318.0	807.1
3.005	303.2	813.8	10.004	303.2	819.5
3.005	296.0	821.3	10.004	295.8	827.1
5.004	333.1	790.2	------	-----	------
5.004	318.0	802.7	------	-----	------
5.004	303.2	815.6	------	-----	------
5.004	295.9	823.0	------	-----	------

Table 4-59: Experimental measured density data of bitumen diluted with mixture 2 as a function of temperature (T) and pressure (P) at a constant mass fraction of mixture 2 (w_s = 0.8) in the mixture.

W_S = 0.8

P (MPa)	T (K)	ρ_m (kg/m^3)	P (MPa)	T (K)	ρ_m (kg/m^3)
1.003	332.9	763.3	7.004	333.0	769.6
1.003	318.0	776.4	7.004	317.9	782.3
1.003	303.2	789.1	7.004	303.2	794.7
1.003	296.1	797.4	7.004	296.0	802.6
3.005	332.9	765.5	10.004	333.0	772.6
3.005	317.9	778.4	10.004	317.9	785.0
3.005	303.2	791.1	10.004	303.2	797.3
3.005	296.0	799.3	10.004	296.0	805.0
5.004	333.0	767.6	------	-----	------
5.004	317.9	780.4	------	-----	------
5.004	303.2	792.9	------	-----	------
5.004	296.0	801.0	------	-----	------

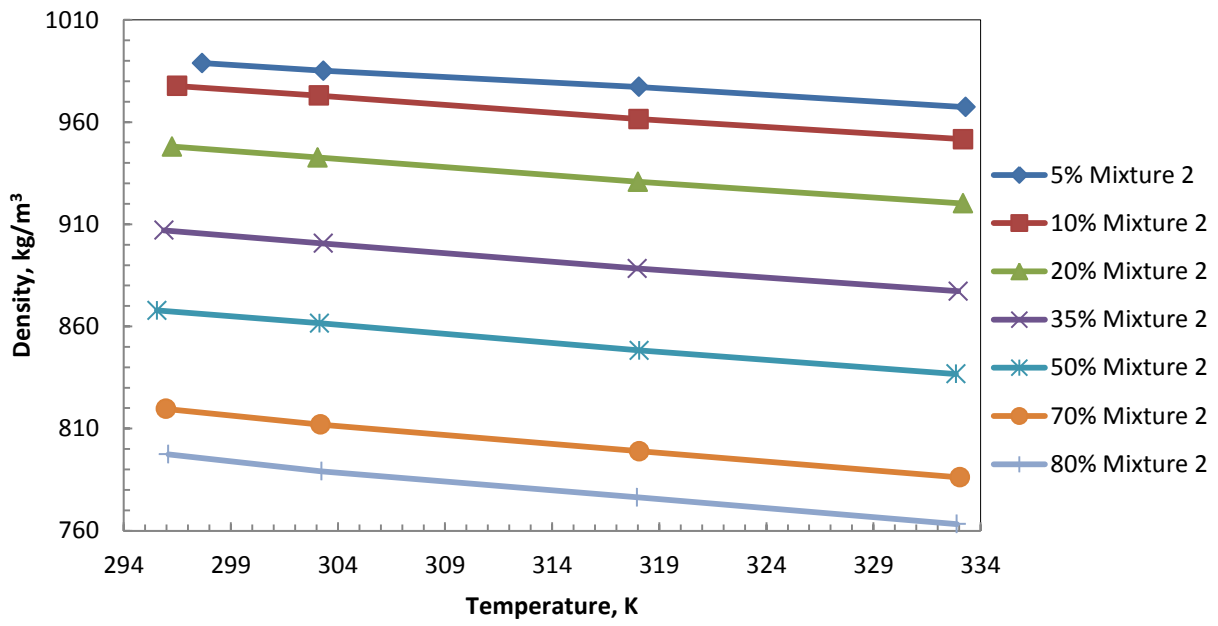

Figure 4-16: Density variations of mixture 2/ bitumen with temperature, at different mass fractions of mixture 2 at a constant pressure of 1 MPa.

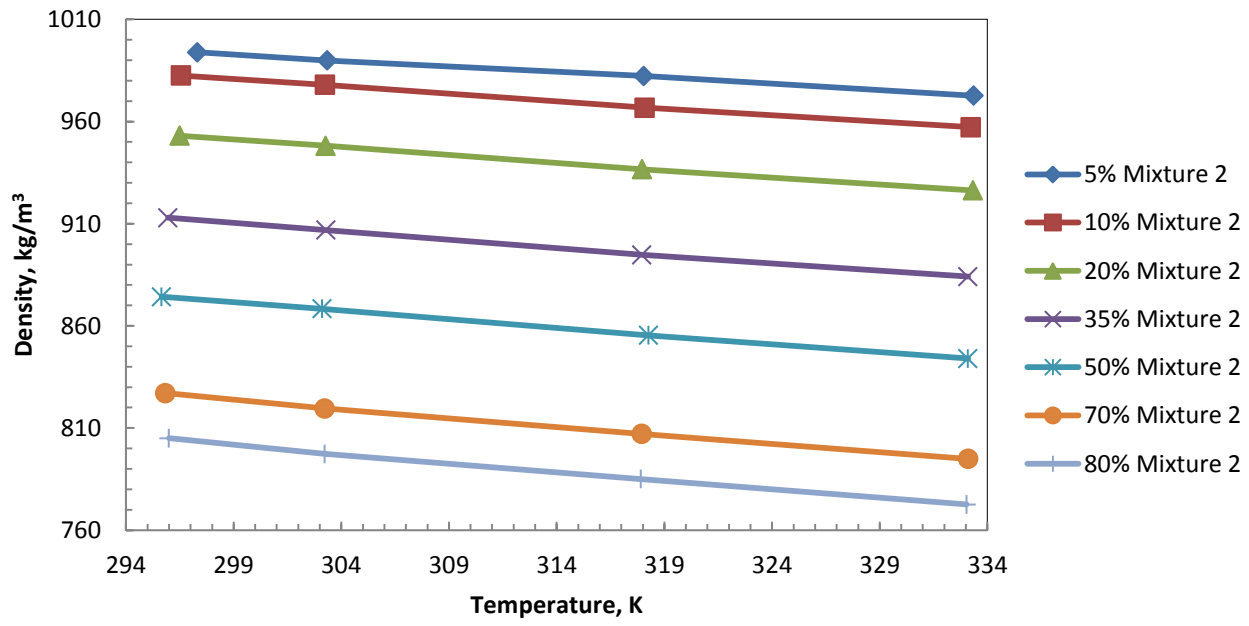

Figure 4-17: Density variations of mixture 2/ bitumen with temperature, at different mass fractions of mixture 2 at a constant pressure of 10 MPa.

4.8 Physical Properties of Bitumen/Mixture 3 (Hexane 25%-Toluene 75%)

4.8.1 Measured Viscosity Data of Mixture 3 Diluted Bitumen

The viscosity of mixture 3 was measured at pressures and temperatures similar to those measured for all previous mixtures. The viscosity was found to be dependent on pressure, temperature, and the composition of solvent mixture.

Tables 4-60 to 4-66 summarize the viscosity data of the mixture under consideration at various temperatures and pressures. In tables 4-60 to 4-66, the mass compositions of mixture 3 are 5%, 10%, 20%, 35%, 50%, 70%, and 80 %, respectively.

Table 4-60: Experimental measured viscosity data for bitumen diluted with mixture 3 as a function of temperature (T) and pressure (P) at a constant mass fraction of mixture 3 (w_s = 0.05) in the mixture.

W_S = 0.05

P (MPa)	T (K)	μ_m (cp)	P (MPa)	T (K)	μ_m (cp)
1.003	344.5	301.3	7.003	344.4	368.2
1.003	327.0	960.1	7.003	327.0	1205.3
1.003	311.2	3841.1	7.003	311.2	4999.9
1.003	302.2	9736.6	7.003	302.2	12984.7
3.004	344.5	320.4	10.003	344.4	419.5
3.004	327.0	1030.9	10.003	327.0	1395.5
3.004	311.2	4248.4	10.003	311.2	5677.9
3.004	302.1	10873.6	10.003	302.1	15099.9
5.004	344.4	342.9	------	-----	------
5.004	327.0	1113.3	------	-----	------
5.004	311.2	4626.4	------	-----	------
5.004	302.2	11825.2	------	-----	------

Table 4-61: Experimental measured viscosity data for bitumen diluted with mixture 3 as a function of temperature (T) and pressure (P) at a constant mass fraction of mixture 3 (w_s = 0.1) in the mixture.

$W_S = 0.1$

P (MPa)	T (K)	μ_m (cp)	P (MPa)	T (K)	μ_m (cp)
1.003	344.5	105.2	7.003	344.5	125.5
1.003	326.9	277.7	7.003	327.0	334.1
1.003	312.8	693.7	7.003	312.7	869.0
1.003	300.9	2169.3	7.003	301.1	2748.8
3.004	344.6	110.6	10.003	344.5	143.7
3.004	326.9	293.2	10.003	327.0	374.5
3.004	312.8	739.4	10.003	312.7	989.0
3.004	301.0	2344.0	10.003	301.1	3095.7
5.004	344.5	117.5	------	-----	------
5.004	327.0	312.5	------	-----	------
5.004	312.7	797.1	------	-----	------
5.004	301.0	2609.1	------	-----	------

Table 4-62: Experimental measured viscosity data for bitumen diluted with mixture 3 as a function of temperature (T) and pressure (P) at a constant mass fraction of mixture 3 (w_s = 0.2) in the mixture.

W_S = 0.2

P (MPa)	T (K)	μ_m (cp)	P (MPa)	T (K)	μ_m (cp)
1.003	343.7	22.58	7.003	343.8	24.47
1.003	327.2	41.56	7.003	327.3	46.52
1.003	311.7	86.29	7.003	311.8	97.25
1.003	301.2	159.83	7.003	301.3	195.46
3.004	343.7	23.18	10.003	343.7	26.23
3.004	327.2	42.83	10.003	327.3	50.18
3.004	311.7	89.75	10.003	311.7	104.69
3.004	301.2	169.11	10.003	301.4	214.30
5.004	343.7	23.55	------	-----	------
5.004	327.3	44.44	------	-----	------
5.004	311.8	93.30	------	-----	------
5.004	301.3	180.43	------	-----	------

Table 4-63: Experimental measured viscosity data for bitumen diluted with mixture 3 as a function of temperature (T) and pressure (P) at a constant mass fraction of mixture 3 (w_s = 0.35) in the mixture.

$W_S = 0.35$

P (MPa)	T (K)	μ_m (cp)	P (MPa)	T (K)	μ_m (cp)
1.003	343.3	4.133	7.003	343.3	4.744
1.003	326.3	6.885	7.003	326.3	7.848
1.003	311.9	10.851	7.003	311.8	12.396
1.003	301.2	15.936	7.003	301.2	18.076
3.004	343.4	4.325	10.003	343.6	5.148
3.004	326.2	7.178	10.003	326.3	8.363
3.004	311.8	11.381	10.003	311.8	13.254
3.004	301.2	16.493	10.003	301.3	19.234
5.004	343.3	4.513	------	-----	------
5.004	326.2	7.475	------	-----	------
5.004	311.8	11.879	------	-----	------
5.004	301.2	17.349	------	-----	------

Table 4-64: Experimental measured viscosity data for bitumen diluted with mixture 3 as a function of temperature (T) and pressure (P) at a constant mass fraction of mixture 3 (w_s = 0.5) in the mixture.

W_S = 0.5

P (MPa)	T (K)	μ_m (cp)	P (MPa)	T (K)	μ_m (cp)
1.003	342.9	1.765	7.003	342.8	1.784
1.003	325.5	2.489	7.003	325.5	2.521
1.003	310.8	3.455	7.003	310.8	3.511
1.003	300.6	4.436	7.003	300.7	4.510
3.004	342.9	1.764	10.003	342.8	1.811
3.004	325.5	2.499	10.003	325.5	2.564
3.004	310.8	3.470	10.003	310.8	3.562
3.004	300.6	4.459	10.003	300.7	4.585
5.004	342.9	1.771	------	-----	------
5.004	325.5	2.504	------	-----	------
5.004	310.8	3.480	------	-----	------
5.004	300.7	4.467	------	-----	------

Table 4-65: Experimental measured viscosity data for bitumen diluted with mixture 3 as a function of temperature (T) and pressure (P) at a constant mass fraction of mixture 3 (w_s = 0.7) in the mixture.

W_S = 0.7

P (MPa)	T (K)	μ_m (cp)	P (MPa)	T (K)	μ_m (cp)
1.003	342.7	0.664	7.003	342.8	0.666
1.003	325.3	0.854	7.003	325.4	0.854
1.003	310.7	1.072	7.003	310.7	1.068
1.003	299.8	1.320	7.003	299.6	1.299
3.004	342.7	0.662	10.003	342.8	0.674
3.004	325.3	0.850	10.003	325.3	0.858
3.004	310.7	1.066	10.003	310.6	1.074
3.004	299.8	1.285	10.003	299.7	1.304
5.004	342.8	0.663	------	-----	------
5.004	325.4	0.850	------	-----	------
5.004	310.7	1.065	------	-----	------
5.004	299.6	1.295	------	-----	------

Table 4-66: Experimental measured viscosity data for bitumen diluted with mixture 3 as a function of temperature (T) and pressure (P) at a constant mass fraction of mixture 3 (w_s = 0.8) in the mixture.

W_S = 0.8

P (MPa)	T (K)	μ_m (cp)	P (MPa)	T (K)	μ_m (cp)
1.003	342.7	0.447	7.003	342.7	0.450
1.003	325.2	0.561	7.003	325.2	0.558
1.003	310.5	0.688	7.003	310.5	0.686
1.003	300.1	0.805	7.003	300.1	0.802
3.004	342.7	0.448	10.003	342.7	0.455
3.004	325.2	0.559	10.003	325.2	0.563
3.004	310.5	0.684	10.003	310.5	0.692
3.004	300.1	0.798	10.003	300.1	0.809
5.004	342.7	0.448	------	-----	------
5.004	325.2	0.557	------	-----	------
5.004	310.5	0.684	------	-----	------
5.004	300.2	0.799	------	-----	------

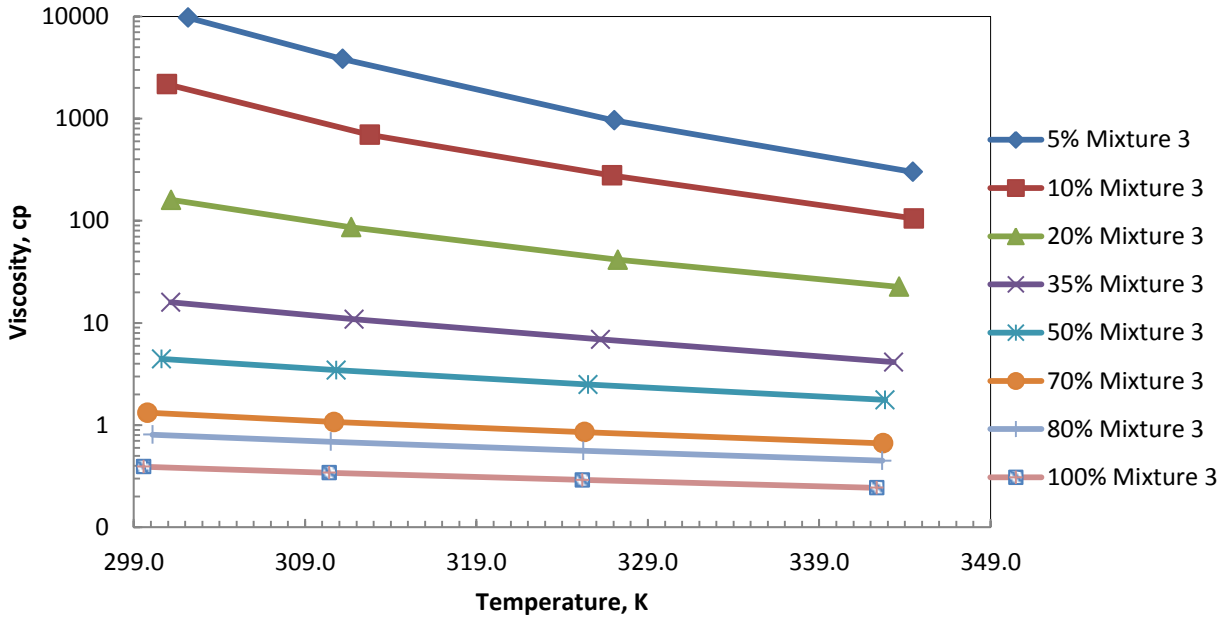

Figure 4-18: Viscosity variations of mixture 3/ bitumen with temperature, at different mass fractions of mixture 3 at a constant pressure of 1 MPa.

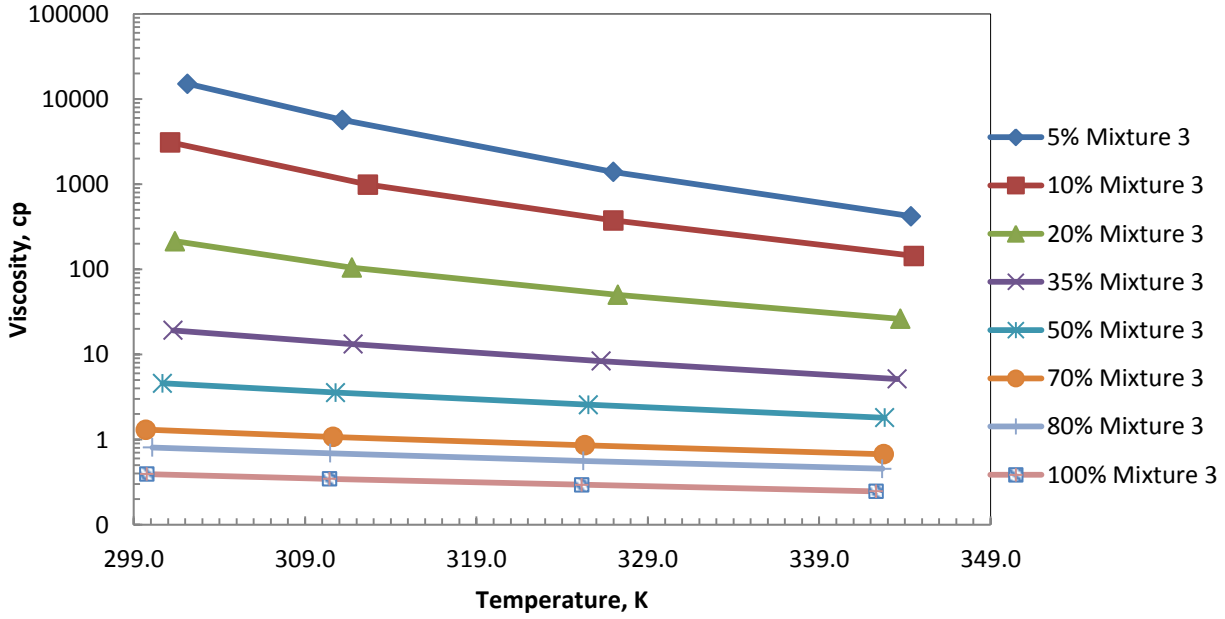

Figure 4-19: Viscosity variations of mixture 3/ bitumen with temperature, at different mass fractions of mixture 3 at a constant pressure of 10 MPa.

4.8.2 Measured Density Data of Mixture 3 Diluted Bitumen

The density data for mixture 3 was measured at pressures and temperatures similar to those for all of the previous mixtures. The viscosity of the mixtures was found to be dependent on pressure, temperature, and the composition of the solvent mixture.

Tables 4-67 to 4-73 summarize the density data of the mixture under consideration at various temperatures and pressures. In tables 4-67 to 4-73, the mass compositions of mixture 3 are 5%, 10%, 20%, 35%, 50%, 70%, and 80 %, respectively.

Table 4-67: Experimental measured density data of bitumen diluted with mixture 3 as a function of temperature (T) and pressure (P) at a constant mass fraction of mixture 3 (w_s = 0.05) in the mixture..

W_S = 0.05

P (MPa)	T (K)	ρ_m (kg/m^3)	P (MPa)	T (K)	ρ_m (kg/m^3)
1.003	333.0	971.0	7.003	333.1	974.7
1.003	318.1	980.8	7.003	318.1	984.3
1.003	303.3	988.7	7.003	303.3	991.9
1.003	297.8	992.5	7.003	297.7	995.7
3.004	333.1	972.3	10.003	333.1	976.4
3.004	318.1	982.0	10.003	318.1	985.9
3.004	303.3	989.8	10.003	303.3	993.5
3.004	297.7	993.6	10.003	297.6	997.2
5.004	333.1	973.5	------	-----	------
5.004	318.1	983.2	------	-----	------
5.004	303.3	990.9	------	-----	------
5.004	297.7	994.6	------	-----	------

Table 4-68: Experimental measured density data of bitumen diluted with mixture 3 as a function of temperature (T) and pressure (P) at a constant mass fraction of mixture 3 (w_s = 0.1) in the mixture.

$W_S = 0.1$

P (MPa)	T (K)	ρ_m (kg/m^3)	P (MPa)	T (K)	ρ_m (kg/m^3)
1.003	333.2	958.5	7.003	333.2	962.3
1.003	317.8	967.3	7.003	317.9	970.8
1.003	303.0	977.1	7.003	303.2	980.4
1.003	296.3	981.6	7.003	296.5	984.7
3.004	333.2	959.8	10.003	333.2	964.1
3.004	317.8	968.5	10.003	318.0	972.5
3.004	303.1	978.2	10.003	303.3	982.0
3.004	296.4	982.6	10.003	296.6	986.2
5.004	333.2	961.1	------	-----	------
5.004	317.9	969.7	------	-----	------
5.004	303.2	979.3	------	-----	------
5.004	296.5	983.7	------	-----	------

Table 4-69: Experimental measured density data of bitumen diluted with mixture 3 as a function of temperature (T) and pressure (P) at a constant mass fraction of mixture 3 (w_s = 0.2) in the mixture.

W_S = 0.2

P (MPa)	T (K)	ρ_m (kg/m^3)	P (MPa)	T (K)	ρ_m (kg/m^3)
1.003	332.9	934.7	7.003	332.9	938.8
1.003	318.3	944.6	7.003	318.6	948.3
1.003	303.2	957.0	7.003	303.2	960.7
1.003	296.0	962.8	7.003	295.9	966.3
3.004	332.9	936.1	10.003	333.0	940.7
3.004	318.4	945.9	10.003	318.6	950.1
3.004	303.2	958.2	10.003	303.2	962.4
3.004	295.9	964.0	10.003	295.9	967.9
5.004	332.9	937.5	------	-----	------
5.004	318.5	947.1	------	-----	------
5.004	303.2	959.5	------	-----	------
5.004	295.9	965.2	------	-----	------

Table 4-70: Experimental measured density data of bitumen diluted with mixture 3 as a function of temperature (T) and pressure (P) at a constant mass fraction of mixture 3 (w_s = 0.35) in the mixture.

$W_S = 0.35$

P (MPa)	T (K)	ρ_m (kg/m^3)	P (MPa)	T (K)	ρ_m (kg/m^3)
1.003	332.9	899.0	7.003	332.9	903.6
1.003	317.9	910.0	7.003	317.9	914.2
1.003	303.3	922.7	7.003	303.3	926.7
1.003	296.2	928.4	7.003	296.3	932.1
3.004	332.9	900.5	10.003	332.9	905.6
3.004	317.9	911.5	10.003	317.9	916.2
3.004	303.3	924.1	10.003	303.3	928.6
3.004	296.3	929.7	10.003	296.4	933.9
5.004	332.9	902.1	------	-----	------
5.004	317.9	912.9	------	-----	------
5.004	303.3	925.4	------	-----	------
5.004	296.3	930.9	------	-----	------

Table 4-71: Experimental measured density data of bitumen diluted with mixture 3 as a function of temperature (T) and pressure (P) at a constant mass fraction of mixture 3 (w_s = 0.5) in the mixture.

W_S = 0.5

P (MPa)	T (K)	ρ_m (kg/m^3)	P (MPa)	T (K)	ρ_m (kg/m^3)
1.003	333.0	868.0	7.003	333.1	872.9
1.003	318.0	879.6	7.003	318.0	884.2
1.003	303.4	892.1	7.003	303.4	896.4
1.003	296.6	898.4	7.003	296.5	902.6
3.004	333.0	869.6	10.003	333.1	875.2
3.004	318.0	881.2	10.003	318.0	886.4
3.004	303.4	893.6	10.003	303.4	898.5
3.004	296.6	899.8	10.003	296.5	904.6
5.004	333.1	871.3	------	-----	------
5.004	318.0	882.7	------	-----	------
5.004	303.4	895.1	------	-----	------
5.004	296.5	901.2	------	-----	------

Table 4-72: Experimental measured density data of bitumen diluted with mixture 3 as a function of temperature (T) and pressure (P) at a constant mass fraction of mixture 3 (w_s = 0.7) in the mixture.

W_S = 0.7

P (MPa)	T (K)	ρ_m (kg/m^3)	P (MPa)	T (K)	ρ_m (kg/m^3)
1.003	333.1	826.9	7.003	333.1	832.5
1.003	317.8	839.9	7.003	317.8	845.0
1.003	303.3	853.1	7.003	303.3	857.9
1.003	295.7	860.4	7.003	295.6	865.1
3.004	333.1	828.9	10.003	333.1	835.1
3.004	317.8	841.6	10.003	317.8	847.4
3.004	303.3	854.8	10.003	303.3	860.2
3.004	295.7	862.0	10.003	295.7	867.2
5.004	333.1	830.7	------	-----	------
5.004	317.8	843.3	------	-----	------
5.004	303.3	856.4	------	-----	------
5.004	295.6	863.6	------	-----	------

Table 4-73: Experimental measured density data of bitumen diluted with mixture 3 as a function of temperature (T) and pressure (P) at a constant mass fraction of mixture 3 (w_s = 0.8) in the mixture.

W_S = 0.8

P (MPa)	T (K)	ρ_m (kg/m^3)	P (MPa)	T (K)	ρ_m (kg/m^3)
1.003	333.2	807.8	7.003	333.1	813.7
1.003	318.1	820.9	7.003	317.9	826.4
1.003	303.0	835.5	7.003	303.1	840.4
1.003	296.2	842.2	7.003	296.1	847.0
3.004	333.1	809.9	10.003	333.1	816.5
3.004	318.0	822.8	10.003	317.9	828.9
3.004	303.1	837.1	10.003	303.1	842.7
3.004	296.2	843.9	10.003	296.1	849.3
5.004	333.1	811.9	------	-----	------
5.004	318.0	824.6	------	-----	------
5.004	303.1	838.7	------	-----	------
5.004	296.2	845.4	------	-----	------

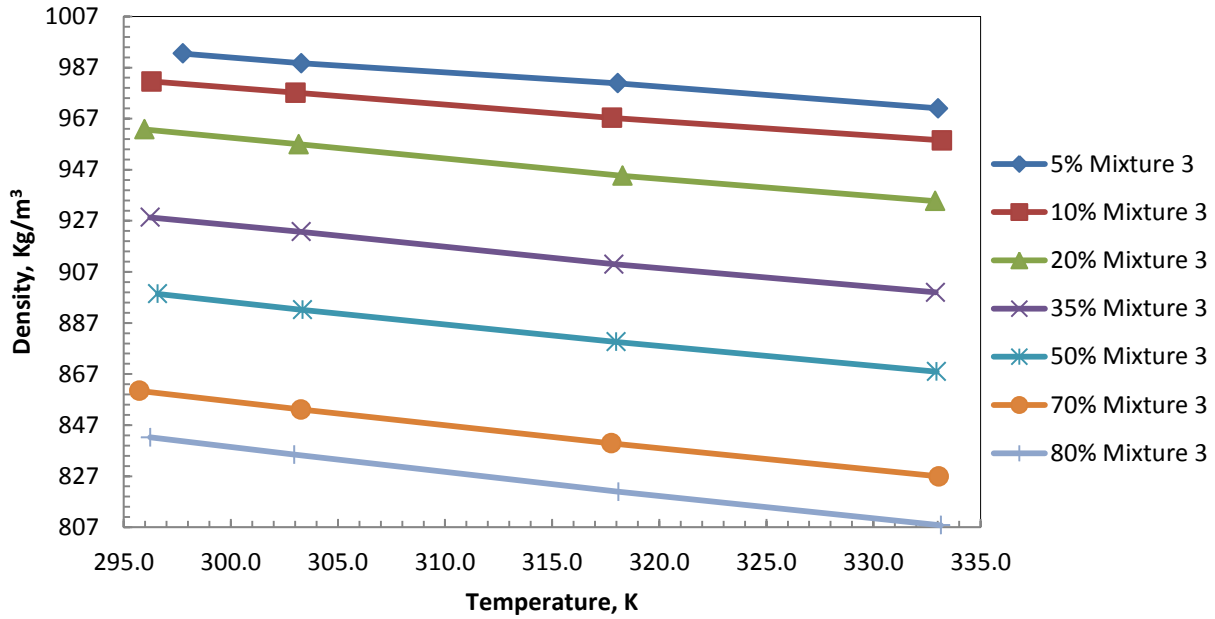

Figure 4-20: Density variations of mixture 3/ bitumen with temperature, at different mass fractions of mixture 3 at a constant pressure of 1 MPa.

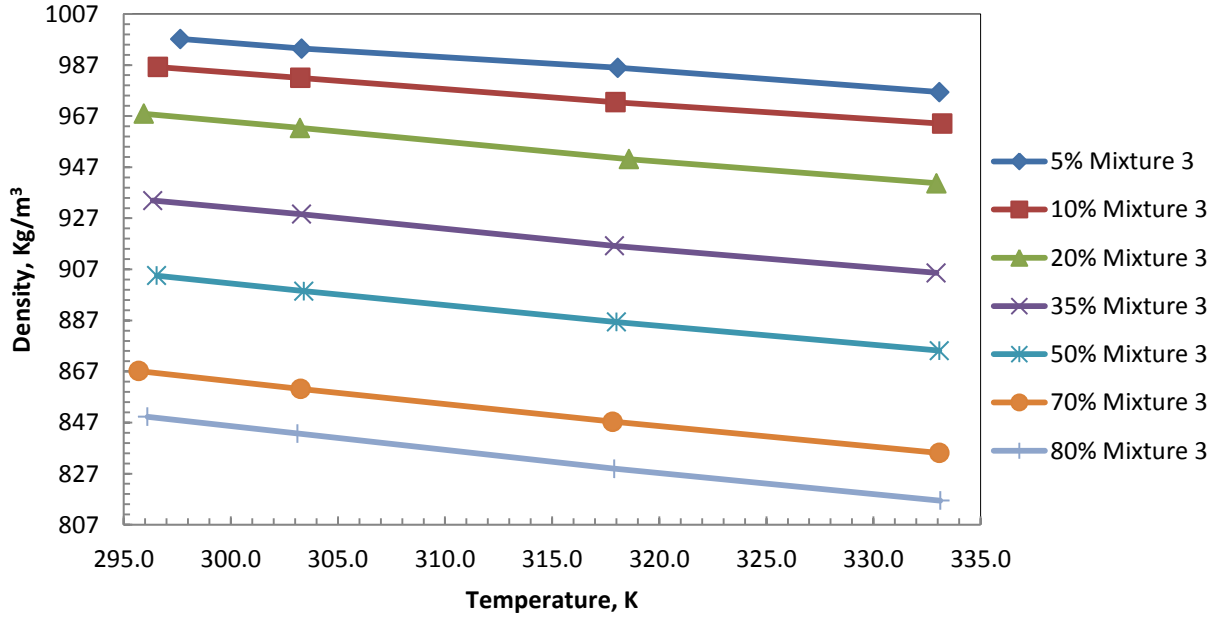

Figure 4-21: Density variations of mixture 3/ bitumen with temperature, at different mass fractions of mixture 3 at a constant pressure of 10 MPa.

Chapter 5 Modelling Investigation of Experimental Data

Various modelling techniques for the viscosity and density of bitumen and its mixtures are presented in the literature. These techniques are based on several assumptions. The details of each correlation and its significance in predicting physical properties will be outlined in this chapter.

5.1 Modelling of Physical Properties of Pure Solvents

5.1.1 Viscosity Modelling

(Andrade, 1934) presented a correlation to predict the viscosities of pure solvents and their mixtures in different mass compositions. This study used toluene, hexane, and their mixtures as the solvents. The Andrade model is a two-parameter semi-logarithmic correlation that gives the variation of liquid viscosity with temperature excluding the minimal effect of pressure on viscosity. Table 4-2 shows the insignificant effect of pressure in the experimental data.

$$\ln(\mu_{solv}) = a + \frac{b}{T} \qquad 5\text{-}1$$

where; solvent viscosity is in mPa.s and Temperature (T) is measured in degrees Kelvin (K)

5.1.2 Density Modelling

(Badamchi-zadeh et al., 2009 a, 2009 b) presented a correlation for the density of pure solvents based on experiments measuring the physical properties of Athabasca bitumen and propane mixtures. The proposed correlation is as follows:

$$\rho = (a_1 + a_2[T - 273.15])exp\{(a_3[T - 273.15] + a_4)P\} \qquad 5\text{-}2$$

where, ρ is the density of the solvent in kg/m^3; a_1, a_2, a_3 and a_4 are adjustable parameters; T is the temperature in Kelvin (K); and P is the pressure in kPa. Using this correlation, the average deviation for the Badamchi-Zadeh experimental data was ±0.4 kg/m^3.

5.2 Modelling of Physical Properties of Raw Bitumen

5.2.1 Viscosity Modelling

(Mehrotra and Svrcek, 1986) presented two models for the viscosity of raw bitumen to define its relationship to pressure and temperature. The details of the models were described in Chapter 2. The average absolute deviation was 2.8% for Eq. [2-7] and 1.8% for Eq. [2-8].

5.2.2 Density Modelling

The correlation presented by (Badamchi-zadeh et al., 2009 a, 2009 b) can also be used to model the density of raw bitumen with different adjustable characteristic parameters.

5.3 Modelling of Physical Properties of Binary Mixture

5.3.1 Viscosity Modelling

(Arrhenius, 1887) proposed a mixing rule for the viscosity of ideal mixtures but it didn't accurately predict for heavy oil and solvents. The equation is as follows:

$$\mu_m = \mu_S^{x_S} * \mu_B^{(1-x_S)} \qquad 5\text{-}3$$

In log form it can be represented as:

$$\ln \mu_m = x_S \ln \mu_S + (1 - x_S) \ln \mu_B \qquad 5\text{-}4$$

where, x_S and x_B are the mole fraction of solvent and bitumen, μ_S and μ_B are the viscosities of the pure solvent and bitumen, respectively.

The Power law model is based on the (Kendall and Monroe, 1917) model in which the viscosity of the mixture is directly dependent on its concentration. The correlation is as follows:

$$\mu_m = [x_s {\mu_s}^n + (1 - x_s){\mu_B}^n]^{\frac{1}{n}} \qquad 5\text{-}5$$

where, x_S and x_B are the mole fraction of the solvent and bitumen and μ_S and μ_B are the viscosities of the pure solvent and bitumen, respectively. The exponent *n* is the adjustable parameter in the Power law model and its value can be determined by the Least Squares regression.

(Lederer, 1933) proposed a modified version of the classic Arrhenius log-type viscosity mixing rule with the following equation.

$$ln\,\mu_m = \left(1 - \frac{\alpha v_B}{\alpha v_B + v_S}\right)\, ln\,\mu_S + \left(\frac{\alpha v_B}{\alpha v_B + v_S}\right) ln\,\mu_B \qquad 5\text{-}6$$

where, υ_s and υ_b are the volume fractions of the solvent and bitumen, respectively, and α is the adjustable parameter with values between 0 and 1.

(Shu, 1984) also investigated Lederer's Model and developed the following equation to calculate the constant α.

$$\alpha = \frac{17.04(\rho_B - \rho_S)^{0.5237} {\rho_B}^{3.2745} {\rho_S}^{1.6316}}{\ln\left(\frac{\mu_B}{\mu_S}\right)} \qquad 5\text{-}7$$

where, μ_S and μ_B are the viscosities of the pure solvent and bitumen and ρ_S and ρ_B are the densities of the pure solvent and bitumen, respectively. Shu correlated his experimental data with this correlation and found that it could be used to determine the viscosity of mixtures of heavy oil, bitumen, and petroleum fractions.

5.3.2 Density Modelling

The density modelling of the mixtures was achieved using the following correlation, based on the assumption that no volume change occurs on mixing of the solvent and bitumen.

$$\rho_m = \frac{1}{\frac{w_S}{\rho_S} + \frac{1-w_S}{\rho_B}} \qquad 5\text{-}8$$

where, w_s is the mass fraction of the solvent. ρ_s and ρ_B are the densities of the pure solvent and bitumen, respectively.

5.4 Results and Discussion

5.4.1 Physical Properties of Pure Solvents

Initially, the experimental apparatus was used to measure the viscosity and density of pure toluene over a wide range of temperatures and pressures. The experimental results found that pressure had an insignificant effect on the viscosity of pure toluene. The effect of temperature on the viscosity of toluene was inversely linear; the viscosity of the solvent decreased with temperature at all pressures. This inverse relationship can be seen in Figures 4-2, 3, 6, 7, 10, 11, 14, 15, 18, and 19. The experimental and correlated viscosity results from Equation [5-1] are presented in Table 5-1 along with the coefficients of the correlation.

The average absolute deviation was calculated as follows:

$$AARD\ \% = \left(\frac{100}{N}\right) \sum \left| \frac{\mu_{corr} - \mu_{exp}}{\mu_{exp}} \right| \qquad 5\text{-}9$$

The AARD % for toluene obtained by regression of the data was 0.2%.

Table 5-1: Measured and correlated viscosities of toluene at different temperatures, T at a pressure of 1 MPa.

Temperature	Measured Viscosities	Correlated Viscosities	ARD%
(K)	(cp)	(cp)	
343.0	0.307	0.306	0.3
325.9	0.366	0.367	0.4
308.8	0.451	0.450	0.3
301.5	0.494	0.494	0.1

$\ln(\mu_{toluene}) = -4.561+1191/T$

The density of the toluene was measured using a density-measuring cell DMA HPM and the results were correlated using equation [5-2]. The densities of the pure solvents decreased with temperature and increase with pressure. Correlation [5-2] predicted the density of toluene within ±0.4 kg/m^3 and the coefficients are summarized in Table 5-2.

Table 5-2: Calculated coefficients for density of pure toluene by using Eq. [5-2]

Coefficients	a_1	a_2	a_3	a_4
Toluene	887.6	-0.9889	7.19E-09	7.13E-07

5.4.2 Physical Properties of Raw Bitumen

5.4.2.1 Raw Bitumen Density

The density of raw bitumen at various temperatures and pressures is shown in Table 4-3. The experimental data for the density of raw bitumen was compared with the predicted density obtained with correlation [5-2]. The regression of the coefficients was performed with the MATLAB curve fitting tool and the coefficients are summarized in Table 5-3 with the coefficients measured by (Guan et al., 2013) for the density of Athabasca bitumen at several pressures and temperatures. The correlated values show a maximum average deviation of ±0.4 kg/m^3 in this study.

Table 5-3: Calculated coefficients for density of bitumen using correlation [5-2]

Coefficients	a_1	a_2	a_3	a_4
This Study	1017	-0.5717	2.23E-09	5.0E-07
Guan et al.	1020.3	-0.63096	2.27E-09	4.49E-07

The variations of experimental and correlated density with pressure at different temperatures are plotted in Figure 5-1. The density of the raw bitumen increased with pressure at all isotherms. Figure 5-1 also shows the variation of bitumen density with temperature. The increase in temperature resulted in a significant decrease in bitumen density for all isobars. Thus, a linear variation of bitumen density was found for pressure and temperature.

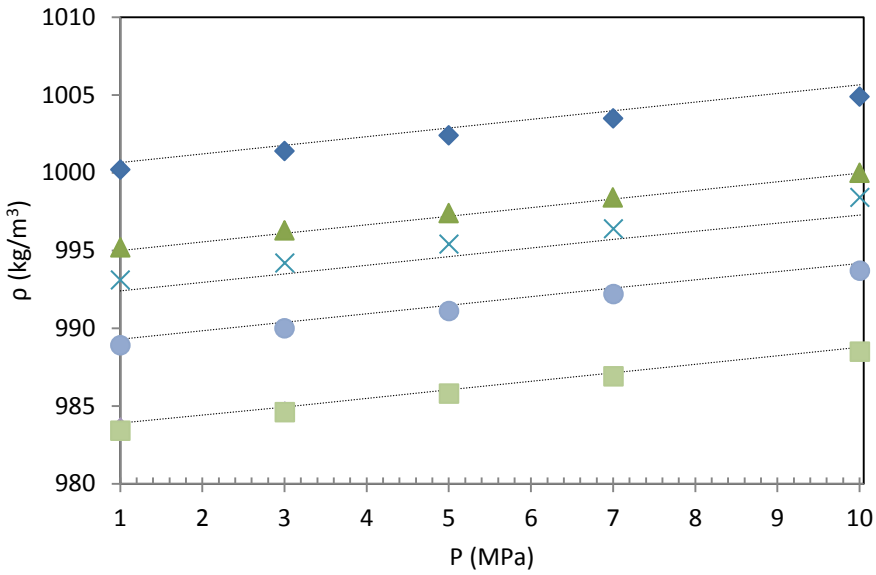

Figure 5-1: Density of raw bitumen, ρ, versus pressure, P, at different temperatures, T; ■,●,×,▲,♦, measured densities; ■, T = 303.3 K; ●, T=313.4 K; ×, T = 318.1 K; ▲, T = 323.6 K, ♦, T = 333.3 K; -----, correlated densities using Eq. [5-2].

5.4.2.2 Raw Bitumen Viscosity

The viscosity of bitumen was measured at four different temperatures (344.7, 333.1, 326, and 321.3 K) and various pressures from 1 to 10 MPa. The experimental data is shown in Table 4-4. Equations 2-7 and 2-8 were used to correlate the experimental data, which was presented by (Mehrotra and Svrcek, 1986). These two correlations include the impact of pressure and temperature on the viscosity of bitumen while the (Khan et al., 1984) correlation only included the impact of temperature. Table 5-4 summarizes the experimental and correlated data from the two correlations along with the ARD % at each data point. The coefficients for equations 2-7 and 2-8 are shown in Table 5-5 and produced AARD%'s of 0.8 and 0.4, respectively.

Table 5-4: Measured μ_{exp}, and correlated, μ_{corr}, viscosity of MacKay River bitumen at different temperatures, T, and pressures, P.

P	T	μ_{exp}	$\ln(\mu_{exp})$	$\ln[\ln(\mu_{exp})]$	μ_{corr}	
(MPa)	(K)	(cp)	(cp)	(cp)	[2-7]	[2-8]
1.004	344.7	1223	7.109	1.961	7.184	1.970
3.005	344.7	1331	7.194	1.973	7.278	1.981
5.004	344.7	1469	7.292	1.987	7.372	1.992
7.006	344.7	1600	7.378	1.998	7.466	2.003
10.006	344.7	1830	7.512	2.017	7.608	2.020
1.005	333.0	3425	8.139	2.097	8.096	2.088
3.003	333.1	3807	8.245	2.110	8.182	2.098
5.005	333.1	4075	8.313	2.118	8.276	2.109
7.005	333.1	4502	8.412	2.130	8.370	2.121
10.006	333.2	5181	8.553	2.146	8.503	2.136
1.002	326.0	6202	8.733	2.167	8.714	2.161
3.004	326.0	6862	8.834	2.179	8.809	2.172
5.003	325.9	7704	8.949	2.192	8.912	2.184
7.005	325.9	8308	9.025	2.200	9.006	2.195
10.006	325.9	9642	9.174	2.216	9.148	2.212
1.004	321.3	8555	9.054	2.203	9.164	2.211
3.003	321.3	9382	9.147	2.213	9.258	2.222
5.000	321.3	10103	9.221	2.221	9.352	2.233

6.999	321.3	11422	9.343	2.235	9.446	2.244
10.003	321.3	13330	9.498	2.251	9.588	2.261

Table 5-5: Calculated coefficients for bitumen viscosity using correlations 2-7 and 2-8

Coefficients		a_1	a_2	a_3
This Study	Eq. [2-7]	22.31	-3.482	0.04709
	Eq. [2-8]	21.97	-3.424	0.00560
Guan et al.	Eq. [2-7]	23.95	-3.767	0.04911
	Eq. [2-8]	23.55	-3.698	0.00576

The relationship between the experimental and correlated viscosity data from the two equations at various pressures and temperatures is shown in Figures 5-2 and 5-3. The solid lines in these figures show the correlated data and the symbols show the experimental data. A comparison of the figures found that Eq. [2-8] gave a better prediction than Eq. [2-7] at all temperatures and pressures. The temperature effect on the viscosity of the bitumen was more pronounced than the effect of pressure.

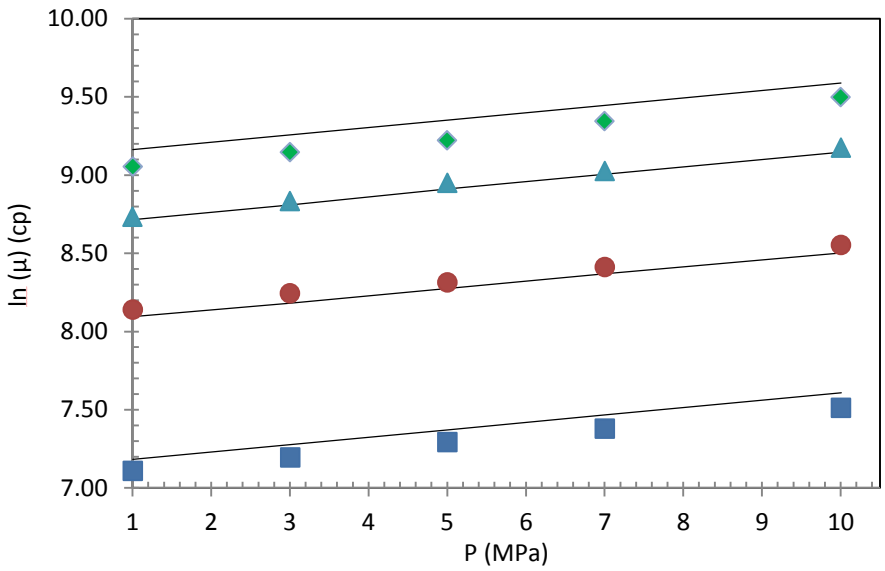

Figure 5-2: Viscosity of bitumen, μ, versus pressure, P, at different temperatures, T; ■,●,▲,♦, measured viscosities; ■, T = 344.7 K; ●, T=333.1 K; ▲, T = 326 K, ♦, T = 321.3 K; − ,correlated viscosities using Eq. [2-7].

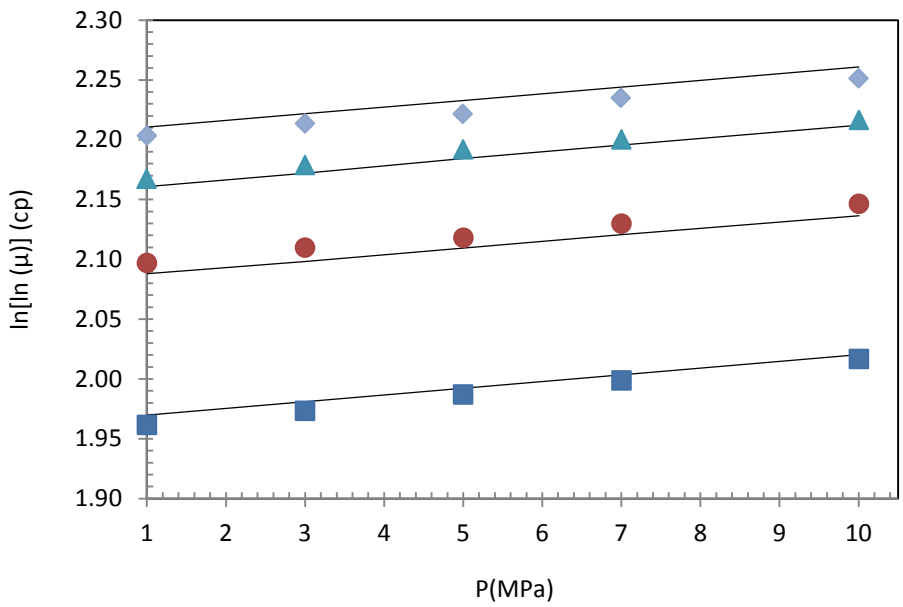

Figure 5-3: Viscosity of bitumen, μ, versus pressure, P, at different temperature, T; ■,●,▲,♦, measured viscosities; ■, T = 344.7 K; ●, T=333.1 K; ▲, T = 326 K, ♦, T = 321.3 K; − ,correlated viscosities using Eq. [2-8].

5.4.3 Physical Properties of Bitumen-Toluene System

The experimental viscosity data for the toluene diluted bitumen system is shown in Tables 4-5 to 4-10 and the density data is shown in Tables 4-11 to 16 at various pressures, temperatures, and toluene concentrations in the bitumen. The density and viscosity of the toluene diluted bitumen mixtures increased with pressure, and decreased with increased temperature and toluene mass fraction.

5.4.3.1 Density of Bitumen/ Toluene Mixtures

The density variations of the mixture with pressure and solvent concentration were linear for the bitumen/toluene system. Eq. [5-8] was used to correlate the density data for all of the binary mixtures. The AARD% for the toluene/bitumen system was 0.1. This equation requires density data for pure toluene and bitumen at all temperatures and pressures, which were measured and correlated using Eq. [5-2]. The experimental and correlated results were well matched as shown in Figures 5-4 and 5-5. The density of the mixture increased when the pressure was increased from 1 MPa (Figure 5-4) to 10 MPa (Figure 5-5). An increase in the solvent concentration resulted in reduced mixture density at all isotherms and pressures.

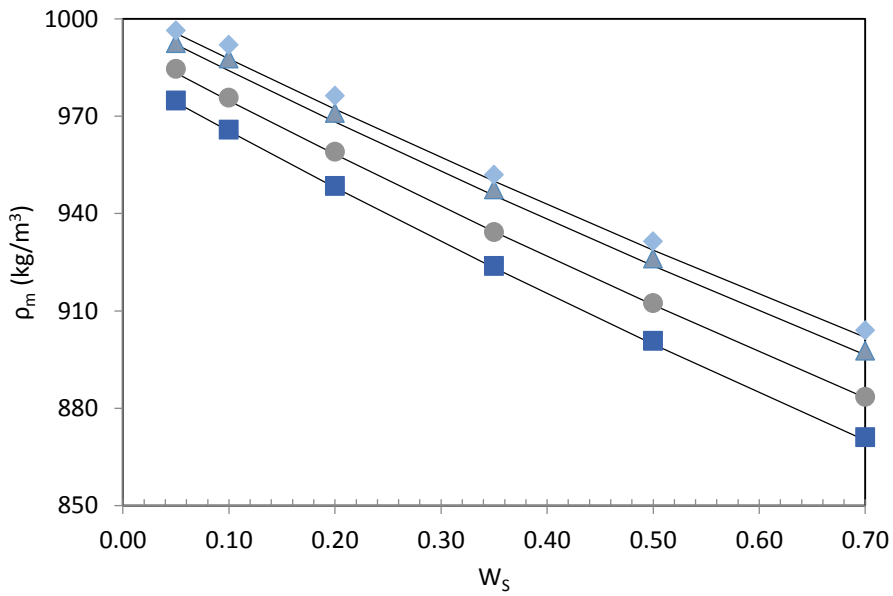

Figure 5-4: Density of toluene/bitumen system, ρ_m, versus toluene concentration, W_S, at different temperatures, T; and a pressure of 1 MPa; measured densities;−, correlated densities; ■, T = 333 K; ●, T=318 K; ▲, T = 303 K, ♦, T = 297.6 K.

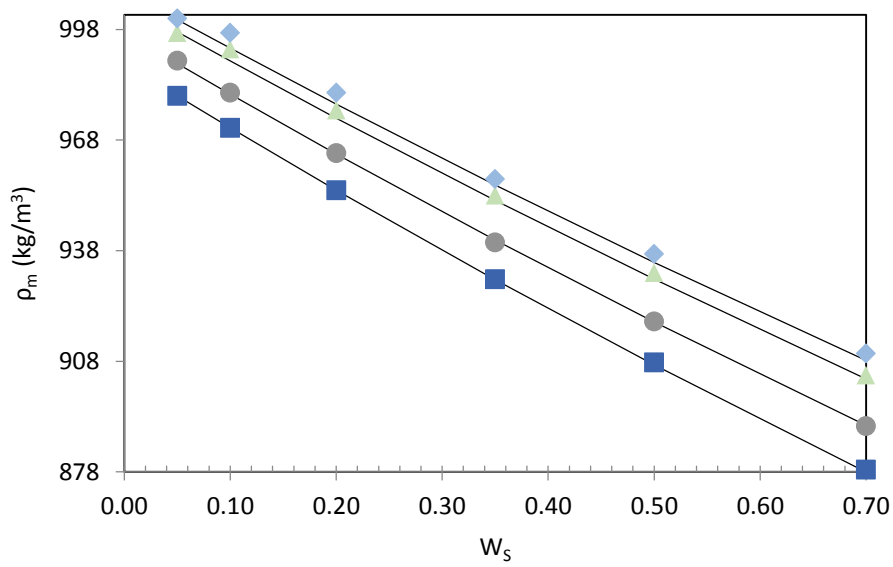

Figure 5-5: Density of toluene/bitumen system, ρ_m, versus toluene concentration, W_S, at different temperatures, T; and a pressure of 10 MPa; measured densities;−, correlated densities; ■, T = 333 K; ●, T=318 K; ▲, T = 303 K, ♦, T = 297.6 K.

The effect of pressure on mixture density was also investigated and illustrated in Figures 5-6 and 5-7. Figure 5-6 and Figure 5-7 represent the measured and experimental density data at toluene concentrations of 0.05 and 0.7. The purpose of plotting the densities at extreme concentration points was to show the magnitude of the reduction of mixture densities when the solvent concentration was significantly increased. The symbols represent the experimental data and the solid lines show the data predicted by Eq. [5-8]. The effect of pressure on the mixture density was significant and linear at all temperatures. The predicted densities at 297.6 K showed a deviation from the measured values at the highest mass fraction for all of the pressures. Therefore, the assumption of ideal mixing for this system is not applicable at lower temperature.

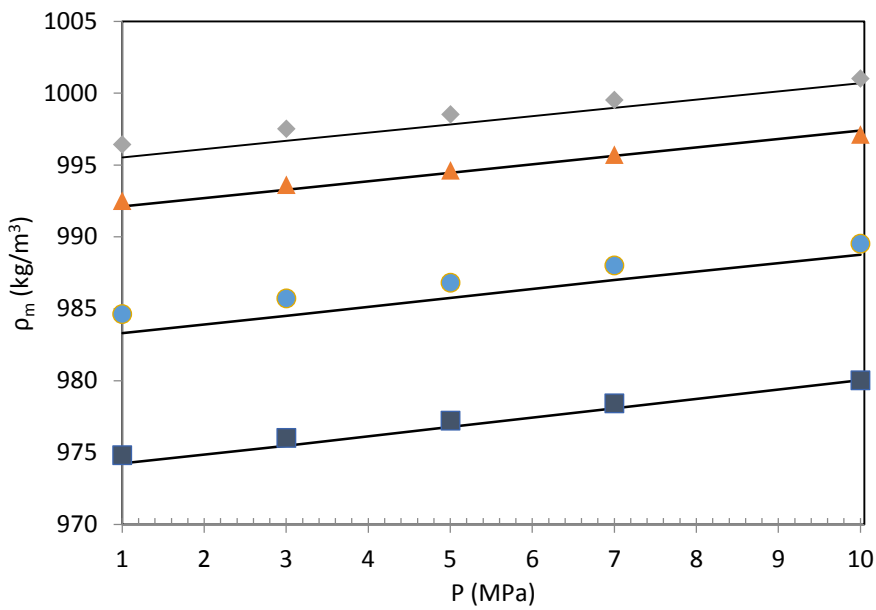

Figure 5-6: Density of toluene/bitumen system, ρ_m, versus pressure, P, at different temperatures, T; and a toluene concentration of 0.05; measured densities;−, correlated densities; ■, T = 333 K; ●, T=318 K; ▲, T = 303 K, ♦, T = 297.6 K.

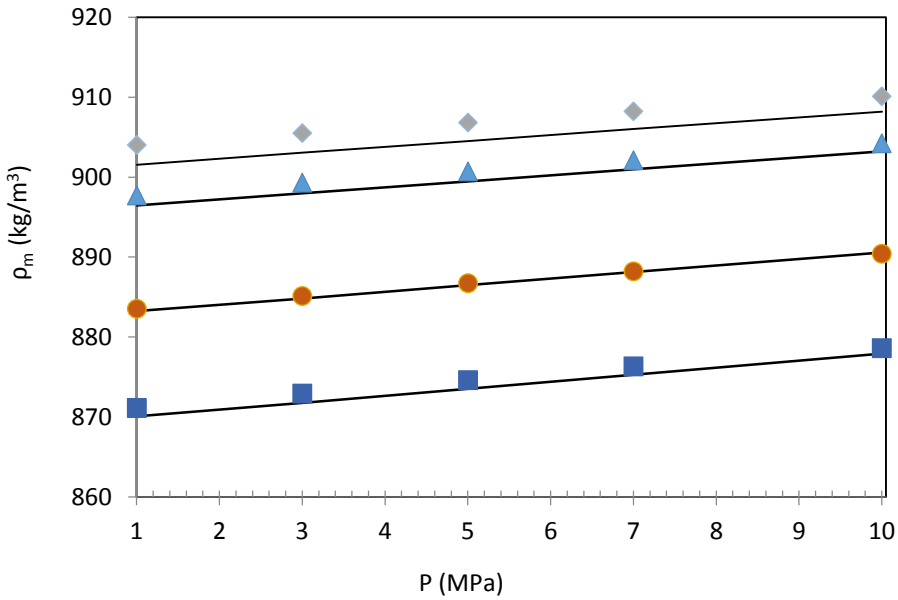

Figure 5-7: Density of toluene/bitumen system, ρ_m, versus pressure, P, at different temperatures, T; and a toluene concentration of 0.7; measured densities;−, correlated densities; ■, T = 333 K; ●, T=318 K; ▲, T = 303 K, ♦, T = 297.6 K.

5.4.3.2 Viscosity of Toluene Diluted Bitumen Mixtures

The experimental viscosity data for the bitumen/toluene system was also correlated with several correlations from literature, which are primarily used for heavy oils diluted with solvents. The viscosities of the mixtures were correlated using the Arrhenius, Power law, Lederer, and Shu models each having its own significance for predicting the viscosities of the mixtures. The effect of pressure on the viscosity was more pronounced when the toluene concentration in the mixtures was low. As the solvent concentration increased, the effect of pressure became insignificant. This behaviour was due to the fact that as the solvent concentration increases, the mixture becomes closer to the pure solvent and the pressure effect on pure solvent was insignificant. Increasing the pressure resulted in higher mixture viscosity values especially at lower solvent concentrations and temperatures.

The comparison between the experimental data and the viscosities predicted by each of these four models is shown in Figure 5-8. The figure demonstrates that the Lederer and Power law models fit the experimental data better than the Shu and Arrhenius models. The Lederer model gave a better prediction for toluene-diluted bitumens with an AARD % of 9.6 while the Power law model had an AARD% of 14.8. The Arrhenius and Shu models did not have any adjustable parameters but the values of adjustable parameters for the other two models were calculated by a regression of the data which gave a value of n = 0.0550 and α = 0.3203 for the toluene/bitumen mixtures.

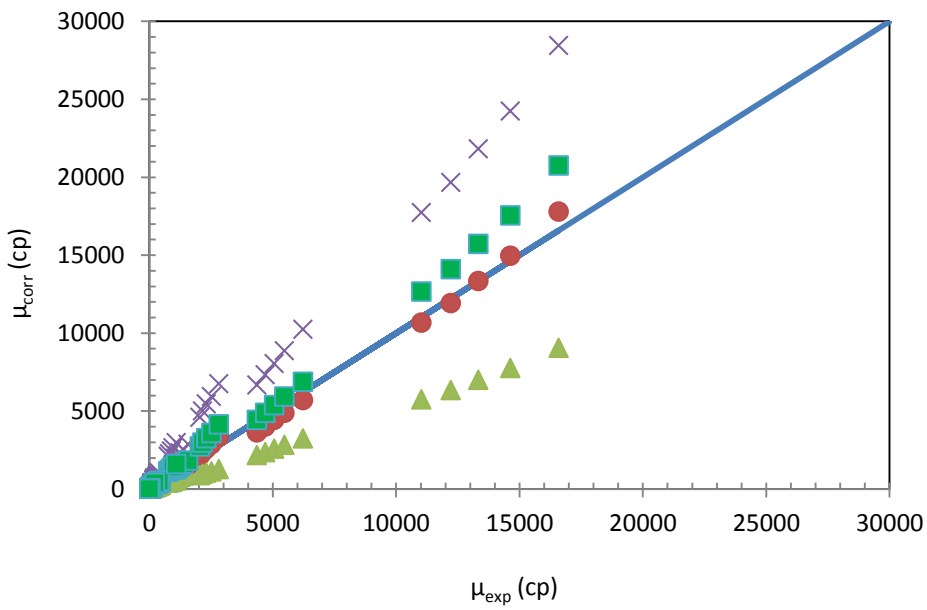

Figure 5-8: Experimental bitumen/toluene mixture viscosities, μ_{exp}, versus correlated viscosities, μ_{corr}, by using several models; ▲, Arrhenius's model; ●, power law model; ■, Lederer's model; ×, Shu correlation.

The predictions obtained with the Power law and Lederer's models were much more accurate than those of the other two models. For this reason, only these two more accurate models were considered to investigate the relationship between the mixture viscosities and three

parameters (pressure, temperature, and solvent concentrations). Figures 5-9 and 5-10 illustrate the effect of solvent concentration on the mixture viscosities at 1 and 10 MPa, respectively. The dashed and solid lines represent the correlated results obtained by the Power law model and the Lederer's model, respectively. The experimental results are shown with symbols.

A curvilinear trend exists among the solvent concentration and mixture viscosity for both pressures. The temperature effect on the viscosity of the mixture was more prominent at lower solvent concentrations and decreased when the toluene concentration was increased. Figures 5-9 and 5-10 show that the Lederer's model produced much better predictions at higher temperatures for most of the experimental data points.

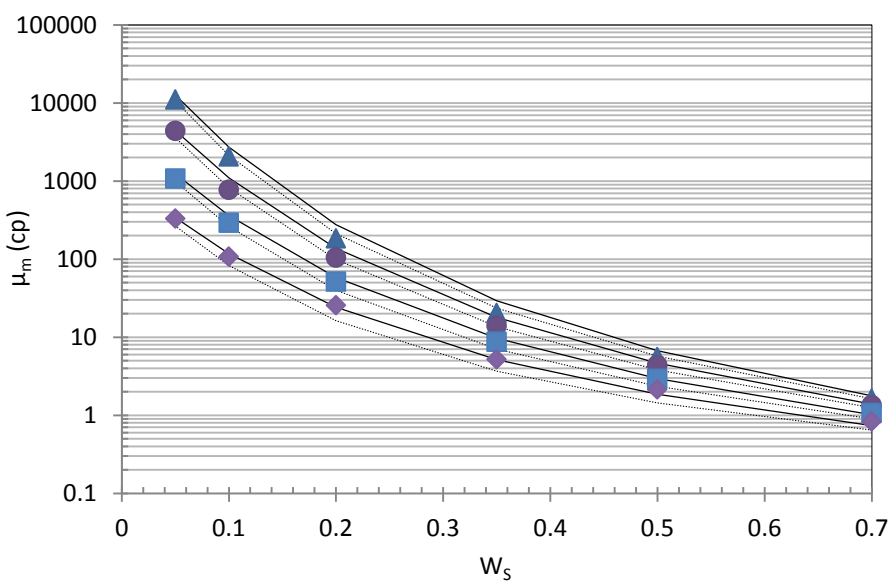

Figure 5-9: Viscosity, μ_m, of toluene diluted bitumen mixtures versus toluene mass fraction, W_S, at different temperatures and a pressure of 1 MPa; ▲,●,■,♦, measured viscosities; −, Lederer's model; ----, power law model; ▲, 302.1 K; ●, 311.3 K; ■, 327 K; ♦, 344.6 K.

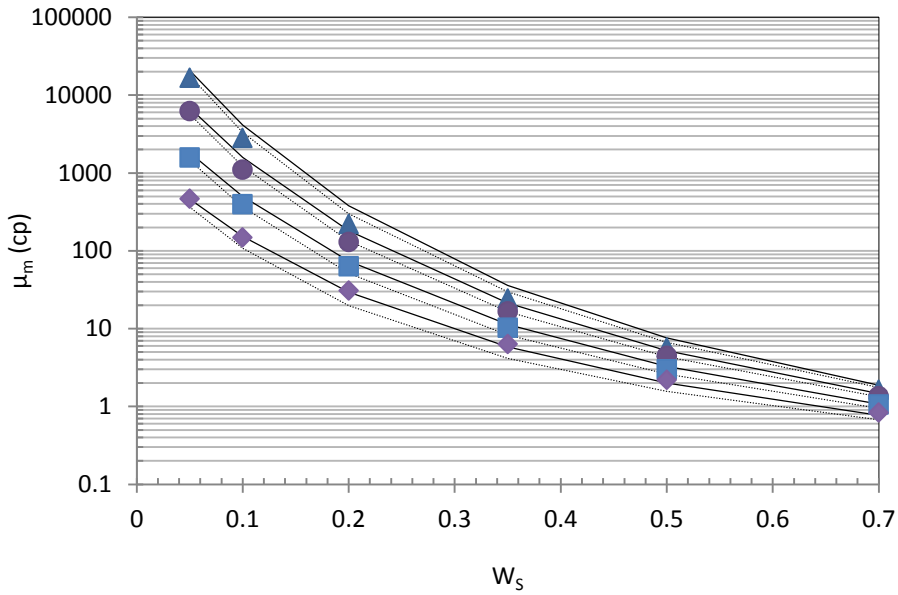

Figure 5-10: Viscosity, μ_m, of toluene diluted bitumen mixtures versus toluene mass fraction, W_S, at different temperatures and a pressure of 10 MPa; ▲,●,■,♦, measured viscosities; −, Lederer's model; ----, power law model; ▲, 302.1 K; ●, 311.3 K; ■, 327 K; ♦, 344.6 K.

5.4.4 Physical Properties of Bitumen-Hexane System

5.4.4.1 Density of Hexane Diluted Bitumen Mixtures

The density of the bitumen/hexane mixtures was also measured at temperatures ranging from ambient to 333 K and pressures from 1 to 10 MPa. The effects of the three parameters, pressure, temperature, and hexane concentration on hexane-diluted bitumen were investigated and observations for asphaltene precipitation were performed at the end of each experiment. The experimental data for bitumen/hexane density is shown in Tables 4-23 to 4-28. The experimental results suggest that the effect of pressure on the density of this mixture is linear, i.e. the density decreased in a linear relationship with increasing pressure at all hexane concentrations and all isotherms. The reduction in the density of the mixture was greater in this case compared to the toluene diluted bitumen mixtures. At $w_{hexane} = 0.5$, asphaltene precipitation was observed in the feeding cell at the end of the experiment. It is not clear which mass composition of hexane marks

the beginning of asphaltene precipitation in the hexane/bitumen system. Asphaltene precipitation may have started between 35 and 50 wt %.

The density of hexane was only measured at room temperature so the density data of hexane at all pressures and temperatures was taken from the (National Institute of Standards and Technology) and the density data of bitumen was taken from Eq. [5-2]. The experimental data for the hexane/bitumen system was also correlated using Eq. [5-8], which produced an AARD% of 0.6. The effect of hexane mass fraction on mixture density at the lowest and highest pressures for all temperatures is presented in Figures 5-11 and 5-12, respectively. The experimental data is represented with symbols and predicted data is represented by solid lines.

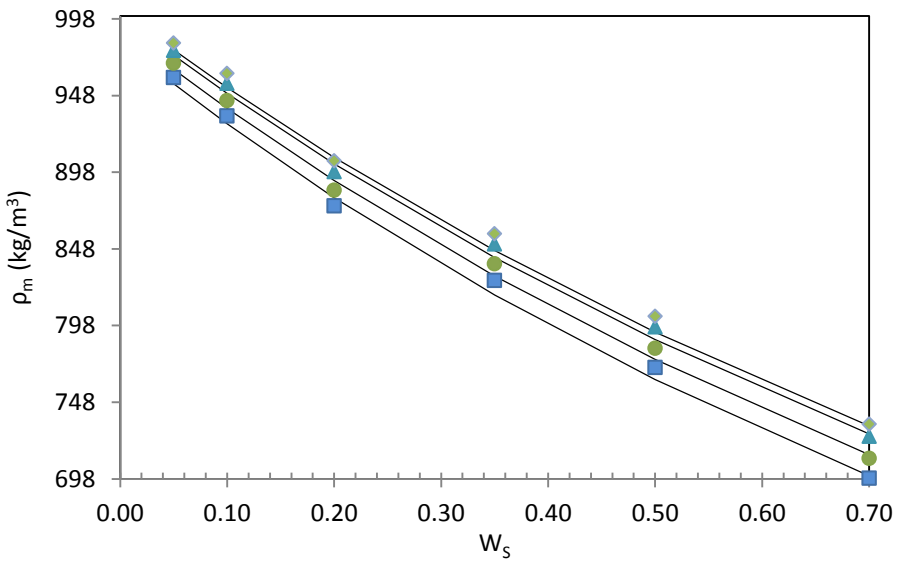

Figure 5-11: Density of hexane/bitumen system, ρ_m, versus hexane concentration, W_S, at different temperatures, T; and a pressure of 1 MPa; measured densities;−, correlated densities; ■, T = 333.2 K; ●, T=318.4 K; ▲, T = 303.4 K, ♦, T = 296.4 K.

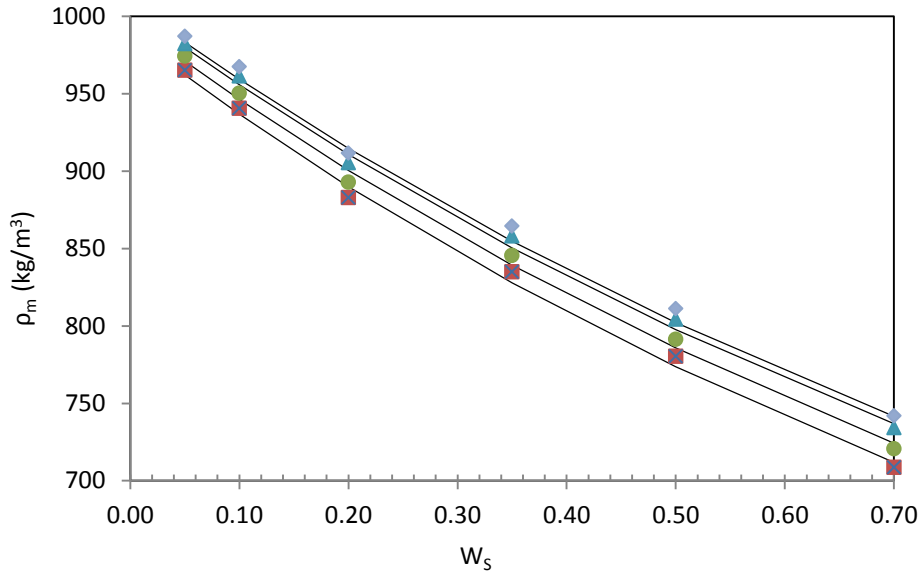

Figure 5-12: Density of hexane/bitumen system, ρ_m, versus hexane concentration, W_S, at different temperatures, T; and a pressure of 10 MPa; measured densities;−, correlated densities; ■, T = 333.2 K; ●, T=318.4 K; ▲, T = 303.4 K, ♦, T = 296.4 K.

5.4.4.2 Viscosity of Hexane Diluted Bitumen Mixtures

The measured viscosities of the hexane diluted bitumen system were correlated using the same procedure and equations that were used for the toluene/bitumen systems. The predicted results using the Arrhenius, Power law, Lederer's, and Shu models are presented in Figure 5-13. The viscosities of hexane were taken from the NIST Chemistry Web Book at all temperatures and pressures. The viscosity of bitumen was obtained with Eq. [2-8] because it produced a better prediction compared to Eq. [2-7]. Similar to the toluene/bitumen systems, the viscosities of the hexane diluted bitumen mixture were also better predicted by the Lederer's and Power law model as compared to the Shu and Arrhenius models. A comparison of AARD% between Lederer's model and the Power law model suggest that Lederer's gives better predictions. The AARD% was 16.2 for Lederer's model and 20 for the Power law model. The adjustable parameters obtained are; $\alpha = 0.3397$ for Lederer's model and $n = 0.0408$ for Power law model.

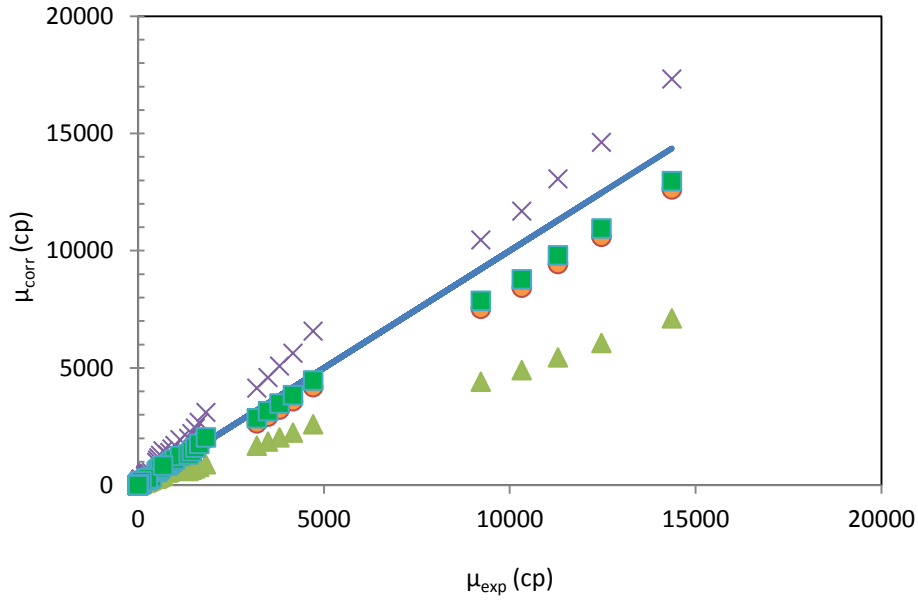

Figure 5-13: Experimental bitumen/hexane mixture viscosities, μ_{exp}, versus correlated viscosities, μ_{corr}, by using several models; ▲, Arrhenius's model; ●, power law model; ■, Lederer's model; ×, Shu correlation.

Only the Lederer's and Power law models were used to describe the mixture viscosity trends because they produced more accurate predictions than the other two models. Figures 5-14 and 5-15 represent the effect of pressure on the viscosities of the hexane/bitumen system at various temperatures. The pressure effect is investigated in these figures at a minimum (0.05) and maximum (0.7) mass fraction of hexane. Comparison of these two figures suggests that a linear relationship exists between mixture viscosity and pressure at all temperatures and solvent concentrations. The Power law and Lederer's model best fit the experimental data at the lowest solvent concentration as shown in Figure 5-14. At the highest mass fraction of solvent there was a significant difference between the experimental data and the results from the models under consideration. There was a dramatic increase in this difference at the lowest temperature for all pressures.

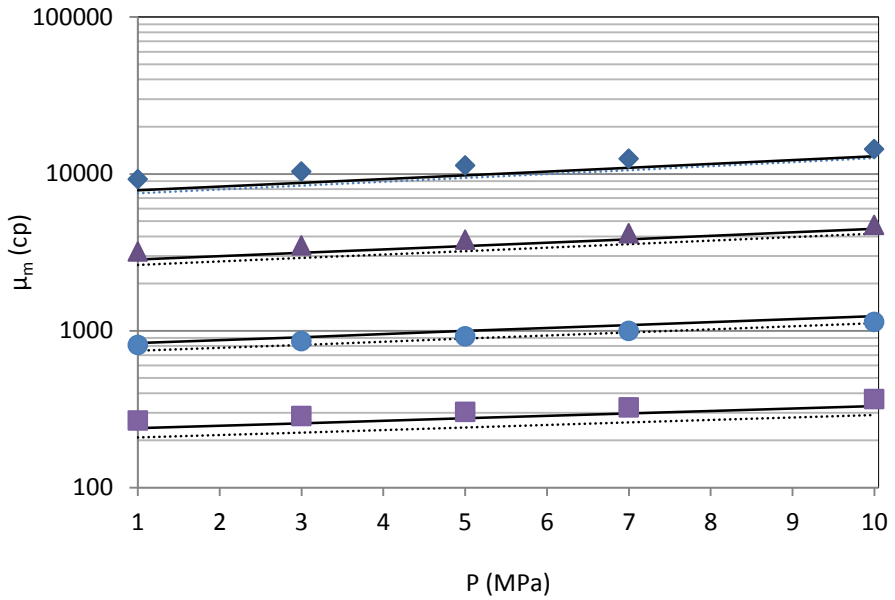

Figure 5-14: Viscosity, μ_m, of hexane diluted bitumen mixtures versus pressure, P, at different temperatures and a hexane concentration of 0.05; ■,●,▲ ,♦, measured viscosities; −, Lederer's model; ····, power law model; ■, 344 K; ●, 328 K; ▲, 311.3 K; ♦, 300.9 K.

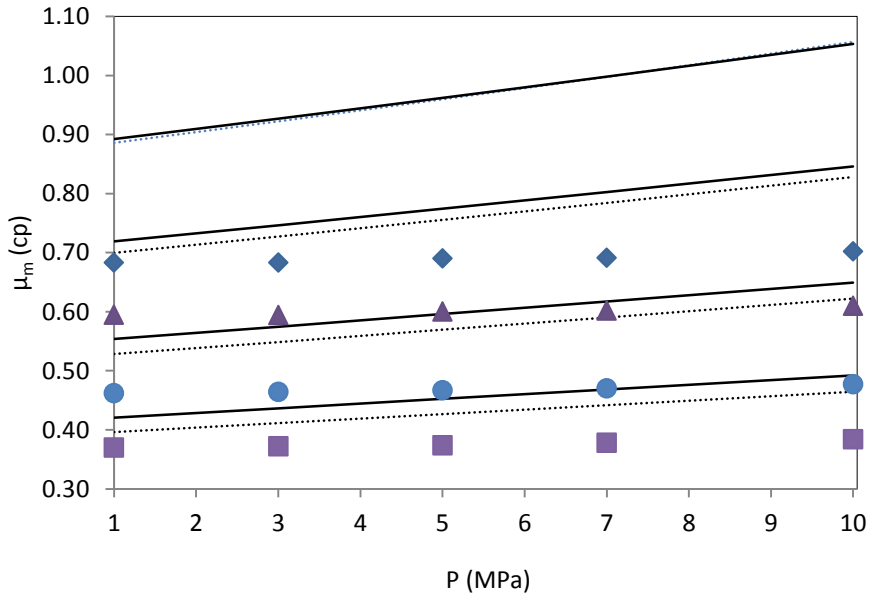

Figure 5-15: Viscosity, μ_m, of hexane diluted bitumen mixtures versus pressure, P, at different temperatures and a hexane concentration of 0.7; ■,●,▲ ,♦, measured viscosities; −, Lederer's model; ·····, power law model; ■, 344 K; ●, 328 K; ▲, 311.3 K; ♦, 300.9 K.

5.4.5 Physical Properties of Pure Mixtures 1, 2, 3

Various mixtures were prepared by mixing toluene and hexane in different proportions. Mixture 1 consisted of 25 wt% toluene and 75 wt% hexane, mixture 2 consisted of equal mass fractions of both solvents, and mixture 3 consisted of 75 wt% toluene and 25 wt% hexane. The densities and viscosities of each mixture were measured at several temperatures and pressures to investigate the effect of pressure and temperature. The pressure effect on the densities of the pure mixtures was insignificant while the temperature increase resulted in a linear decrease in the densities. The effect of pressure and temperature on the viscosities of the mixtures was prominent. The experimental densities and viscosities of the mixtures were correlated using the same equations used for the pure solvents. The results from the correlation of the experimental data are presented in Tables 5-6 to 5-9 along with the correlation parameters.

Table 5-6: Measured and correlated viscosities of mixture 1 at different temperatures, T.

Temperature	Measured Viscosities	Correlated Viscosities	ARD%
(K)	(cp)	(cp)	
343.5	0.185	0.184	0.6
325.7	0.222	0.226	2.0
310.2	0.282	0.276	2.3
298.3	0.324	0.326	0.6

$\ln(\mu_{mixture\ 1}) = -5.463 + 1295/T$

Table 5-7: Measured and correlated viscosities of mixture 2 at different temperatures, T.

Temperature	Measured Viscosities	Correlated Viscosities	ARD%
(K)	(cp)	(cp)	
342.7	0.218	0.218	0.0
325.2	0.257	0.256	0.4
310.3	0.297	0.298	0.4
300.3	0.334	0.333	0.3

$$\ln(\mu_{mixture\ 2}) = -4.523 + 1028/T$$

Table 5-8: Measured and correlated viscosities of mixture 3 at different temperatures, T.

Temperature	Measured Viscosities	Correlated Viscosities	ARD%
(K)	(cp)	(cp)	
342.4	0.243	0.244	0.1
325.1	0.290	0.291	0.0
310.4	0.342	0.343	0.3
299.7	0.391	0.391	0.0

$$\ln(\mu_{mixture\ 3}) = -4.736 + 1138/T$$

Table 5-9: Calculated coefficients for density of pure mixture 1, 2, 3 by using Eq. [5-2]

Coefficients	a_1	a_2	a_3	a_4	Deviation (±)
Mixture 1	725.1	-0.9862	1.22E-08	1.12E-06	0.4
Mixture 2	776.6	-0.9888	1.10E-08	9.40E-07	0.2
Mixture 3	827.8	-0.9826	8.27E-09	8.54E-07	0.3

5.4.6 Physical Properties of Bitumen/Mixture 1 System

5.4.6.1 Density of Mixture 1 Diluted Bitumen

The density of bitumen-diluted mixture 1 at different mass fractions was also measured at various temperatures and pressures. The measured density data for the bitumen/mixture 1 system was presented in Tables 4-39 to 4-45. This experimental data was correlated using Eq. [5-8] and produced a 0.5 AARD%. This equation required the density of pure mixture 1, the density of raw bitumen, and the mass fractions of each component. The correlated density data of pure mixture 1 and raw bitumen was used in this equation. To investigate the effect of temperature on the density of bitumen/mixture 1, the experimental and correlated densities found with Eq. [5-8] are plotted at different solvent concentrations in Figures 5-16 and 5-17. In these figures, the solvent concentrations were measured at two extreme pressures (1 and 10 MPa). The symbols represent the experimental data, while the predicted results are shown with solid lines. These figures suggest that density decreases linearly with increased temperature for all solvent concentrations and the experimental and correlated results matched each other at all conditions.

The comparison of Figures 5-16 and 5-17 shows that even at the highest pressure (10 MPa) the density reduction trend of this system remains the same. Higher mixture density values were obtained in Figure 5-17 because the pressure was at its maximum value. The linear reduction trend of density with temperature increases with solvent concentration and becomes more linear at the highest solvent concentration of 0.8 wt%.

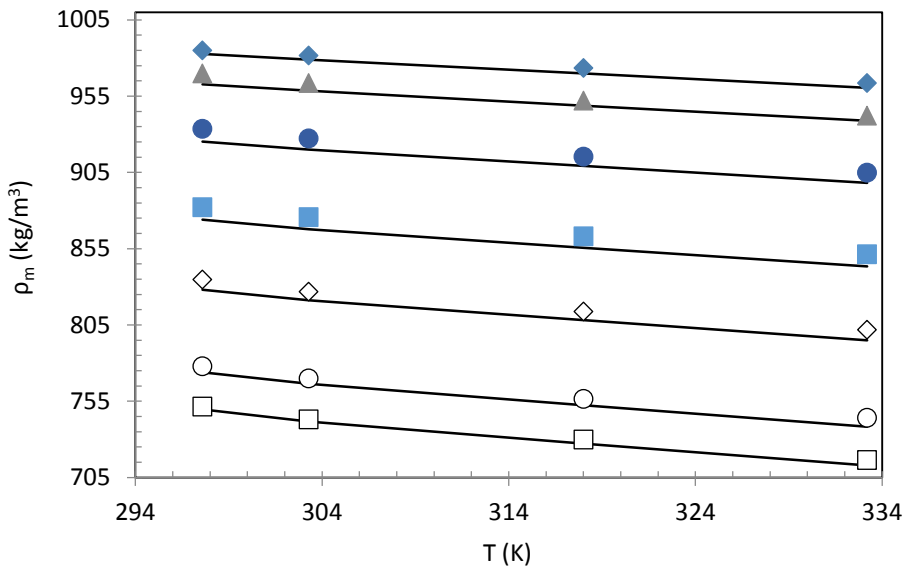

Figure 5-16: Density of bitumen/mixture 1 system, ρ_m, versus temperature, T, at different mixture 1 concentrations, W_S; and at a pressure of 1 MPa; measured densities;–, correlated densities; □, $W_S = 0.8$; ○, $W_S = 0.7$; ◊, $W_S = 0.5$; ■, $W_S = 0.35$; ●, $W_S = 0.2$; ▲, $W_S = 0.1$, ♦, $W_S = 0.05$.

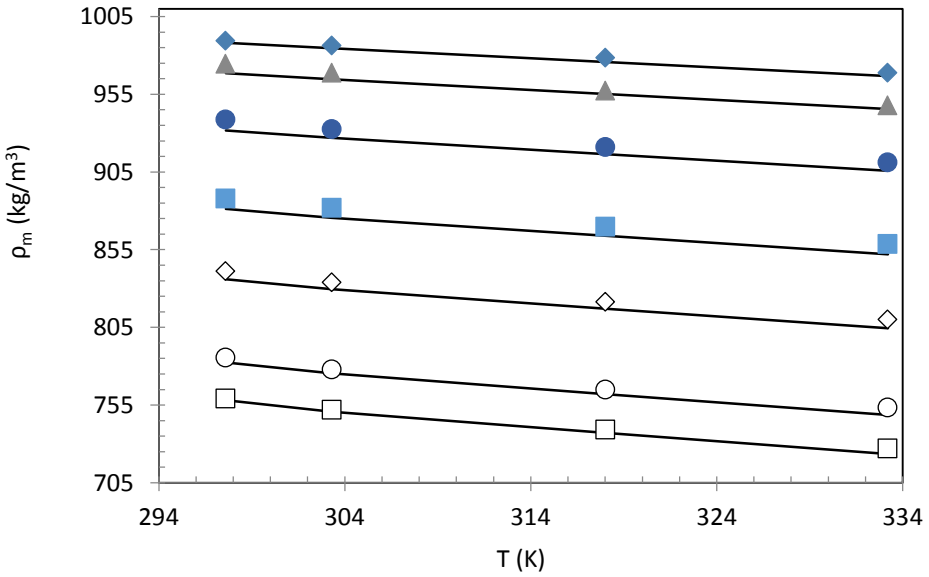

Figure 5-17: Density of bitumen/mixture 1 system, ρ_m, versus temperature, T, at different mixture 1 concentrations, W_S; and at a pressure of 10 MPa; measured densities;–, correlated densities; □, $W_S = 0.8$; ○, $W_S = 0.7$; ◊, $W_S = 0.5$; ■, $W_S = 0.35$; ●, $W_S = 0.2$; ▲, $W_S = 0.1$, ♦, $W_S = 0.05$.

5.4.6.2 Viscosity of Mixture 1 Diluted Bitumen

The measured viscosities of bitumen/mixture 1 were also investigated using the correlations from the literature. The viscosities of this system were correlated by four different models, Arrhenius, Lederer's, Power law, and Shu. The models all gave reasonable results for the bitumen/mixture 1 systems. The use of these models requires viscosity data for both components, therefore, the data generated by Eq. [5-1] was used for pure mixture 1 viscosity and Eq. [2-8] was used for the viscosity of bitumen. These four models can be compared with each other and with the experimental data as shown in Figure 5-18. The Figure indicates that the Lederer's and Power law model produce better predictions than the other two models. The AARD was 14.4% and 15% for the Power law model and Lederer's model, respectively. The adjustable parameter values of these two models were $n = 0.0512$ and $\alpha = 0.3291$.

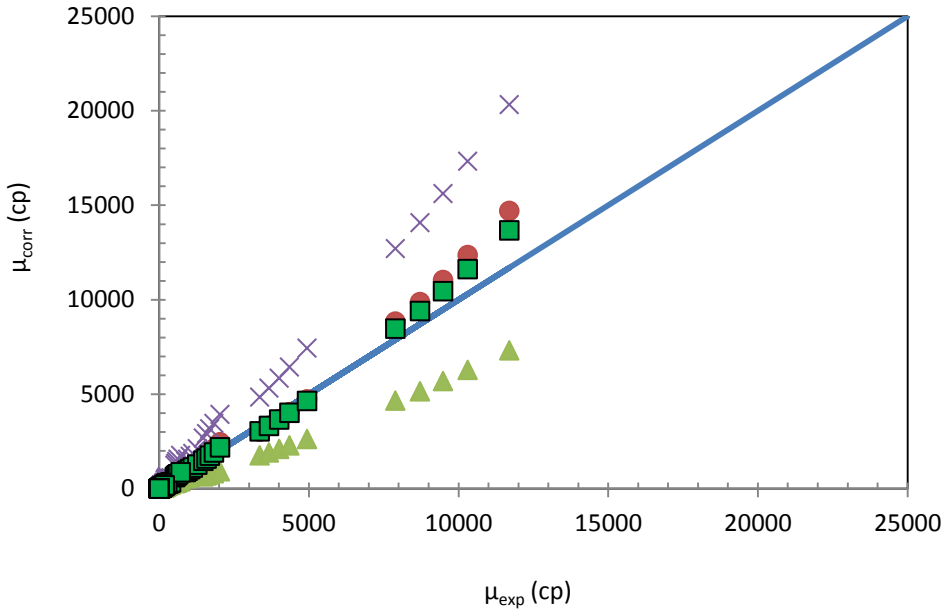

Figure 5-18: Experimental bitumen/ mixture 1 viscosities, μ_{exp}, versus correlated viscosities, μ_{corr}, by using several models; ▲, Arrhenius's model; ●, power law model; ■, Lederer's model; ×, Shu correlation.

The Lederer and Power law models were also considered while investigating the relationship between the viscosity of the bitumen/mixture 1 and pressure at different temperatures and solvent concentrations as shown in Figures 5-19 and 5-20. Comparison of the experimental and correlated data from these two models at the highest temperature is shown in Figure 5-19. Figure 5-20 presents the same comparison but at the lowest temperature (299 K). The correlated data values of the two models were somewhat different from the experimental data at the lowest temperature. This difference increased at the highest temperature especially with increased solvent concentration. A comparison of Figures 5-19 and 5-20 revealed that the difference between the experimental and correlated viscosities of the bitumen/mixture 1 increased at the highest temperature and highest solvent concentration.

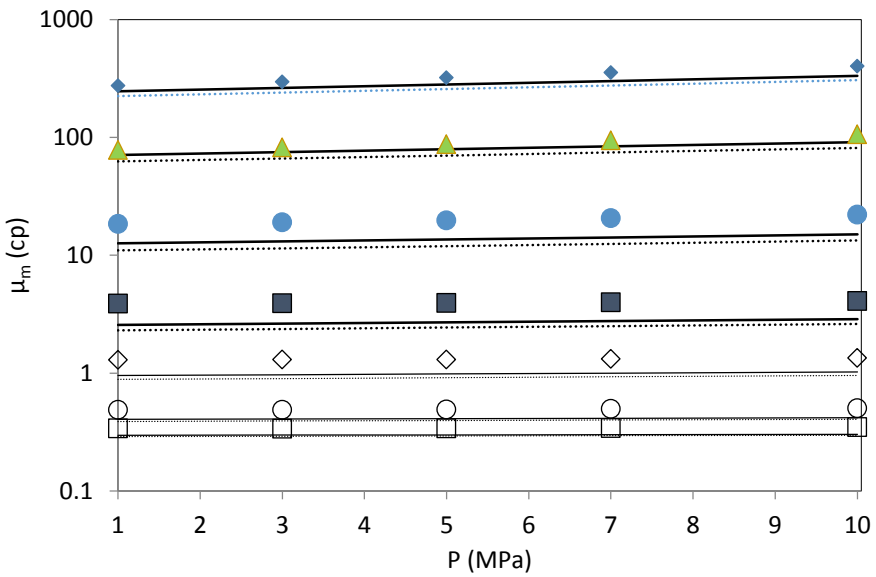

Figure 5-19: Viscosity of bitumen/mixture 1 system, μ_m, versus pressure, P, at different mixture 1 concentrations, W_S; and at a Temperature of 344 K; measured viscosities;−, correlated viscosities; □, $W_S = 0.8$; ○, $W_S = 0.7$; ◊, $W_S = 0.5$; ■, $W_S = 0.35$; ●, $W_S = 0.2$; ▲, $W_S = 0.1$, ♦, $W_S = 0.05$.

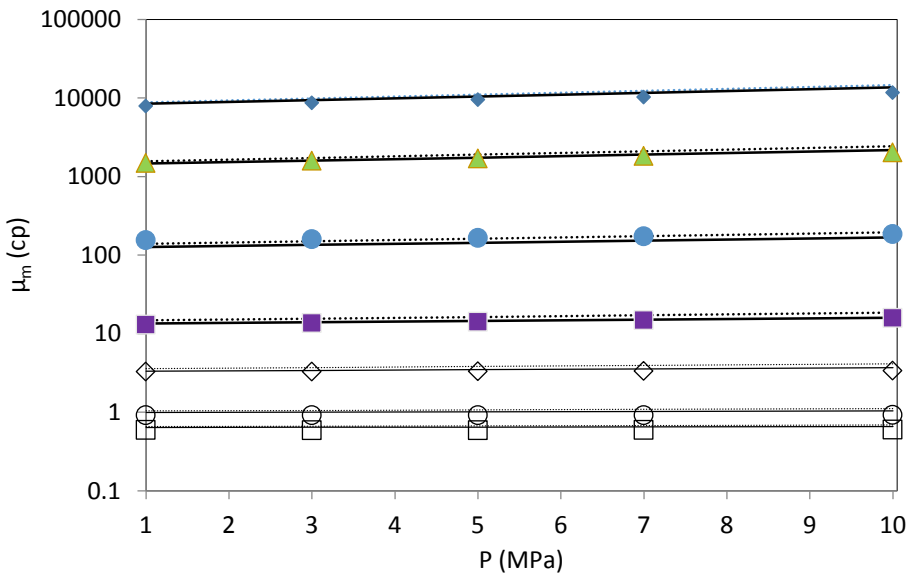

Figure 5-20: Viscosity of bitumen/mixture 1 system, μ_m, versus pressure, P, at different mixture 1 concentrations, W_S; and at a Temperature of 299 K; measured viscosities;−, correlated viscosities; □, $W_S = 0.8$; ○, $W_S = 0.7$; ◊, $W_S = 0.5$; ■, $W_S = 0.35$; ●, $W_S = 0.2$; ▲, $W_S = 0.1$, ♦, $W_S = 0.05$

5.4.7 Physical Properties of Bitumen/Mixture 2 System

5.4.7.1 Density of Mixture 2 Diluted Bitumen

The experimental density data for bitumen/mixture 2 was presented in Tables 4-53 to 4-59 in Chapter 4. The solvent used in this study was prepared by mixing hexane and toluene in equal mass fractions and then the solvent mixture was mixed with bitumen. The densities and viscosities of the mixture were measured at different temperatures, pressures, and solvent concentrations. Eq. [5-8] was used to correlate the density data for the bitumen/mixture 2 system. The AARD% for this system was 0.5. The correlated densities of pure mixture 2 and raw MacKay River bitumen previously found by Eq. [5-2] were used.

The relationship between the densities of bitumen/mixture 2 and pressures at different isotherms is presented in Figures 5-21 and 5-22. The experimental and correlated densities are plotted in Figures 5-21 and 5-22 at the extreme mixture 2 mass fractions of 0.05 and 0.8. The purpose of plotting the densities at the extreme points was to show the magnitude of the density reduction when the solvent concentration is significantly increased. The symbols and solid lines in these figures represent the experimental and correlated density data, respectively. The increase in pressure resulted in a decrease in the mixture densities at all isotherms. The experimental and correlated data do not match very well, especially at the lowest temperatures. This difference is considerably more at similar conditions in Figure 5-22, which is plotted at the highest mass fraction. Therefore, the initial assumption of ideal mixing for the mixture 2 and bitumen system is not applicable at the lowest temperatures and highest solvent concentrations.

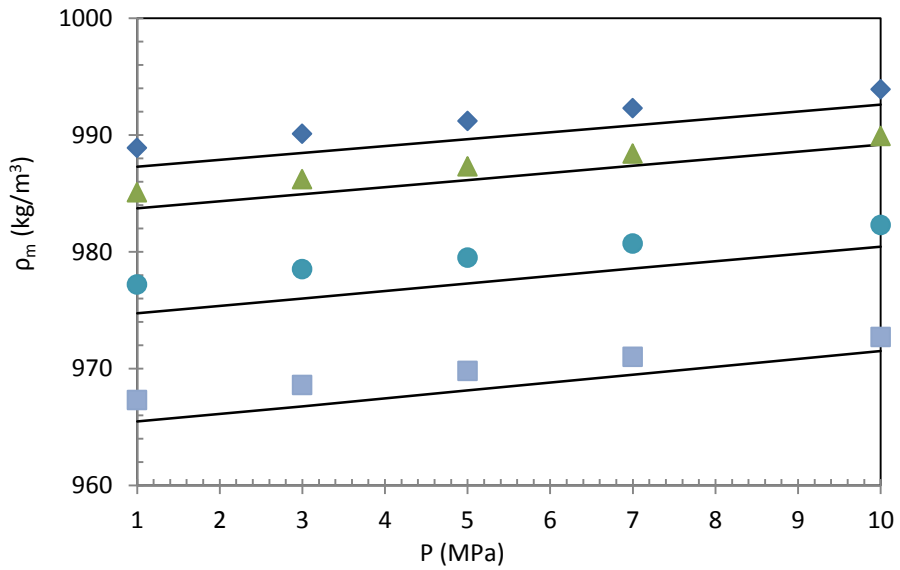

Figure 5-21: Density of bitumen/mixture 2 system, ρ_m, versus pressure, P, at different temperatures, T; and a mixture 2 concentration of 0.05; measured densities;−, correlated densities; ■, T = 333 K; ●, T=318 K; ▲, T = 303 K, ♦, T = 298 K.

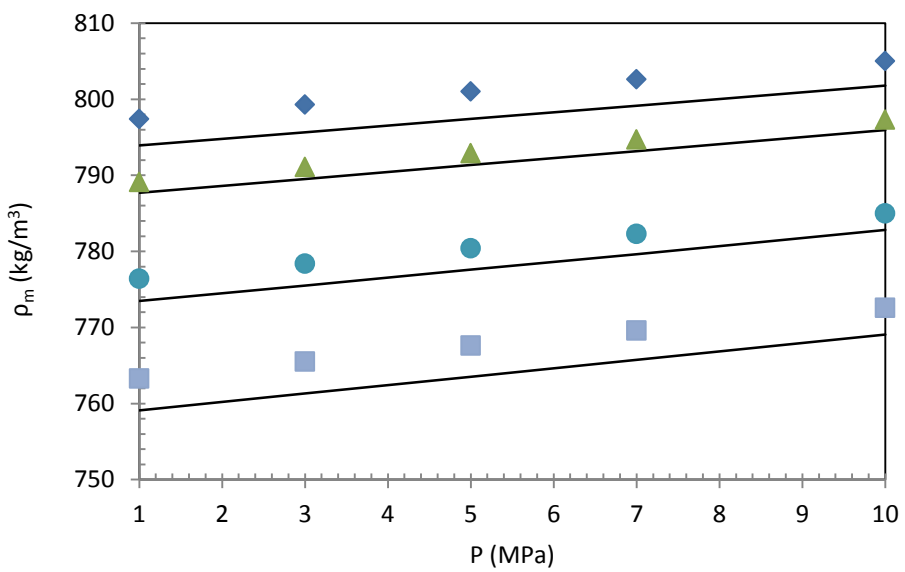

Figure 5-22: Density of bitumen/mixture 2 system, ρ_m, versus pressure, P, at different temperatures, T; and a mixture 2 concentration of 0.8; measured densities;−, correlated densities; ■, T = 333 K; ●, T=318 K; ▲, T = 303 K, ♦, T = 298 K.

5.4.7.2 Viscosity of Mixture 2 Diluted Bitumen

The viscosity of the bitumen/mixture 2 systems was measured with the same apparatus under the same temperature and pressure conditions. The experimental viscosity values for this case are presented in Tables 4-46 to 4-52. The data suggests that the effect of pressure on the viscosity of the bitumen/mixture 2 was more pronounced when the mass fraction of mixture 2 was the least and diminishes when the concentration was increased to the maximum value of 0.8. The system becomes more similar to pure mixture 2 when its concentration is increased and, as previously mentioned, the pressure effect on the pure solvent was insignificant.

The experimental viscosity data for this system was also correlated with four different correlations, the Arrhenius, Power law, Lederer's, and Shu models. These models required the viscosities of pure mixture 2 and raw bitumen, which were obtained using Eq. [5-1] and [2-8], respectively. Figure 5-23 illustrates the comparison between the experimental data and the viscosities predicted by each of the four models. For the bitumen/mixture 2 system, the predictions from the Shu and Arrhenius models didn't match the experimental results as well as those from the Power law and Lederer's model. The AARD%s, which were 58.8, 44, 13.5 and 8.6 for the Shu, Arrhenius, Power law, and Lederer's models, respectively, confirmed the result. The values of the adjustable parameters for the Power law and Lederer's models were calculated by the optimization toolbox in MATLAB which produced a value of $n = 0.0550$ and $\alpha = 0.3332$, respectively.

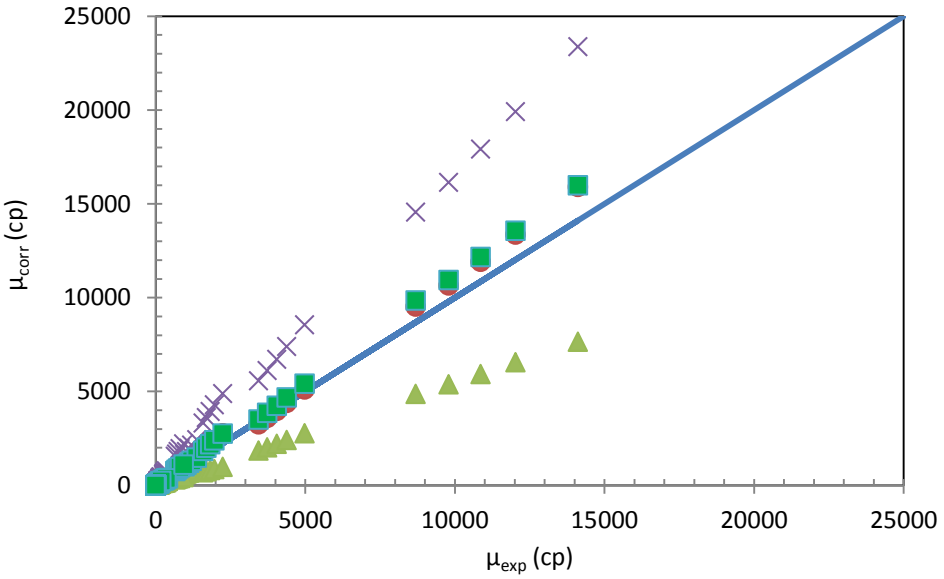

Figure 5-23: Experimental bitumen/ mixture 2 viscosities, μ_{exp}, versus correlated viscosities, μ_{corr}, by using several models; ▲, Arrhenius's model; ●, power law model; ■, Lederer's model; ×, Shu correlation.

Figures 5-24 and 5-25 demonstrate the effect of solvent concentration on the viscosity of the mixture at all temperatures. The experimental viscosities are depicted as symbols, the dashed lines represent the Power law model, and the solid lines represent the data correlated by Lederer's model. The mixture viscosity versus solvent concentration plot reveals a curvilinear relationship at extreme pressures. The reduction in mixture viscosity with temperature is more significant at the lower solvent concentrations. However, as the solvent concentration increases to the maximum mass fraction of solvent the reduction in viscosity as a result of temperature is not distinct. The difference in pressure between Figure 5-24 and Figure 5-25 resulted in considerably higher viscosities in Figure 5-25 at the same temperatures and solvent concentrations.

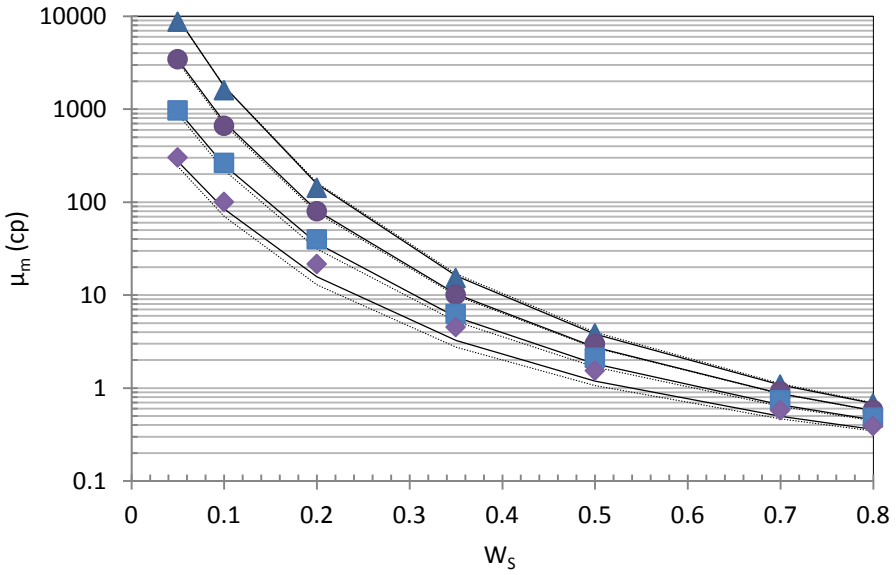

Figure 5-24: Viscosity, μ_m, of mixture 2 diluted bitumen system versus mixture 2 mass fraction, W_S, at different temperatures and a pressure of 1 MPa; ▲,●,■,♦, measured viscosities; −, Lederer's model; ⋯⋯, power law model; ▲, 300 K; ●, 311 K; ■, 327 K; ♦, 344 K.

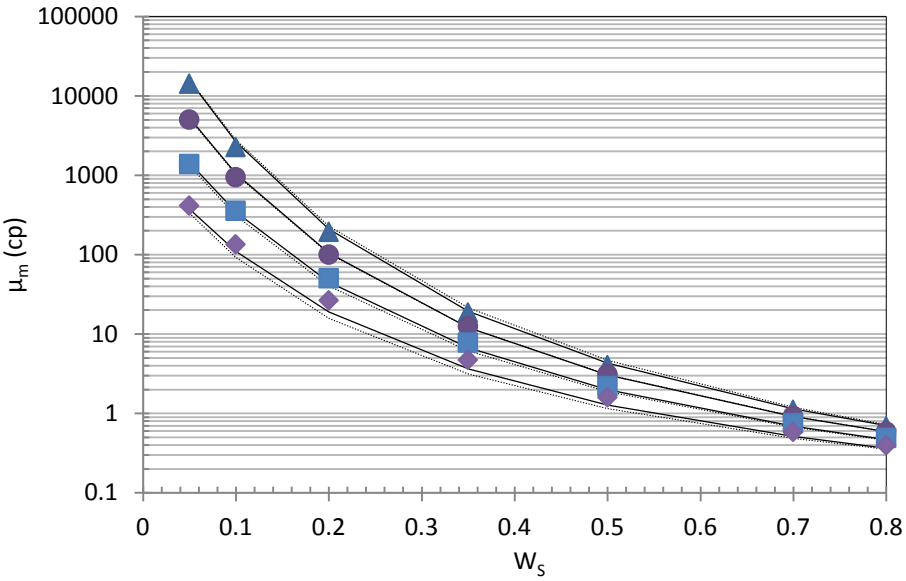

Figure 5-25: Viscosity, μ_m, of mixture 2 diluted bitumen system versus mixture 2 mass fraction, W_S, at different temperatures and a pressure of 10 MPa; ▲,●,■,♦, measured viscosities; −, Lederer's model; ⋯⋯, power law model; ▲, 300 K; ●, 311 K; ■, 327 K; ♦, 344 K.

5.4.8 Physical Properties of Bitumen/Mixture 3 System

5.4.8.1 Density of Mixture 3 Diluted Bitumen

The density of the bitumen/mixture 3 system was measured at various temperatures ranging from ambient to 333 K and pressures from 1 to 10 MPa. This study also investigated the effects of pressure, temperature, and mixture 3 concentrations. The experimental data for the bitumen/mixture 3 densities is shown in Tables 4-67 to 4-73.

When compared with previous cases, the relationship of density with solvent concentration and pressure were found to be similar. However, the experimental results obtained at similar temperatures, pressures, and solvent concentrations were different from the previous studies. The experimental results were correlated using Eq. [5-8] which produced an AARD% of 0.3. The relationship between the densities of the bitumen/mixture 3 and the solvent mole fraction is demonstrated in Figures 5-26 and 5-27. The correlated densities, denoted by solid lines, are also plotted in these figures for comparison with the experimental data. A linear relationship was observed previously when the densities of the different mixtures were plotted against mass fraction. However, plotting the mixture densities against mole fraction did not produce a linear relationship. A similar trend was observed for the density and mole fraction of the solvent at the lowest and highest pressures.

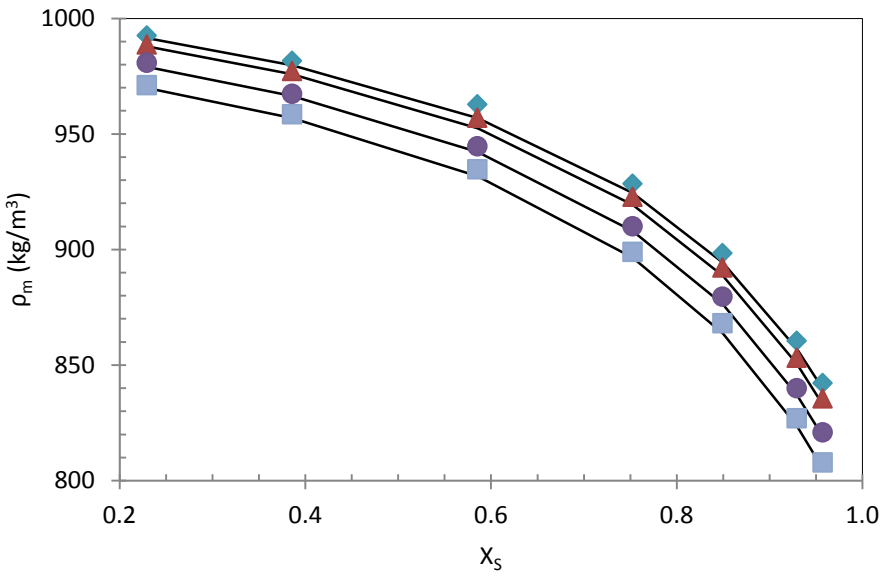

Figure 5-26: Density of bitumen/mixture 3 system, ρ_m, versus mixture 3 mole fraction, X_S, at different temperatures, T; and a constant pressure of 1 MPa; measured densities;−, correlated densities; ■, T = 333 K; ●, T=318 K; ▲, T = 303 K, ♦, T = 296 K.

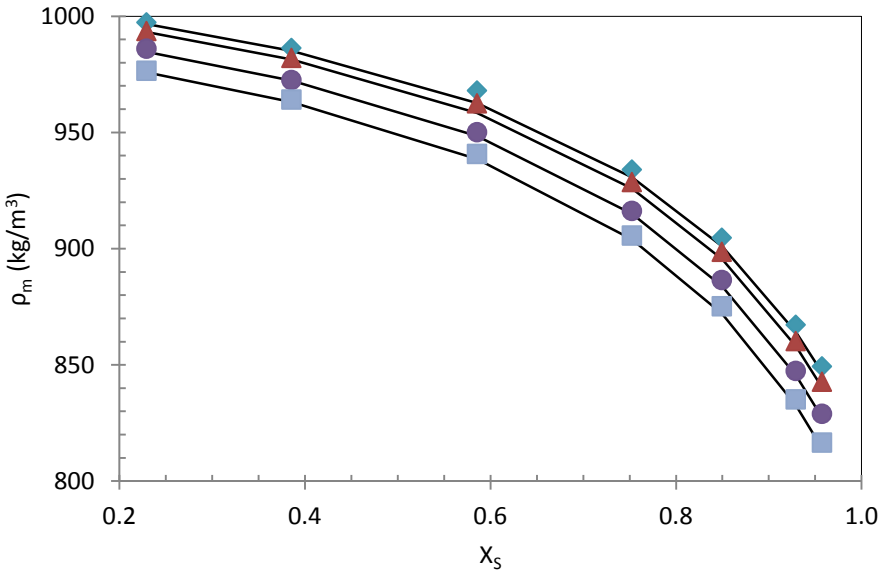

Figure 5-27: Density of bitumen/mixture 3 system, ρ_m, versus mixture 3 mole fraction, X_S, at different temperatures, T; and a constant pressure of 10 MPa; measured densities;−, correlated densities; ■, T = 333 K; ●, T=318 K; ▲, T = 303 K, ♦, T = 296 K.

5.4.8.2 Viscosity of Mixture 3 Diluted Bitumen

Experiments were conducted to measure the viscosities of bitumen/mixture 3 systems in order to fully understand their complex nature. After the experimental viscosity measurements were completed, the data was correlated using the Arrhenius, Power law, Lederer, and Shu models from the literature. The use of these correlations gave acceptable results in this study and the results predicted by the Lederer and Power law models were much more accurate than those of the Shu and Arrhenius models. The AARD% for Lederer's model and the Power law model were 9.4 and 13.5, respectively. The adjustable parameters for this study were $\alpha = 0.3222$ (Lederer's model) and $n = 0.0547$ (Power law model). Comparison of results predicted by these four models and the experimental viscosities is shown in Figure 5-28.

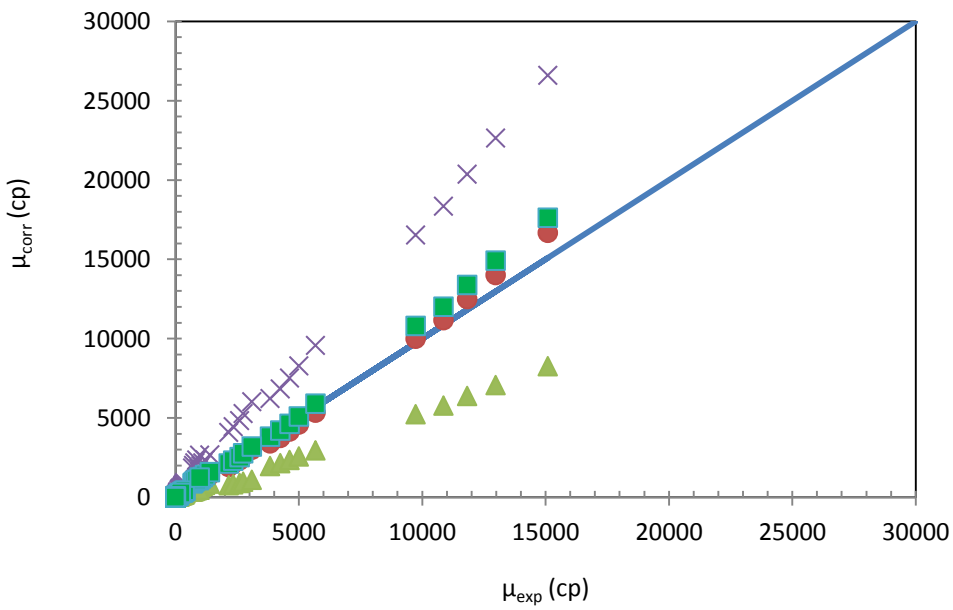

Figure 5-28: Experimental bitumen/ mixture 3 viscosities, μ_{exp}, versus correlated viscosities, μ_{corr}, by using several models; ▲, Arrhenius's model; ●, power law model; ■, Lederer's model; ×, Shu correlation.

Only the Lederer and Power law models were considered for further study because they gave the most accurate predictions. This portion of the study investigated of the effect of varying the mole fraction of mixture 3 on the viscosities of bitumen/mixture 3 systems at various isotherms. The effect of mole fraction was studied at two extreme pressure values (1 and 10 MPa) and is represented in Figures 5-29 and 5-30. A comparison of these two figures suggests that an almost linear relationship exists between the system viscosities and the mole fraction of the solvent at all temperatures and pressures. The viscosity reduction is more pronounced at the lower mole fractions and as the mole fraction reaches near unity the temperature effect is less pronounced at all pressures. The Power law and Lederer's model fit the experimental data best at lower solvent mole fractions as shown in Figures 5-29 and 5-30. The difference between the experimental and model results increases as the mole fraction increases.

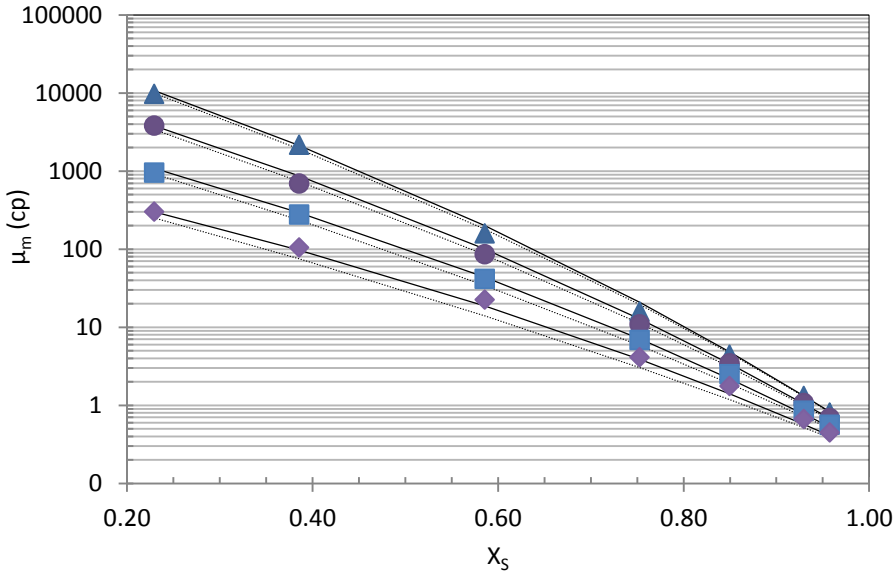

Figure 5-29: Viscosity μ_m, of bitumen/mixture 3 systems, versus mixture 3 mole fraction, X_S, at different temperatures, T; and a pressure of 1 MPa; measured data;−, correlated data; ■, T = 343 K; ●, T=326 K; ▲, T = 311.7 K, ♦, T = 301.3 K.

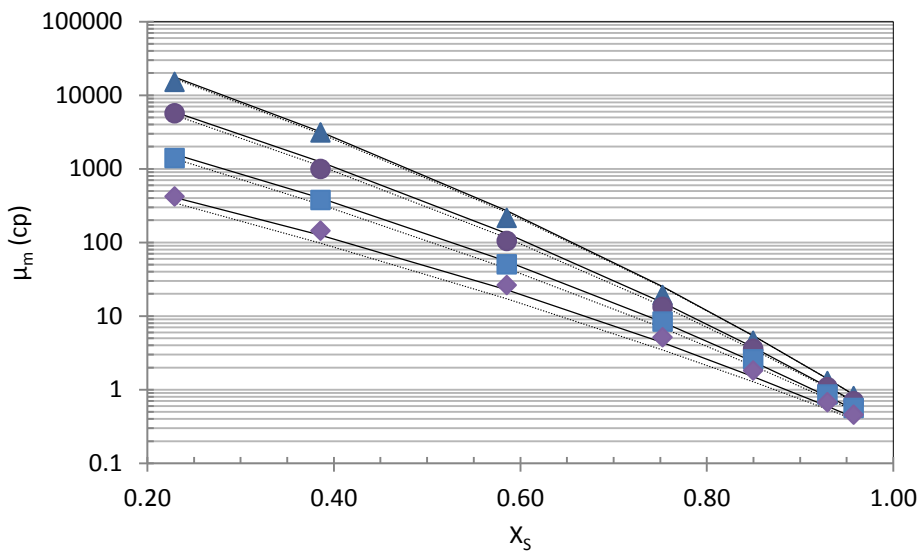

Figure 5-30: Viscosity μ_m, of bitumen/mixture 3 systems, versus mixture 3 mole fraction, X_S, at different temperatures, T; and a pressure of 10 MPa; measured data;−, correlated data; ■, T = 343 K; ●, T=326 K; ▲, T = 311.7 K, ♦, T = 301.3 K

Chapter 6 Conclusion

A previously designed and calibrated apparatus was used in this study to accurately measure the physical properties of the various fluids. The data was acquired at pressures from 1 to 10 MPa in stepwise increments of 2 MPa and temperatures from ambient to 344 K in stepwise increments of 15 K. The physical properties of the mixtures were measured to determine the effect of concentration with pressure and temperature. The concentration was observed and recorded from 5 to 80% solvent. The chemicals and fluids used in these experiments were MacKay River bitumen, toluene, and hexane. Toluene was also used to clean the experimental apparatus. Mixing the fluids in the desired proportions formed the experimental mixtures. The data generated by the experimental apparatus was fitted to the correlations from the literature and several mixing rules were investigated depending on the case and physical property being considered.

6.1 Asphaltene Precipitation

The focus of this research was also to investigate the critical concentration at which asphaltene precipitation starts; along with determining and correlating measured experimental data for several bitumen/solvents mixtures. In order to measure the delay in the critical mass fraction, by the addition of an aromatic solvent i.e. toluene to hexane, three different mixtures were prepared. The asphaltene precipitation results observed in binary and ternary mixtures of bitumen and solvents are presented in their respective section.

6.2 Case Study of Raw MacKay River Bitumen

Raw bitumen has a much higher viscosity than conventional crude oil at ambient and near ambient temperatures. Therefore, at temperatures below 321 K and all pressures, the bitumen viscosity was out of the range of the viscometer.

Table 4-4 presents the viscosity data at different temperatures and pressures. The viscosity of raw bitumen varied quite significantly with temperature at a constant pressure. For example, at 10 MPa, increasing the temperature from 321.3 to 344.7 K decreased the viscosity from 13330 to 1830 cp. The effect of pressure on viscosity was also analyzed and was determined to be less significant than the effect of temperature. For instance, at 321.3 K, a 9 MPa pressure increase results in only a 4775 cp increase in the viscosity of bitumen.

The experimental viscosity data for raw MacKay River bitumen was correlated by Eq. [2-7] and Eq. [2-8] presented by (Mehrotra and Svrcek, 1986). These two correlations contain the adjustable parameters a_1, a_2 and a_3, which were obtained by regression of the experimental data. The values of these parameters to fit the experimental data at various temperatures and pressures are presented in Table 5-5. The use of both of these equations produced much more accurate predictions and resulted in an AARD% of 0.8 and 0.4 for Eq. [2-7] and [2-8], respectively. It is evident from the AARD% that Eq. [2-8] produced the best predictions for the viscosity data of raw bitumen.

The density of raw bitumen was measured and the data obtained from these experiments is shown in Table 4-3. The influence of temperature and pressure on density was similar but of a different magnitude. The density of the bitumen increased linearly with pressure and decreased with temperature (Figure 5-1). The density of raw bitumen was measured at temperatures above

ambient and at all pressures. The density modeling of bitumen was completed using Eq. [5-2] and a regression of data provided us with the values of the adjustable parameters a_1, a_2, a_3, and a_4 as presented in Table 5-3. The model developed using Eq. [5-2] resulted in a maximum average deviation of ± 0.4 kg/m^3.

6.3 Case Study of Pure Solvents: Toluene and Hexane

The viscosity and density of the pure solvents were measured at temperatures and pressures similar to those at which the physical properties of raw bitumen were measured. The data in Tables 4-1 and 4-2 provides the viscosity and density variation of the pure solvents with temperature and pressure. According to these tables, the effect of pressure on the viscosity of toluene and hexane was so small that it can be ignored especially when compared with the effect of temperature on the viscosities. Therefore, an inverse relationship between the natural logarithm of viscosity and temperature was observed for each pure solvent. The experimental data for the viscosity of toluene was correlated with the Andrade equation [5-1] which contains two adjustable parameters; a and b. Regression of the measured data resulted in different values of a and b as presented in Chapter 5. The AARD% for the viscosity of toluene was 0.2.

The influence of pressure and temperature on density was significant. The density of the pure solvents decreased as the temperature increased from ambient to 333 K as illustrated in Table 4-1. The effect of pressure on the density of pure toluene was proportional. In depth comparison of the measured density data for both bitumen and toluene shows that the effect of both temperature and pressure on bitumen density is more significant than the effect on toluene. The same correlation that was used to fit the density data of raw bitumen was also used to fit the density of toluene. Eq. [5-2] produced different adjustable parameters for toluene, which are presented in Table 5-2. These values fit the experimental data with a maximum average deviation

of ± 0.4 kg/m^3. Hexane was not modelled due to the lack of experimental data because the density and viscosity values were only measured at room temperature over a pressure range of 1 to 10 MPa.

6.4 Case Study of Bitumen/Toluene and Bitumen/Hexane Binary Mixtures

The density of bitumen/toluene and bitumen/hexane at various temperatures, pressures, and solvent compositions was shown in Tables 4-11 to 4-16 and 4-23 to 4-28, respectively. According to these tables, the relationship between the pressure and density of each mixture is linear and the temperature has an inverse relationship with the density of each mixture. The bitumen/toluene mixture had a higher viscosity and density at almost all similar conditions of pressure and temperature than the bitumen/hexane mixture because the viscosity and density of the pure toluene was higher than the pure hexane at all conditions.

The density also decreased with increasing solvent concentration because the addition of solvent to bitumen makes the mixture lighter. The mixture density data can also be analyzed from Figures 4-4 and 4-5 for the bitumen/toluene mixture and Figures 4-8 and 4-9 for the bitumen/hexane system. According to these figures, the same increase in temperature at a high solvent composition results in a greater density decrease than it would at a lower solvent composition.

The density data of the binary mixtures was correlated with Eq. [5-8] which requires the densities of the pure solvents and the mass fractions of the raw bitumen. This equation produced an AARD% of 0.1 and 0.6 for the density of toluene and hexane diluted bitumen systems, respectively. The predicted densities of the toluene-bitumen system at lower temperatures deviated from the measured values at the highest mass fraction for all pressures. Therefore, the

assumption of ideal mixing is not applicable for this system at lower temperatures. The deviation of the predicted values from the experimental data was quite large in the hexane diluted bitumen systems (Figures 5-11 and 5-12).

The viscosities of the mixtures were dependent on temperatures and pressures but the magnitude of variation was different at various solvent concentrations. The viscosity data is presented in Tables 4-5 to 4-10 for the bitumen/toluene and Tables 4-17 to 4-35 for the bitumen/hexane systems. The viscosity decreased with increasing temperature and increased with increasing pressure at all solvent concentrations. The magnitude of influence of pressure and temperature on viscosity was dependent on the solvent concentration. As the mass fraction of the pure solvent increased to a maximum value of 0.7, the mixture became more like the pure solvent resulting in a negligible pressure effect on the viscosity of the mixture. The tabulated viscosity data can also be represented in a graphical manner (Figures 4-2, 3, 6, and 7).

A curvilinear relationship was observed between the viscosities and pressures of the mixtures with respect to all temperatures and solvent concentrations. The rise in temperature at lower solvent concentrations resulted in a significant decrease in viscosities at a constant pressure and mass fraction. The measured viscosity of the binary mixtures was correlated using four different models from the literature. The modelling results showed that the viscosity of the binary mixture is better predicted by the Lederer and Power law models than by the Shu correlation and Arrhenius's model. The Lederer and Power law models gave similar predictions for both binary mixture systems. In depth analysis of these models show that in the case of the toluene diluted bitumen system, the AARD%s were 9.6 and 14.8 for the Lederer and Power law model, respectively. In the case of the hexane diluted bitumen system, the AARD%s were 16.2 and 20.

Asphaltene precipitation for each binary mixture was also observed. In the case of the bitumen/toluene mixtures, no asphaltene precipitation was observed up to the maximum toluene mass composition of 70%. In the case of the bitumen/hexane mixture, asphaltene precipitation was observed at the hexane mass compositions of 50 and 70%.

6.5 Case Study of Pure Mixtures 1, 2, and 3

Three different solvent mixtures were prepared by the addition of an aromatic solvent i.e. toluene to hexane. The viscosity and density of the pure solvent mixtures were measured at conditions similar to those for pure toluene. The data in Tables 4-29, 30, and 31 provides the viscosity and density variation of pure solvent mixtures 1, 2, and 3 with temperature and pressure.

Similar to the case of pure solvents, the influence of pressure on the viscosity of each mixture was so small that it can be disregarded compared to the effect of temperature. The density of the pure solvent mixtures varied considerably with pressure and temperature. Mixtures with a greater composition of toluene showed higher physical property values at all conditions compared to those which contained less toluene. Of the mixtures considered, mixture 3 (hexane 25 wt % + toluene 75 wt %), showed the highest density and viscosity values at all temperatures and pressures.

The experimental data for the viscosity of pure mixture 1, mixture 2, and mixture 3 was correlated using the Andrade equation [5-1] which contains two adjustable parameters (a and b). The regression of the experimental data generated different values of these adjustable parameters for each case. The AARD% for the viscosities of mixture 1, mixture 2, and mixture 3 were 1.4,

0.3, and 0.1, respectively. The correlated and experimental viscosity data of the mixtures was presented in Tables 5-6 to 5-8.

Eq. [5-2] was used to fit the density data of each solvent mixture, this equation was also used to fit the density of pure toluene and raw bitumen. The adjustable parameters obtained by using this equation were presented in Table 5-9 for each solvent mixture. These values fit the experimental data for mixtures 1, 2, and 3 with a maximum average deviation of ± 0.4, 0.2 and 0.3 kg/m^3, respectively.

6.6 Case Study of Bitumen/Mixture 1, Bitumen/Mixture 2, and Bitumen/Mixture 3

The density of bitumen/mixture 1, bitumen/mixture 2, and bitumen/mixture 3 at various temperatures, pressures, and solvent mixture compositions was shown in Tables 4-39 to 4-45, 4-53 to 4-59, and 4-67 to 4-73. According to these tables, the pressure influences the density of each system linearly while the temperature has an inverse relationship with the density of the mixtures. The density decreased with when the ratio of solvents mixture concentration to bitumen was increased. The mixture density data can also be analyzed in Figures 4-12, 13, 16, 17, 20 and 21 for each system. According to these figures, at higher mixture compositions, the temperature rise results in a greater decrease in density than it would at lower mixture compositions.

The density data of bitumen diluted with mixtures 1, 2, and 3 was correlated with Eq. [5-8]. The AARD%s for this equation in the cases of mixture 1, 2, and 3 were 0.5, 0.5, and 0.3, respectively. In each case, the predictions matched the experimental data for most of the data points. The density of each mixture decreased linearly with increasing temperature at all pressures and solvent concentrations. The pressure versus mixture density plot showed

significant difference between the predicted and experimental data at higher temperatures and higher solvent concentrations. This behaviour invalidates our assumption of no volume change at these conditions.

This study also measured the influence of temperature and pressure on the viscosity of the systems, but the magnitude of this influence was dependent on the bitumen composition of the mixtures. The viscosity data was presented in Tables 4-33 to 4-38, 4-46 to 4-52, and 4-60 to 4-66 for the bitumen/mixture 1, bitumen/mixture 2 and bitumen/mixture 3 systems. The viscosity decreased as the result of increasing temperature at each pressure, and increased when the pressure was increased at a constant temperature. Figures 4-10, 11, 14, 15, 18, and 19 represent the viscosity data for bitumen diluted with the mixtures.

The experimental viscosities for bitumen diluted with the pure solvent mixtures were correlated with several models and predictions. Four different models were used to model the data. Of these, the Lederer and Power law models produced much more accurate predictions for all cases, whereas the Shu correlation and Arrhenius's model gave poor predictions (Figures 5-18, 5-23, and 5-28). The AARD% for mixture 1 using the Power law and Lederer's models were 14.4 and 15, respectively. In the case of mixture 2, the AARD% obtained using the Power law and Lederer's models were 13.5 and 8.6, respectively. The AARD% for Lederer's model and the Power law model were 9.4 and 13.5, respectively, in the case of bitumen diluted with mixture 3.

Asphaltene precipitation was also studied for each system. In the case of bitumen/mixture 1, asphaltene precipitation was observed only at the maximum mixture 1 mass composition of 80%. In the case of bitumen/mixture 2 and bitumen/mixture 3, no asphaltene precipitation was observed up to the maximum mixture compositions of 80% for both systems as the concentration of toluene was higher in these systems than in mixture 1.

6.7 Future Work

In oil industry, naphtha and condensate are used for the in-situ recovery and in transportation of bitumen through pipeline. Naphtha or condensate contains the mixture of hydrocarbons (5 to 15 carbon atoms). The main problem that is faced by oil industry is the low solubility of asphaltene fraction in n-alkanes. The critical concentration at which asphaltene precipitation occurs has been determined in various studies (Badamchi-zadeh et al., 2009 a; Nourozieh et al., 2013) for the bitumen diluted with n-alkanes (propane, hexane, and decane). In future, it will be quite interesting to find the magnitude of delay in asphaltene critical concentration for bitumen diluted with n-alkanes (pentane, heptane, octane, or nonane) by the addition of aromatic solvents either toluene or xylene along with the measurement of physical properties of considered systems.

Bibliography

Allan, J. M.; Teja, A. S. Correlation and Prediction of the Viscosity of Defined and Undefined Hydrocarbon Liquids. *Can. J. Chem. Eng.* **1991**, *69*, 986–991.

Arrhenius, S. A. Ueber Die Dissociation Der in Wasser Gelosten Stoffe, Z. *Phys. Chem.* **1887**, *1*, 631–648.

Badamchi-zadeh, A.; Yarranton, H. W.; Svrcek, W. Y.; Maini, B. B. Phase Behaviour and Physical Property Measurements for VAPEX Solvents: Part I. Propane and Athabasca Bitumen. *J. Can. Pet. Technol.* **2009 a**, *48*, 54–61.

Badamchi-zadeh, A.; Yarranton, H. W.; Maini, B. B.; Satyro, M. A. Phase Behaviour and Physical Property Measurements for VAPEX Solvents: Part II. Propane, Carbon Dioxide and Athabasca Bitumen. *J. Can. Pet. Technol.* **2009 b**, *48*, 57–65.

Das, S. K.; Butler, R. M. Mechanism of the Vapor Extraction Process for Heavy Oil and Bitumen. *J. Pet. Sci. Eng.* **1998**, *21*, 43–59.

Dealy, J. M. Rheological Properties of Oil Sand Bitumens. *Can. J. Chem. Eng.* **1979**, *57*, 677–683.

Guan, J. G.; Kariznovi, M.; Nourozieh, H.; Abedi, J. Density and Viscosity for Mixtures of Athabasca Bitumen and Aromatic Solvents. *J. Chem. Eng. Data* **2013**, *58*, 611–624.

Jacobs, F. A.; Donnelly, J. K.; Stanislav, J. Viiscosity of Gas-Saturated Bitumen. *J. Can. Pet. Technol.* **1980**, *19*, 46–50.

Johnson, S. E.; Svrcek, W. Y.; Mehrotra, A. K. Viscosity Prediction of Athabasca Bitumen Using the Extended Principle of Corresponding States. *Ind. Eng. Chem. Res.* **1987**, *26*, 2290–2298.

Kariznovi, M.; Nourozieh, H.; Abedi, J. Experimental Apparatus for Phase Behavior Study of Solvent–bitumen Systems: A Critical Review and Design of a New Apparatus. *Fuel* **2010**, *90*, 536–546.

Kariznovi, M.; Nourozieh, H.; Abedi, J. Experimental and Modeling Study of Vapor-Liquid Equilibrium for Propane/heavy Crude Systems at High Temperature Conditions. In *SPE Annual Technical Conference and Exhibition*; Society of Petroleum Engineers, 2011.

Kariznovi, M.; Nourozieh, H.; Abedi, J. Phase Behavior and Viscosity Measurements of Heavy Crude Oil with Methane and Ethane at High-Temperature Conditions. In *SPE Western Regional Meeting*; Society of Petroleum Engineers, 2012.

Kendall, J.; Monroe, K. P. The Viscosity of Liquids. II. The Viscosity-Composition Curve for Ideal Liquid Mixtures. *J. Am. Chem. Soc.* **1917**, *39*, 1787–1802.

Khan, M. A. B.; Mehrotra, A. X.; Svrcek, W. Y. Viscosity Models for Gas-Free Athabasca Bitumen. *J. Can. Pet. Technol.* **1984**, *23*, 47–53.

Lederer, E. L. Viscosity of Mixtures with and without Diluents. *Proc. First World Pet. Congr. London* **1933**, *2*.

Mehrotra, A. K. Development of Mixing Rules for Predicting the Viscosity of Bitumen and Its Fractions Blended with Toluene. *Can. J. Chem. Eng.* **1990**, *68*, 839–848.

Mehrotra, A. K. A Generalized Viscosity Equation for Pure Heavy Hydrocarbons. *Ind. Eng. Chem. Res.* **1991**, *30*, 420–427.

Mehrotra, A. K. A Generalized Viscosity Equation for Liquid Hydrocarbons: Application to Oil-Sand Bitumens. *Fluid Phase Equilib.* **1992**, *75*, 257–268.

Mehrotra, A. K.; Svrcek, W. Y. Measurement and Correlation of Viscosity, Density and Gas Solubility for Marguerite Lake Bitumen Saturated with Carbon Dioxide. *AOSTRA J. Res.* **1984**, *1*, 51 – 62.

Mehrotra, A. K.; Svrcek, W. Y. Viscosity, Density and Gas Solubility Data for Oil Sand Bitumens. Part I : Athabasca Bitumen Saturated with CO and C_2H_6. *AOSTRA J. Res.* **1985 a**, *1*, 263 – 268.

Mehrotra, A. K.; Svrcek, W. Y. Viscosity, Density and Gas Solubility Data for Oil Sand Bitumens. Part II: Peace River Bitumen Saturated with N_2, CO, CH_4, CO_2 and C_2H_6. *AOSTRA J. Res.* **1985 b**, *1*, 269–279.

Mehrotra, A. K.; Svrcek, W. Y. Viscosity, Density and Gas Solubility Data for Oil Sand Bitumens. Part III: Wabasca Bitumen Saturated with N_2, CO, CH_4, CO_2 and C_2H_6. *AOSTRA J. Res.* **1985 c**, *2*, 83–93.

Mehrotra, A. K.; Svrcek, W. Y. Viscosity of Compressed Athabasca Bitumen. *Can. J. Chem. Eng.* **1986**, *64*, 844–847.

Mehrotra, A. K.; Svrcek, W. Y. Corresponding States Method for Calculating Bitumen Biscosity. *J. Can. Pet. Technol.* **1987 a**, *26*, 2290–2298.

Mehrotra, A. K.; Svrcek, W. Y. Viscosity of Compressed Cold Lake Bitumen. *Can. J. Chem. Eng.* **1987 b**, *65*, 672–675.

Mehrotra, A. K.; Svrcek, W. Y. Properties of Cold Lake Bitumen Saturated with Pure Gases and Gas Mixtures. *Can. J. Chem. Eng.* **1988**, *66*, 656–665.

Mehrotra, A. K.; Eastick, R. R.; Svrcek, W. Y. Viscosity of Cold Lake Bitumen and Its Fractions. *Can. J. Chem. Eng.* **1989**, *67*, 1004–1009.

Miadonye, A.; Singh, B.; Puttagunta, V. R. Viscosity Estimation for Bitumen-Diluent Mixtures. *Fuel Sci. Technol. Int.* **1995**, *13*, 681–698.

Miadonye, A.; Latour, N.; Puttagunta, V. R. A Correlation for Viscosity and Solvent Mass Fraction of Bitumen-Diluent Mixtures. *Pet. Sci. Technol.* **2000**, *18*, 1–14.

Moran, K.; Yeung, A. Determining Bitumen Viscosity through Drop Shape Recovery. *Can. J. Chem. Eng.* **2004**, *82*, 813–820.

Nourozieh, H.; Kariznovi, M.; Guan, J. G.; Abedi, J. Measurement of Thermophysical Properties and Modeling for Pseudo-Binary Mixtures of N-Decane and Athabasca Bitumen. *Fluid Phase Equilib.* **2013**, *347*, 62–75.

Puttagunata, V. R.; Singh, B.; Miadonye, A. Correlation of Bitumen Viscosity with Temperature and Pressure. *Can. J. Chem. Eng.* **1993**, *71*, 447–450.

Shu, W. R. A Viscosity Correlation for Mixtures of Heavy Oil, Bitumen, and Petroleum Fractions. *Soc. Pet. Eng. J.* **1984**, *24*, 277–282.

Svrcek, W. Y.; Mehrotra, A. K. Gas Solubility, Viscosity and Density Measurements for Athabasca Bitumen. *J. Can. Pet. Technol.* **1982**, *21*, 31–38.

Takamura, K. Microscopic Structure of Athabasca Oil Sand. *Can. J. Chem. Eng.* **1982**, *60*, 538–545.

Ukwuoma, O.; Ademodi, B. The Effects of Temperature and Shear Rate on the Apparent Viscosity of Nigerian Oil Sand Bitumen. *Fuel Process. Technol.* **1999**, *60*, 95–101.

Ward, S. H.; Clark, K. A. Determination of the Viscosities and Specific Gravities of the Oils in Samples of Athabasca Bituminous Sand. **1950**.

Wen, Y.; Kantzas, A. Evaluation of Heavy Oil/bitumen-Solvent Mixture Viscosity Models. *J. Can. Pet. Technol.* **2006**, *45*, 56–61.

Zhang, C.; Zhao, H.; Hu, M.; Xiao, Q.; Li, J.; Cai, C. A Simple Correlation for the Viscosity of Heavy Oils from Liaohe Basin, NE China. *J. Can. Pet. Technol.* **2007**, *46*, 8–11.

National Institute of Standards and Technology http://webbook.nist.gov/chemistry/fluid.